



**PHD**

**Tear propagation behaviour in structural nets and coated fabrics.**

Gaafar, Ismail Abd Elrazik

*Award date:*  
1981

*Awarding institution:*  
University of Bath

[Link to publication](#)

## **Alternative formats**

If you require this document in an alternative format, please contact:  
[openaccess@bath.ac.uk](mailto:openaccess@bath.ac.uk)

Copyright of this thesis rests with the author. Access is subject to the above licence, if given. If no licence is specified above, original content in this thesis is licensed under the terms of the Creative Commons Attribution-NonCommercial 4.0 International (CC BY-NC-ND 4.0) Licence (<https://creativecommons.org/licenses/by-nc-nd/4.0/>). Any third-party copyright material present remains the property of its respective owner(s) and is licensed under its existing terms.

### **Take down policy**

If you consider content within Bath's Research Portal to be in breach of UK law, please contact: [openaccess@bath.ac.uk](mailto:openaccess@bath.ac.uk) with the details. Your claim will be investigated and, where appropriate, the item will be removed from public view as soon as possible.

Tear Propagation behaviour in structural  
nets and coated fabrics

submitted by Ismail Abd Elrazik Gaafar

for the degree of PhD  
of the University of Bath

1981

COPYRIGHT

- I. "Attention is drawn to the fact that copyright of this thesis rests with its author. This copy of the thesis has been supplied on condition that anyone who consults it is understood to recognise that its copyright rests with its author and that no quotation from the thesis and no information derived from it may be published without the prior written consent of the author".
- II. "This thesis may be made available for consultation within the University Library and may be photocopied or lent to other libraries for the purposes of consultation".

*I. A. Gaafar*

ProQuest Number: U322185

All rights reserved

INFORMATION TO ALL USERS

The quality of this reproduction is dependent upon the quality of the copy submitted.

In the unlikely event that the author did not send a complete manuscript and there are missing pages, these will be noted. Also, if material had to be removed, a note will indicate the deletion.



ProQuest U322185

Published by ProQuest LLC(2015). Copyright of the Dissertation is held by the Author.

All rights reserved.

This work is protected against unauthorized copying under Title 17, United States Code.  
Microform Edition © ProQuest LLC.

ProQuest LLC  
789 East Eisenhower Parkway  
P.O. Box 1346  
Ann Arbor, MI 48106-1346

UNIVERSITY OF BATH LIBRARY		
36	28 APR 1982	FRO
PHD		



## ABSTRACT

The problem of crack (tear) propagation in structural nets and fabrics is investigated. A theoretical solution which predicts the crack propagation behaviour under the effect of biaxial stress fields is presented. This was achieved by abstracting the most important interrelations from the Phenomena under study and expressing them as a partial differential equation, which was solved to give particular solutions corresponding to a given boundary and initial conditions.

The proposed expression was modified to account for the behaviour of coated fabrics under a uniaxial stress field. The scope of the investigation included other topics relevant to the crack propagation phenomena such as, the effect of joint slipping on the redistribution of stresses in structural nets. Experimental and analytical work was conducted to evaluate the reliability of the proposed expression and to explore its limitations. The results obtained were found to be in close agreement with the predicted crack propagation behaviour.

The excellent correlation between the proposed expression and the different theoretical and experimental work previously published which apparently seemed to be contradictory, established the validity and the reliability of the proposed solution.

## CONTENTS

### Abstract

### Chapter 1 Fracture

- 1.1 Fracture : Historic outlook .. .. . 1
- 1.2 Introduction to Fracture mechanics of homogeneous.. 3  
isotropic material
- 1.3 Fracture of structural nets and fabrics:. .. 5  
introduction and literature review.

### Chapter 2 Theoretical analysis of fracture of nets and fabrics

- 2.1 Introduction . . . . . 15
- 2.2 Equilibrium equation for a flat net under plane .. 15  
stress
- 2.3 Analytical solution for the infinite boundary case . 19
  - 2.3.1. Checking that the boundary conditions are .. ..20  
satisfied
  - 2.3.2 General equation for the shape function .. .. 22
- 2.4 Analytical solution for the fixed grips case .. 23
  - 2.4.1. General equation for the shape function .. .. 24
  - 2.4.2 Checking that the analytic function satisfies 25  
the required boundary conditions
- 2.5 Compatability of the two solutions . . . . . 29
- 2.6 Crack propagation and the fracture toughness value . 30
  - 2.6.1. Infinite boundary case .. .. . 31
  - 2.6.2 "Fixed grips leading" case .. .. . 32
  - 2.6.3 Recommended test for calculating the fracture 35  
toughness value " $\gamma$ " and the shear modulus of the  
coated fabric "G"

### Chapter 3 Discussion and comparison with previous work

- 3.1 Influence of stress fields biaxiality on the crack . 51  
propagation behaviour
- 3.2 Correlation between Topping's work (12) and the .. .55  
proposed solution for coated fabrics subjected to  
a biaxial stress field.

3.3	Comparison between Racah's experimental work (15) and the proposed solution for coated fabrics under a uniaxial stress field.	57
3.4	Comparison between Minami's work (9) and the proposed solution.	59
Chapter 4	Discrete analysis approach to crack propagation of structural nets	
4.1	Introduction	67
4.2	Discrete analysis method	69
4.3	Discrete analysis of nets subjected to biaxial tension	73
4.3.1.	Evaluating the reliability of the theoretical solution proposed	73
4.3.2.	Practical applications	76
4.3.3	Discussion and comparison with previous work	81
4.4	Discrete analysis of nets subjected to uniaxial tension	84
4.4.1.	The effect of the net length and width	85
Chapter 5	The effect of joint slipping on the crack propagation behaviour of structural nets	
5.1	Introduction	110
5.2	Factors affecting the value of the slipping force	111
5.3	Method of evaluation	113
5.4	Presentation of the work done	113
5.4.1.	Description of net configurations studied and the procedure adopted.	114
5.4.2.	Different joint slipping patterns encountered	115
5.4.3.	Detailed Results	118
Chapter 6	Experimental investigation of tear propagations in coated fabrics	
6.1	Introduction	125
6.2	Properties of coated fabric used	125
6.3	Shape of the specimens	126
6.4	Method of testing	127

	6.5	Results and discussion							
	6.5.1.	Biaxial tests	..	..	..	..	..	..	127
	6.5.2	Uniaxial tests	.	...	..	..	..	..	129
Chapter 7		Conclusions	..	..	..	..	..	..	141
References			..	..	..	..	..	..	143
Appendix	1.1	Confermal transformation	.	..	..	..	..	..	146
	1.2	Crack area for the fixed grips case	..	..	..	..	..	..	143
	1.3	Strain energy released for the fixed grips case							149
Appendix	2	Discrete analysis program	..	..	..	..	..	..	150
Appendix	3	Joint slippage program	..	..	..	..	..	..	158

## CHAPTER 1

### FRACTURE

## CHAPTER 1

### FRACTURE

#### 1.1. Fracture: Historic Outlook (21)

Man has been aware of the phenomenon of fracture since the beginnings of history, yet the emergence of the fracture theory as a true scientific discipline based on first principles has been surprisingly slow. It would seem that the urgent demand for the "practical solution" has had an overriding influence in determining the approach to the majority of fracture problems, resulting in the evolution of empirically-based fracture theories. This situation was changed in 1920 when Griffith (1) published his classic paper on the energy-balance concept of fracture.

Griffith's idea is eminently simple, by accounting for all energy terms which vary during a small change in a given crack system, one may write down a basic equation for describing crack growth. The principle is therefore based on the energy conservation laws of mechanics and thermodynamics. It was found (20) that once a crack occurs, the local stresses at the crack tip increases to a level several times that of the applied stresses, creating a stress concentration region around the crack tip. This meant that even the smallest of flaws does represent a potential source of weakness in the material.

Griffith's theory was developed for materials which behave in a purely elastic manner prior to crack propagation, such as glass, and although in most practical situations, some plastic deformation may take place before crack extension, thus presenting great difficulties in evaluating these energy terms, this did not limit its use because, provided that the plastic zone is small in comparison with the crack length and thickness, the energy released by crack extension could still be calculated from an elastic analysis with sufficient degree of accuracy. (2), (3).

From this brief introduction it is not difficult to appreciate the

fact, that all soundly based fracture theories were derived either directly from the Griffith concept or from some alternative starting assumption with underlying equivalence. Fracture mechanics of homogeneous isotropic materials is by now a well established part of engineering science, and although the present investigation is mainly concerned with the fracture behaviour of structural nets, it would be useful to mention some aspects of the former in order to relate it to the discussion in later chapters.

## 1.2. Introduction to Fracture Mechanics of Homogeneous Isotropic Material

There are three fundamental modes of crack surface displacements, Fig. (1.1).

1. In plane opening mode
2. Sliding or shear mode
3. Out of plane tearing mode

For a linear elastic body, the stress field produced around the crack tip may be described by either of two related approaches.

### 1. Stress analysis approach

The crack tip stress field may be described by a stress distribution that is common to all crack problems and a magnitude that is characterised by the stress intensity factor "K" for each mode of crack surface displacements.

The determination of stress intensity factors is a specialist task necessitating the use of a number of analytical and numerical techniques.

The fracture event is interpreted as being characterised by the attainment of a critical value of the stress intensity factor  $K_c$ , which represents the fracture toughness of the material and the knowledge of  $K_c$ , in a specimen provides the means for predicting similar crack extension behaviour in a structural member of the same material under similar conditions.

Dimensional analysis of the equations giving the stress and displacement fields in the vicinity of crack tips subjected to the three modes of deformation, indicates that the stress intensity factor is linearly related to stress, which in turn is inversely proportional to the square root of the crack length, thus

$$\sigma = \frac{K}{(b)^{\frac{1}{2}}} \quad \text{or} \quad \sigma \cdot (b)^{\frac{1}{2}} = K = \text{constant.}$$

where  $b$  : half the crack length



## 2. Energy balance approach (based on Griffith's theory)

Unstable crack propagation takes place when the strain energy released in an incremental crack extension exceeds the energy absorbed by creating new crack surface.

So alternatively, the magnitude of the stress field may be described in terms of an energy rate that could be regarded as a force,  $G$ , which is defined as the irreversible energy loss per unit area of newly created surface, this force would have a critical value  $G_c$  when a crack starts to propagate.

Precise determination of absorbed energy from independent measurement does not provide a satisfactory means of predicting the fracture event. However, the practical approach proposed by Irwin (2) does enable the onset of unstable fracture to be predicted in real structures provided suitable fracture experiments on cracked specimens have been carried out.

In situations where fracture is preceded by limited plastic deformation there is strict equivalence between the strain energy rate concept,  $G$ , and the stress intensity factor but when extensive plastic deformation occurs prior to failure the relationship between both approaches becomes more tenuous and great care is needed when interpreting the fracture behaviour in these situations.

### 1.3. Fracture of Structural Nets & Fabrics

#### Introduction and Literature Review

In recent years the need for new structural forms capable of fulfilling the growing demands in the field of construction, and for a more efficient use of building materials, has brought into focus the use of stressed membranes to form tensile structures of different types and shapes.

The rapid development of tensile structures is mainly due to their simplicity of construction, economy in cost for large spans, and for their considerable architectural potential.

Tensile structures can be classified into two main groups, according to the type of the stretched membrane. In the first group the membrane is an assembly of high tensile strength cables, forming a net which is then used in many different ways to cover large enclosures without the need for any intermediate supports, like the cable suspended roofs and other forms of cable networks. And in the second group, the tensioned membrane is made of woven fabrics either coated or uncoated. This group can be furthermore divided into two subgroups depending on the type of the structural support, whether

1. The membrane is stabilised by the pressure difference on both sides, as in air houses, flexible transport containers, water reservoirs, parachutes and a variety of military and civil engineering works.
2. The membrane is supported by cables, columns or any other conventional method, as in tents.

With the increased popularity of tensile structures, the need for a better understanding of their behaviour increased, in order to overcome the problems associated with this type of construction, and to achieve safer and more efficient methods for design and construction.

Although the two types of tension structures differ substantially in many ways, the stressed membrane in both cases is essentially a structural net, comprising of a number of linking elements intersecting at a finite number of nodal points.

Fracture in a structural net means the sequential breakage of a number of cables, (or yarns in the case of woven fabrics), along a line through the net.

After the initiation of the crack in the stressed membrane, the crack may retain its initial length or propagate resulting in the eventual failure of the structure.

It was found (4), (5) that the primary mode of failure in air houses is by tearing of the membrane, with large tears initiated mainly by sharp flying objects in high winds, internal scaffolding, fork-lift trucks and vandals.

Thus tear propagation resistance is the single most important mechanical property of an air house membrane.

The difference in fracture behaviour between solids and structural nets is attributed to the low shear stiffness, if any, of the latter which enables it to rotate relatively and spread the stress concentration in the region of the crack tip over a greater area ahead of the crack tip, thus a higher resistance to crack propagation is achieved.

Topping (6) has demonstrated by a rather simple analysis the superiority of structural nets to isotropic sheets and films in crack (tear) resistance.

Numerous studies have been made concerning the fracture mechanics of homogeneous isotropic materials, but the actual data existing which deals with the fracture of structural nets is very limited.

Abbott and Skelton (7) studied the tear propagation of woven fabrics, and adopting the energy balance approach they obtained an equation in the form

$$\frac{m T_c^2}{1 + m T_c} \leq 6 K_c + (1 - f) \frac{m T_R^2}{1 + m T_R}$$

This equation gives the critical tension " $T_c$ ", the tension below which crack will not propagate from a deliberately induced failure site, in terms of the tensile modulus " $m$ ", the energy resilience " $f$ " (recovery energy expressed as a fraction of strain energy to rupture for a yarn), the rupture tension " $T_R$ ", and the sum of the kinetic energy, heat energy and shear energy at the critical stress " $K_c$ ".

The authors acknowledged the fact, that accurate values of these parameters have never been obtained, and as a result the equation given cannot be used for calculating the critical stress, but hoped that it would give a useful insight into the nature of the phenomenon and the characteristics of the fibre or the structure on which it depends.

The main factors affecting the tearing strength can be summarised as follows (8).

#### (1) Yarn Strength

It has been amply confirmed experimentally that the tearing strength, force required to propagate a tear, is at least roughly proportional to the single yarn strength.

#### (2) Yarn Breaking Elongation

A high elongation normally produces a high tearing strength, due to its obvious influence on the interyarn spacing at the point of break.

#### (3) Fabric Density

In a densely woven structure there is less free space, less ultimate deformation potential, higher interyarn frictional forces, and hence a lower tearing strength.

#### (4) Weave Pattern

(5) The influence of finishing treatments like the application of

coating material, which essentially immobilises the yarns, and thus inevitably produces a large reduction in tearing strength.

Minami (9) considered the possibility of expressing the fracture toughness as a value of the inherent property of the material independent of all external factors such as tension and crack length.

He derived an expression for the fracture toughness of woven fabrics, having linear elastic properties, under uniaxial tensile stresses applied normal to the direction of the crack. The fracture toughness value, given as a rate of energy release, was transformed into an algebraic equation by Hedgepeth's theory (10), which applies an influence function to solve the discrete differential equation using Hedgepeth's analytical model. (The model neglects the yarns running perpendicular to the direction of the tension).

The theoretical formula for the fracture toughness was given as:

$$G_c = \frac{\pi}{8\sqrt{E_t G_t}} \left( 4b + \frac{1}{n_c} \right) T_c^2$$

This equation gives the fracture toughness value  $G_c$ , in terms of Young's modulus " $E_t$ " and the shear modulus " $G_t$ " of the coated fabric, the yarn count per unit length " $n_c$ ", half the crack length " $b$ " and the critical tension " $T_c$ ". To evaluate the validity of the proposed equation, experimental work was carried out, four types of coated fabrics were tested uniaxially, and the invariance of the fracture toughness value, as predicted by the equation, with respect to the crack length was checked using the experimental results.

Although this check showed linear growth of the fracture toughness value with respect to the crack length, this was attributed to the use of the maximum tension value  $T_p$  instead of  $T_c$  which was difficult to measure, after making a correction based on experimental observations, and repeating the check, an almost constant value for the

fracture toughness, independent of the crack length, was achieved, though not for all the specimens.

Minami also tested two specimens in the presence and absence of coating, and the result showed negligible effect on the fracture toughness value.

Anderson, et al., (11) have found, however, that the tear strength may be either increased or decreased by varying the properties and thickness of the coating material.

Similar tests, under different conditions, to study the effect of coating were conducted by Abbot and Skelton (7), in which a significant drop in the critical tensions after coating was recorded. If a crack is to propagate, sufficient energy must be released after a yarn is ruptured to supply the work required to strain the next yarn to rupture. So in order to establish the relationship between the propagation velocity, which should simulate the rate of energy release with time, and the critical tension, the same authors attempted to measure the propagation velocity in the high tension region.

The results showed that for levels above the critical tension, the propagation velocity varies linearly with tension, and that there are considerable differences in behaviour between the light and heavy fabrics of the same weave. The heavier fabrics have a higher rupture load and hence a greater critical tension, in spite of which, both the absolute value of propagation velocity and its rate of increase with tension are smaller than for lighter fabrics. Results also showed that the speed of crack initiation had no effect on the value of the critical tension.

Topping (12) compared four different theories which predicts the burst strength of longitudinally slit pressurised fabric cylinders with tests of warp cylinders having various diameters and lengths, containing slits of various lengths and widths. These theories are:

### 1. Modified Griffith Theory

Griffith's original solution for a narrow elliptical crack in an infinite isotropic elastic plate subjected to a uniform uniaxial stress normal to the crack, is:

$$f = \frac{c}{(\ell/\rho)^{3/2}}$$

This equation gives failure stress  $f$  in terms of the crack length  $\ell$  and the crack tip radius  $\rho$ , was modified by Williams (22) for use in pressurised cylinders, the final form is:

$$Pr = \frac{c_1}{\ell^n (1 + K \ell/r)}$$

(since  $f = Pr$  in a pressurised cylinder)

where  $r$  : cylinder radius and  $(1 + K \ell/r)$  is the cylinder curvature factor and where  $n, c_1$  are empirical constants.

### 2. Elementary Fabric Theory

Topping (12), derived an equation from elementary considerations for a flat sheet of single-ply fabric slit parallel to one set of threads, assuming an effective number  $n_y$ , of uniformly loaded threads at the edges of the slit, carried the load from the cut threads. After the incorporation of the cylinder curvature factor this equation becomes:

$$Pr = \frac{P_0 \cdot r}{(1 + c_y \ell/2 n_y) (1 + K \ell/r)}$$

where  $P_0$  : undamaged cylinder's burst pressure, and  $c_y$  : thread count per unit width.

### 3. Hedgepeth's Stress Concentration Factor

Hedgepeth (10) assumed a sheet of parallel, tension carrying filaments embedded in a matrix which carries only shear, he obtained a

static stress concentration factor:

$$K_n \approx \frac{\sqrt{\pi n} (n + 1)}{2n + 1} \xrightarrow{n \rightarrow \infty} \frac{\sqrt{\pi n}}{2}$$

and accordingly for the cylinder curvature factor gives:

$$\frac{K_n}{(1 + K \ell/r)} = \frac{F}{f}$$

where  $F$  : stress at the end of the slit,  $n$ : number of threads cut.

#### 4. Deaton's Fracture Mechanics Approach

Deaton (13) employed a fracture mechanics analysis developed by Anderson and Sullivan (23) for sheet materials. The equation given by them is:

$$Pr = \frac{K_{cn}}{(1 + K \ell/r) \sqrt{\frac{\pi \ell}{2} + \frac{K_{cn}^2}{2 F_{YB}^2}}}$$

where  $K_{cn}$  : fracture toughness for flat sheet determined from tests  
and  $F_{YB}$  : is the yield strength in a biaxial stress field.

Only the modified Griffith equation, requiring three empirical constants, such that:

$$Pr = \frac{40.6}{\ell^{0.65} (1 + .76 \frac{\ell}{r})}$$

fitted the test data.

Inspection of the test data also revealed that neither the cylinder length nor the slit width has an effect on slit-cylinder tear pressure.

William, L. Ko (14) investigated experimentally the fracture behaviour of non-linear woven fabrics, monolayered and laminated sheets, and found that the  $K_n$  curve, Hedgepeth's stress concentration factor, when shifted horizontally gave good correlation with



the experimental data, specially for the monolayer case.

Further experimental work was conducted by Racah (15). The crack propagation behaviour of woven fabrics was investigated by determining the empirical relation between the nominal crack propagation strength and the initial crack length for PVC coated polyester fabrics under uniaxial tension. The relation found is similar, though not identical, to the one used in linear elastic fracture mechanics. The influence of the width and length of the specimens, compared with the crack length was also investigated.

Although it has been suggested that in air houses, the tear propagates in an in-plane opening mode rather than an out-of-plane tearing mode, in the current design and analysis practice the most common method used for the measurement of tearing strength is probably the tongue tear test, in which an out-of-plane stresses are applied to the flawed specimens. In 1976 a "draft for discussion" (16) was issued by the British Standards Institution, which also prescribes an out-of-plane tear test. Racah (15) suggested, since this mode of failure is irrelevant to tear propagation in air houses, that this test should be replaced by a new one, which consists of tensioning flat flawed specimens. The purpose of such test will be to relate the nominal fracture strength with initial length of the crack.

Huisman, Bleker (17) and Abbott, Skelton (7) suggested the integration of a grid with higher strength into the woven fabric net to serve as tear-stops or crack arresters.

Another way to improve the tear resistance behaviour, suggested by the latter, is to treat the woven fabric net with liquid lubricant. Tests showed that the treated specimens had higher tearing resistance.

At the present time, the knowledge of the subject and existing information is still incapable of accounting for many aspects of

the fracture behaviour of structural nets, and until a much better understanding for the crack propagation phenomenon is achieved, the ultimate utilisation of the structural materials in stressed membranes will remain a dream to be realised.

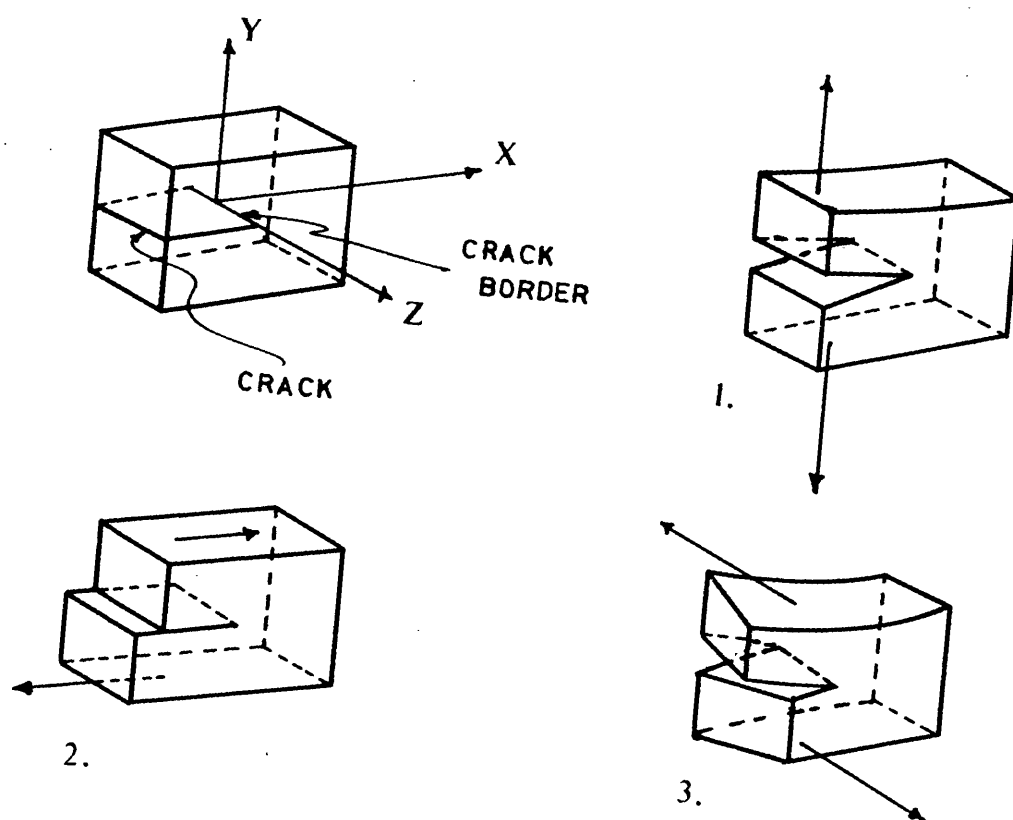


FIG (1.1)  
FUNDAMENTAL MODES OF CRACK SURFACE  
DISPLACEMENT.

## CHAPTER 2

### THEORETICAL ANALYSIS OF FRACTURE OF NETS AND FABRICS

## CHAPTER 2

### THEORETICAL ANALYSIS OF FRACTURE OF NETS & FABRICS

#### 2.1. Introduction

The physical phenomena which can be represented by fields are related from point to point in ways which can usually be expressed in terms of partial differential equations. A change in the field at one point usually affects its value at nearby points, and these changes affect the values still further away, and so on, a step-wise interrelation which is most naturally expressed in terms of space derivatives. The field which corresponds to a particular physical situation is, therefore, usually a solution of some partial differential equation, that particular solution which satisfies the particular set of 'boundary conditions' appropriate to the situation.

The theoretical expressions proposed in this research work were achieved in a similar way by abstracting the most important inter-relations from the phenomena under study and expressing them as partial differential equations, which was solved to give particular solutions corresponding to given boundary and initial conditions.

#### 2.2. Equilibrium Equation for a Flat Net Under Plane Stress

Before presenting the work done, it would be better to examine first a simple one dimensional field, so as to bring out some of the concepts in their simplest form.

The flexible string shown in Fig. (2.1) is in equilibrium under the effect of transverse forces uniformly distributed along its length and the differential equation for the equilibrium shape is given by:

$$\frac{d^2\phi}{dx^2} = - P/T_o \quad (1)$$

This is a one dimensional case of Poisson's equation, and its

general solution is given in the form:

$$\phi = a + bx - \left\{ \frac{P}{2T_0} \right\} x^2$$

where a, b are determined by the boundary condition

$$\phi = 0 \quad \text{at } x = 0, L$$

and the final solution of this problem is

$$\phi = \left\{ \frac{P}{2T_0} \right\} x(x - L)$$

which gives the shape equation as a parabola.

This simple string case can be modified to represent a typical intermediate cable line in a flat net subjected to a constant plane stress by taking "P" as a variable  $P(x)$ , its magnitude at each node along the x axis is proportional to the relative displacement of the two adjacent nodes as each side along the y axis. (The horizontal component of  $P(x)$  is neglected) from Fig. (2.2), the transverse displacement  $Y_k$  and  $Y_{k+1}$  at successive loaded points differ by

$$Y_{k+1} - Y_k = h \cdot \tan \theta_k \quad (2)$$

where h is the horizontal spacing and also for force equilibrium at point "K".

$$\therefore T_k \cos \theta_k - T_{k-1} \cos \theta_{k-1} = 0$$

and

$$T_k \sin \theta_k + T_{k-1} \sin \theta_{k-1} + P_k = 0 \quad (3)$$

$$\therefore T_0 = T_k \cos \theta_k = T_{k-1} \cos \theta_{k-1} = \text{constant}$$

and substituting in (3) gives:

$$T_o (\tan \theta_k - \tan \theta_{k-1}) + P_k = 0 \quad (4)$$

using (2) to eliminate  $\theta_k$  from (4), yields the relation

$$T_o \left[ \left( Y_{k+1} - Y_k \right) - \left( Y_k - Y_{k-1} \right) \right] + h P_k = 0$$

or

$$\frac{T_o}{h} \delta^2 Y_k + P_k = 0 \quad (5)$$

for  $P_k = P = \text{constant}$  this equation become the difference form for the differential equation (1), but for the general case of a flat net, since  $P_k \neq \text{constant}$

$$\begin{aligned} \therefore P_k &= \left( Y_{k,m+1} - Y_{k,m} - L_o \right) \frac{AE}{L_o} - \left( Y_{k,m} - Y_{k,m-1} - L_o \right) \frac{AE}{L_o} \\ &= \left( \Delta Y_{k,m} - \nabla Y_{k,m-1} \right) \frac{AE}{L_o} \end{aligned}$$

where

AE : extensional stiffness of the cables  
 $L_o$  : original cable length in Y direction

substituting for  $P_k$  in equation (5) gives

$$\frac{T_o h}{AE L_o} \delta^2 Y_{k(m)} + \delta^2 Y_{m(k)} = 0$$

$$\therefore \left[ \frac{T_o h}{AE L_o} \right] \frac{\partial^2 \phi}{\partial x^2} + \frac{\partial^2 \phi}{\partial y^2} = 0 \quad (6)$$

where  $\phi$  : the node movement in the Y direction from zero tension

and by transformation of the x axis, so that

$$\left[ \frac{T_o h}{AE L_o} \right] \frac{\partial^2 \phi}{\partial x^2} = \frac{\partial^2 \phi}{\partial X^2}$$

this transformation is equivalent to changing the scale in the x direction and will be readjusted later on.

∴ Equation (6) becomes

$$\frac{\partial^2 \phi}{\partial x^2} + \frac{\partial^2 \phi}{\partial y^2} = 0$$

$$\therefore \nabla^2 \phi = \frac{\partial^2 \phi}{\partial x^2} + \frac{\partial^2 \phi}{\partial y^2} = 0$$

which is Laplace's potential equation (harmonic) and this means that Laplace's equation is the governing equation for flat nets in biaxial field, provided that:

1. Linear elastic behaviour of the cable material is assumed.
2. The horizontal component of the initially vertical cables is neglected.

It is interesting to notice that if  $\nabla^2 \phi$  is negative at some point, this would mean a tendency for " $\phi$ " to concentrate at that point, as illustrated by the one dimensional Poisson's equation (1).

$$\frac{\partial^2 \phi}{\partial x^2} = -P/T_0$$

and for  $P = 0$  or  $T_0 = \infty$  equation (1) becomes a one dimensional Laplace equation  $\nabla^2 \phi = 0$   
or

$$\frac{\partial^2 \phi}{\partial x^2} = 0, \text{ which simply means a straight line.}$$

So one can say that the laplacian operator measures the bulginess of the shape function  $\phi$ , and in a region where  $\nabla^2 \phi = 0$ ,  $\phi$  can have no maxima or minima (19).

Laplace's equation was solved to find the shape function  $\phi$  for flat



nets with a central slit under Biaxial tension.

Using conformal transformations, a method developed in connection with the theory of complex analytic functions, a solution was found for two different boundary conditions.

1. Infinite net, constant force (dead-weight loading).  
i.e. the applied force remains constant as the crack extends.
2. Finite net, constant displacement. ("fixed grips" loading), i.e. the applied loading system suffers no displacement as the crack extends.

In complex analysis, the general solution of the potential equation is the real part of any analytic function of the complex variable ( $z = x + iy$ ).

Conformal transformations were deployed to find the analytic function which satisfies the required boundary conditions in each case.

### 2.3. Analytical Solution for the Infinite Boundary Case

The solution is the real part of the analytic function which satisfies the following boundary conditions.

$$1. \quad \frac{\partial \phi}{\partial y} = 0 \quad \text{at} \quad \begin{cases} y = 0 \\ |x| < b \end{cases}$$

where  $b$  = half the crack length

$$2. \quad \frac{\partial \phi}{\partial y} \rightarrow T \quad (\text{constant tension})$$

as  $y \rightarrow \infty$

$$3. \quad \phi = 0 \quad \text{at} \quad \begin{cases} y = 0 \\ |x| > b \end{cases}$$

as shown in Fig. (2.3) using conformal mapping (Appendix (1.1)) yields the function;

$$\omega(z) = \phi + i\psi = -iT(z^2 - b^2)^{\frac{1}{2}}$$

where  $z = x + iy$

### 2.3.1. Checking that the boundary conditions are satisfied

$$(1) \quad \therefore \frac{dw}{dz} = \frac{\partial \phi}{\partial x} + i \frac{\partial \psi}{\partial x}$$

$$= \frac{\partial \psi}{\partial y} - i \frac{\partial \phi}{\partial y}$$

$$\therefore \quad \frac{\partial \phi}{\partial x} = \frac{\partial \psi}{\partial y}, \quad \frac{\partial \phi}{\partial y} = - \frac{\partial \psi}{\partial x}$$

$\therefore$  Using the Cauchy-Riemann equations, which are not only necessary but also sufficient for a function to be analytic, we find that:

$$\frac{\partial \phi}{\partial y} = - \frac{\partial \psi}{\partial x} = - \frac{\partial}{\partial x} (\text{Im } \omega)$$

$$= - \text{Im} \left( \frac{d\omega}{dz} \right) = - \text{Im} (\omega'(z))$$

$$= - \text{Im} \left\{ \frac{-i T z}{(z^2 - b^2)^{\frac{1}{2}}} \right\}$$

for  $y = 0$ ,  $|x| < b$   $\therefore (z^2 - b^2)^{\frac{1}{2}}$  is imaginary

$$\therefore \frac{\partial \phi}{\partial y} = - \text{Im} \{ \text{real quantity} \}$$

$$= \text{zero}$$

(2) as  $y \rightarrow \infty$

$$\therefore \omega(z) = -i T z \left( 1 - \frac{b^2}{z^2} \right)^{\frac{1}{2}} \approx -i T z \left( 1 - \frac{b^2}{2z^2} \right)$$

$$\approx -i T \left( z - \frac{b^2}{2z} \right) \approx -i T z$$

$$\therefore \frac{\partial \phi}{\partial y} \rightarrow T$$

and when there is no crack  $b = 0$

$$\omega(z) = -i T z$$

$$\frac{\partial \phi}{\partial y} = T \quad \text{for all } y \text{ values}$$

(3) for  $y = 0$

$$\omega(z) = -i T (x^2 - b^2)^{\frac{1}{2}}$$

$$\text{for } |x| > b \quad \omega(z) = \text{imaginary value}$$

$$\therefore \phi = 0$$

$$\text{and for } |x| = b \quad \omega(z) = \text{zero}$$

$$\therefore \phi = 0 \quad \text{for } |x| \geq b$$

thus it can be seen that the analytic function satisfies all the boundary conditions.

It can be seen from Fig. (2.4) that by expressing

$$z \text{ as } z = b + q$$

and since the tension in the Y direction is proportional to  $\frac{\partial \phi}{\partial y}$

$$\begin{aligned} \therefore \frac{\partial \phi}{\partial y} &= \text{Im} \left[ \frac{i T z}{(z^2 - b^2)^{\frac{1}{2}}} \right] \\ &= \text{Im} \left[ \frac{i T (b + q)}{\{(b+q)^2 - b^2\}^{\frac{1}{2}}} \right] \\ &= \text{Im} \left[ \frac{i T (b + q)}{(2bq + q^2)^{\frac{1}{2}}} \right] \\ &= \text{Im} \left[ \frac{i T (b + q)}{(2bq)^{\frac{1}{2}} \left(1 - \frac{q}{2b}\right)^{\frac{1}{2}}} \right] \\ &= \text{Re} \left[ \frac{T (b + q)}{(2bq)^{\frac{1}{2}} \left(1 - \frac{q}{2b}\right)^{\frac{1}{2}}} \right] \end{aligned}$$

for  $q \ll b$

$$\therefore \approx \text{Re} \frac{Tb^{\frac{1}{2}}}{(2q)^{\frac{1}{2}}}$$

$\therefore$  at a given point

$$\text{stress} \propto T b^{\frac{1}{2}}$$

∴ critical tension  $\propto \frac{1}{b^2}$

which is similar to that in a homogeneous isotropic material.

### 2.3.2. General equation for the shape function $\phi$

$$\omega(z) = \phi + i\psi = -iT(z^2 - b^2)^{\frac{1}{2}}$$

where  $z = x + iy$

$$\begin{aligned} \therefore \phi + i\psi &= -iT \left[ (x^2 - y^2 - b^2) + 2xyi \right]^{\frac{1}{2}} \\ &= -iT \left[ (x^2 - y^2 - b^2)^2 + (2xy)^2 \right]^{\frac{1}{4}} (\cos \theta/2 + i \sin \theta/2) \end{aligned}$$

where

$$\cos \theta = \frac{(x^2 - y^2 - b^2)}{\left[ (x^2 - y^2 - b^2)^2 + (2xy)^2 \right]^{\frac{1}{2}}}$$

$$\sin \theta = \frac{2xy}{\left[ (x^2 - y^2 - b^2)^2 + (2xy)^2 \right]^{\frac{1}{2}}}$$

∴ The shape function  $\phi$

$$\phi = T \left[ x^4 + y^4 + b^4 - 2b^2x^2 + 2b^2y^2 \right]^{\frac{1}{4}} \sin \theta/2$$

where

$$\sin \theta/2 = \sqrt{\frac{1 - \cos \theta}{2}}$$

and in order to account for the axis transformation each dimension in the  $x$  direction is divided by:

$$C = \left[ \frac{T_o h}{AE L_o} \right]^{\frac{1}{2}}$$

∴ The final shape function

$$\therefore \phi = T \left[ \frac{x^4}{C^4} + y^4 + \frac{b^4}{C^4} - \frac{2b^2x^2}{C^4} + \frac{2b^2y^2}{C^2} \right]^{\frac{1}{4}} \sin \theta/2$$

Equating  $Y = 0$  in the shape function  $\phi$

$$\therefore \phi = \frac{T}{C} (b^2 - x^2)^{\frac{1}{2}}$$

$$\therefore \frac{\phi^2}{\left(\frac{Tb}{C}\right)^2} + \frac{x^2}{(b)^2} = 1 \quad \text{where } T = \frac{V_o}{AE}$$

Which gives the crack shape as an ellipse.

Figure (2.5) shows a computer plot for the shape function using arbitrary values.

It can be seen that the crack shape for the infinite boundary case will always be an ellipse and that an increase in the crack length while maintaining the other arbitrary values does not alter the shape of that ellipse, as shown in Fig. (2.6) which could almost be considered as a magnification of Fig. (2.5), and only varying the boundary tension or the extensional stiffness changes the ratio between its major and minor axis.

#### 2.4. Analytical Solution for the Fixed Grips Case

Similarly, the solution is the real part of the analytic function which satisfies the following boundary conditions.

$$1. \quad \frac{\partial \phi}{\partial y} = 0 \quad \text{at} \quad \begin{cases} y = 0 \\ |x| < b \end{cases}$$

$$2. \quad \phi \rightarrow \Delta \quad (\text{constant displacement}) \\ \text{as } y \rightarrow \frac{a}{2} \quad \text{where } a = \text{length of the net}$$

$$3. \quad \phi = 0 \quad \text{at} \quad \begin{cases} y = 0 \\ |x| \geq b \end{cases}$$

Using conformal mapping (Appendix (1.1)) yields the analytic function:

$$\omega(z) = -\frac{T a i}{\pi} \cosh^{-1} \left[ \frac{\cosh \left( \frac{\pi z}{a} \right)}{\cosh \left( \frac{\pi b}{a} \right)} \right]$$

where  $z = x + iy$

2.4.1. Derivation of the general equation for the shape function  $\phi$

$$\omega(z) = \phi + i\psi = -\frac{Ta}{\pi} \operatorname{Cosh}^{-1} \left[ \frac{\operatorname{Cosh}(\frac{\pi z}{a})}{\operatorname{Cosh}(\frac{\pi b}{a})} \right]$$

$$\therefore \omega = -iK \operatorname{Cosh}^{-1} H$$

$$\text{where } K = \frac{Ta}{\pi}, \quad H = u + iv = \frac{\operatorname{Cosh}(\frac{\pi z}{a})}{\operatorname{Cosh}(\frac{\pi b}{a})}$$

$$\therefore i\omega = K \operatorname{Cosh}^{-1} H$$

$$\begin{aligned} \therefore H &= \operatorname{Cosh} \frac{i\omega}{K} = \cos \frac{\omega}{K} = \cos \left( \frac{\phi}{K} + i \frac{\psi}{K} \right) \\ &= \cos\left(\frac{\phi}{K}\right) \cosh\left(\frac{\psi}{K}\right) - i \sin\left(\frac{\phi}{K}\right) \sinh\left(\frac{\psi}{K}\right) \end{aligned}$$

$$\therefore u = \cos\left(\frac{\phi}{K}\right) \cosh\left(\frac{\psi}{K}\right)$$

$$v = \sin\left(\frac{\phi}{K}\right) \sinh\left(\frac{\psi}{K}\right)$$

$$\therefore \frac{u^2}{\cos^2\left(\frac{\phi}{K}\right)} - \frac{v^2}{\sin^2\left(\frac{\phi}{K}\right)} = 1$$

$$\therefore u^2 \sin^2\left(\frac{\phi}{K}\right) - v^2 \left[1 - \sin^2\left(\frac{\phi}{K}\right)\right] = \sin^2\left(\frac{\phi}{K}\right) \left[1 - \sin^2\left(\frac{\phi}{K}\right)\right]$$

$$\text{put } \sin^2\left(\frac{\phi}{K}\right) = \alpha$$

$$\therefore u^2 \alpha - v^2 [1 - \alpha] = \alpha [1 - \alpha]$$

$$\therefore \alpha^2 + \alpha(u^2 + v^2 - 1) - v^2 = 0$$

$$\therefore \alpha = \sin^2\left(\frac{\phi}{K}\right) = \frac{-u^2 - v^2 + 1 + \sqrt{(u^2 + v^2 - 1)^2 + 4v^2}}{2}$$

$$\therefore \phi = K \left\{ \sin^{-1} \left[ \frac{-u^2 - v^2 + 1 + \sqrt{(u^2 + v^2 - 1)^2 + 4v^2}}{2} \right]^{\frac{1}{2}} \right\}$$

Where  $\dots H = u + iv = \frac{\cosh(\frac{\pi z}{a})}{\cosh(\frac{\pi b}{a})}$

$$\therefore u = \frac{\cosh(\frac{\pi x}{a}) \cos(\frac{\pi y}{a})}{\cosh(\frac{\pi b}{a})}$$

$$v = \frac{\sinh(\frac{\pi x}{a}) \sin(\frac{\pi y}{a})}{\cosh(\frac{\pi b}{a})}$$

Similarly, to account for the axis transformation each dimension in the x direction is divided by:

$$c = \left[ \frac{T_o h}{AE L_o} \right]^{\frac{1}{2}}$$

$$\therefore u = \frac{\cosh(\frac{\pi x}{ac}) \cos(\frac{\pi y}{a})}{\cosh(\frac{\pi b}{ac})}$$

$$v = \frac{\sinh(\frac{\pi x}{ac}) \sin(\frac{\pi y}{a})}{\cosh(\frac{\pi b}{ac})}$$

#### 2.4.2. Checking that the analytic function satisfies the required boundary conditions

1. By the Cauchy-Riemann conditions

$$\frac{\partial \phi}{\partial y} = - \frac{\partial \psi}{\partial x} = - \frac{\partial}{\partial x} (\text{Im } \omega)$$

$$= - \text{Im} [\omega'(z)]$$

$$\therefore \cosh\left(\frac{\omega \pi}{T_{ai}}\right) = - \frac{\cosh(\frac{\pi z}{a})}{\cosh(\frac{\pi b}{ac})}$$

differentiating with respect to  $z$

$$\sinh\left(\frac{\omega\pi}{T a i}\right) \frac{\pi}{T a i} \frac{\partial \omega}{\partial z} = \frac{-\pi/a \sinh\left(\frac{\pi z}{a}\right)}{\cosh\left(\frac{\pi b}{ac}\right)}$$

$$\frac{\partial \omega}{\partial z} = \omega'(z) = \frac{-iT \sinh\left(\frac{\pi z}{a}\right)}{\sqrt{\cosh^2\left(\frac{\pi z}{a}\right) - \cosh^2\left(\frac{\pi b}{ac}\right)}}$$

$$\text{where } z = \frac{x}{c} + iy$$

$$\therefore \frac{\partial \phi}{\partial y} = - \operatorname{Im} \left[ \frac{-iT \sinh\left(\frac{\pi z}{a}\right)}{\sqrt{\sinh^2\left(\frac{\pi z}{a}\right) - \sinh^2\left(\frac{\pi b}{ac}\right)}} \right]$$

$$= - \operatorname{Im} \left[ \frac{-iT}{\sqrt{\frac{1 - \sinh^2\left(\frac{\pi b}{ac}\right)}{\sinh^2\left(\frac{\pi z}{a}\right)}}} \right] \quad (7)$$

$$\text{for } \begin{cases} Y = 0 \\ |x| < b \end{cases} \therefore \frac{\partial \phi}{\partial y} = - \operatorname{Im} [\text{real quantity}] = \text{zero}$$

$$2. \text{ at } Y = \frac{a}{2}$$

$$u = \frac{\cosh\left(\frac{\pi x}{ac}\right) \cos\left(\frac{\pi y}{a}\right)}{\cosh\left(\frac{\pi b}{ac}\right)} = \text{zero}$$

$$\therefore \sin^2\left(\frac{\phi}{K}\right) = 1 \quad \text{for all values of } v$$

$$\therefore \frac{\phi}{K} = \frac{\pi}{2} \quad \therefore \phi = \frac{\pi}{2} \wedge \frac{T a}{\pi} = \frac{T a}{2} = \text{constant}$$



$$3. \quad \omega(z) = -\frac{Tai}{\pi} \cosh^{-1} \left[ \frac{\cosh \left( \frac{\pi z}{a} \right)}{\cosh \left( \frac{\pi b}{ac} \right)} \right]$$

$$\text{where } z = \frac{x}{c} + iy$$

$$\therefore \text{ for } y = 0, \quad |x| \geq b$$

$$\cosh^{-1} \left[ \frac{\cosh \left( \frac{\pi x}{ac} \right)}{\cosh \left( \frac{\pi b}{ac} \right)} \right] \quad \text{is real}$$

$$\therefore \phi = \text{zero}$$

$\therefore$  all boundary conditions are satisfied.

And as before, if there is no crack ( $b = 0$ )

$$\therefore \omega(z) = \frac{-Tai}{\pi} \cosh^{-1} \left[ \cosh \left( \frac{\pi z}{a} \right) \right]$$

$$\therefore \omega(z) = -iTz \quad \therefore \frac{\partial \phi}{\partial y} = T$$

i.e. constant tension for all  $y$  values.

Equating  $y = 0$

$$v = 0, \quad u = \frac{\cosh \left( \frac{\pi x}{ac} \right)}{\cosh \left( \frac{\pi b}{ac} \right)}$$

$$\therefore \sin^2 \left( \frac{\phi}{k} \right) = \frac{-u^2 + 1 + \sqrt{(u^2 - 1)^2}}{2}$$

$$\text{for } |x| < b \quad u < 1 \quad \therefore -u^2 + 1, \sqrt{(u^2 - 1)^2} \text{ are +ve}$$

$$\therefore \sin^2 \left( \frac{\phi}{k} \right) = 1 - u^2$$

The shape of the crack is given by;

$$\phi = \frac{Ta}{\pi} \cos^{-1} \left[ \frac{\cosh \left( \frac{\pi x}{ac} \right)}{\cosh \left( \frac{\pi b}{ac} \right)} \right]$$

Figure (2.7) shows a computer plot for the shape function using arbitrary values, and in which the effect of the fixed grips loading on the shape of the boundary is evident. A magnification of the crack region is shown in Fig (2.8). while in the infinite boundary case the crack shape is always an ellipse, the shape of the crack in the case of fixed grips loading is determined by the combined effect of the different parameters, i.e. the boundary tension, extensional stiffness and the crack length compared with the length of the net. e.g. the effect of a reduction in the boundary tension on the shape of the crack can be seen in Fig. (2.9). When it comes to assessing the difference in the crack area in both cases, which is directly related to the strain energy released, the simplest way is by comparing the two expressions giving the crack area in each case.

1. for the infinite case

$$\text{crack area} = 4 \cdot \frac{\pi b^2}{4} \cdot \frac{T}{c} = \pi b^2 \frac{T}{c}$$

2. for the fixed grips loading case

$$\text{crack area} = 2 a^2 T \frac{c}{\pi} \cdot \ln \cosh \left( \frac{\pi b}{ac} \right)$$

(see Appendix 1.2)

The relation between the crack area in each case and the crack length is shown in Fig. (2.10), while the ratio between the two areas and  $a/b$  is plotted in Fig. (2.11) for various values of "T". The fixed grips loading case was examined further adopting arbitrary values, equation (7) was used, except for the singular points, to calculate the stress distribution in a given net and then the value of the tension at each point was expressed as the vertical co-ordinates at that point, Fig. (2.12).

A closer examination of the stress distribution at the crack region is given in Fig. (2.13) while Fig. (2.14a,b, c) show the same stress distribution from different angles.

### 2.5. Comparability of the Two Solutions

\* For the case of fixed grips loading:

$$\omega(z) = - \frac{Tai}{\pi} \cosh^{-1} \left[ \frac{\cosh \left( \frac{\pi z}{a} \right)}{\cosh \left( \frac{\pi b}{ac} \right)} \right]$$

as  $a \rightarrow \infty$

$$\therefore \omega(z) = - \frac{Tai}{\pi} \cosh^{-1} \left[ \frac{1 + \frac{1}{2} \left( \frac{\pi z}{a} \right)^2}{1 + \frac{1}{2} \left( \frac{\pi b}{ac} \right)^2} \right]$$

$$= - \frac{Tai}{\pi} \cosh^{-1} \left[ 1 + \frac{1}{2} \frac{\pi^2}{a^2} \left( z^2 - \frac{b^2}{c^2} \right) \right]$$

$$\therefore \cosh^{-1} (1 + K) = Y \quad \therefore \cosh Y = 1 + K = 1 + \frac{Y^2}{2}$$

$$\therefore Y = \sqrt{2K}$$

$$\therefore \omega(z) = - \frac{Tai}{\pi} \left[ \frac{\pi}{a} \left( z^2 - \frac{b^2}{c^2} \right)^{\frac{1}{2}} \right]$$

$$\therefore \omega'(z) = - Ti \left( z^2 - \frac{b^2}{c^2} \right)^{\frac{1}{2}}$$

$$\text{where } z = \frac{x}{c} + iy$$

which is the solution for the infinite case.

\* for the finite or fixed grips loading case

$$\text{crack area} = 2 a^2 \frac{T}{\pi} C. \quad \text{In } \cosh \left( \frac{\pi b}{ac} \right)$$

as  $a \rightarrow \infty$

$\left( \frac{\pi b}{ac} \right)$  becomes very small

$$\therefore \ln \cosh(x) = \ln \cos(ix)$$

$$\ln |\cos x| = -\frac{x^2}{2} - \frac{x^4}{12} - \frac{x^6}{45} \dots$$

$$\therefore \text{for very small } x \quad \therefore \ln |\cos x| = -\frac{x^2}{2}$$

$$\therefore \text{as } a \rightarrow \infty$$

$$\therefore \ln \cosh\left(\frac{\pi b}{ac}\right) = \ln \cos\left(\frac{i\pi b}{ac}\right) = +\frac{\pi^2 b^2}{2a^2 c^2}$$

$$\therefore \text{crack area} = 2 a^2 \frac{T C}{\pi} \left[ \frac{\pi^2 b^2}{2 a^2 c^2} \right]$$

$$= \pi b^2 \frac{T}{c} = \text{crack area for the infinite boundary case.}$$

## 2.6. Crack Propagation and the Fracture Toughness Value

Adopting the concept of Griffith's energy balance theory, which states that unstable propagation of a crack takes place if an increment of crack growth results in more stored energy being released than is absorbed by the creation of the new crack surface, and accounting for all energy terms which vary during a crack growth.

$$\therefore u = (W_L + W_r) + W_s + K$$

where  $u$  : The total energy of the system

$W_L$  : Work done by the external forces due to a crack growth

$W_r$  : Strain energy released

$W_s$  : Energy absorbed in the fracture process

$K$  : Energy independent of crack presence

and the expression giving the stability of the new crack system is;

$$\frac{\partial u}{\partial(2b)} = \frac{\partial u}{\partial b} = 0$$

where  $b$  : half the crack length.

Applying this energy concept to the two cases under consideration.

### 2.6.1. Infinite boundary case

$$W_L = 0$$

$$W_r = -4 \int_0^b \frac{1}{2} V_o \phi \, dx = -\frac{1}{2} V_o (\text{area of the crack})$$

$$= -2 V_o \left[ \frac{\pi}{4} b \frac{Tb}{c} \right]$$

$$\text{where } T = \frac{V_o}{AE}, \quad C = \left[ \frac{T_o h}{AE L_o} \right]^{\frac{1}{2}}$$

$$\therefore W_r = -\frac{\pi}{2} b^2 \frac{V_o^2}{AE} \frac{1}{c}$$

$$W_s = 2 b \gamma$$

where  $\gamma$  : the force required to produce a unit length crack extension

or

fracture toughness value

$$\therefore u = -\frac{\pi b^2}{2} \frac{V_o^2}{AE} \frac{1}{c} + 2b\gamma + k$$

and for stable equilibrium

$$\frac{\partial u}{\partial b} = 0$$

$$\therefore \frac{\partial u}{\partial b} = 2\gamma - \frac{\pi b}{AE} V_o^2 \frac{1}{c}$$

$$\therefore 2\gamma = \frac{\pi b}{AE} \frac{V_o^2}{c}$$

$$\therefore V_o = \left[ \frac{2\gamma AE}{\pi} C \right]^{\frac{1}{2}} \frac{1}{(b)^{\frac{1}{2}}} \quad (8)$$

$$\text{where } c = \left[ \frac{T_o h}{AE L_o} \right]^{\frac{1}{2}}$$

This equation gives the relation between the critical tension and half the crack length for uncoated nets under biaxial tension applied at infinity.

For coated fabrics, an approximate solution can be obtained by adding the term " $G S^2 Y_k$ " in the difference equation (5) to account for the effect of coating, where "G": the shear modulus of the coating material and following the same procedures, we obtain the desired relation in a form identical to equation (8) but with c having a modified value equals

$$\left[ \frac{T_o h + G h^2}{A E L_o} \right]^{\frac{1}{2}}$$

$$\therefore V_o = \left[ \frac{2\gamma}{\pi} A E c \right]^{\frac{1}{2}} \frac{1}{(b)^{\frac{1}{2}}}$$

$$\therefore V_o = \left\{ \frac{2\gamma}{\pi} A E \left( \frac{T_o h + G h^2}{A E L_o} \right)^{\frac{1}{2}} \right\}^{\frac{1}{2}} \frac{1}{(b)^{\frac{1}{2}}} \quad (8a)$$

#### 2.6.2. "Fixed grips loading" case

$$W_L = 0$$

$$W_r = -4 \int_0^b \frac{1}{2} V_o \phi \, dx$$

$$= -2 V_o \int_0^b \frac{T_a}{\pi} \cos^{-1} \left[ \frac{\cosh \left( \frac{\pi x}{ac} \right)}{\cosh \left( \frac{\pi b}{ac} \right)} \right] dx$$

This integration cannot be evaluated directly\*, but since we require the partial derivative of  $W_r$  with respect to b, i.e.  $\frac{\partial W_r}{\partial b}$

$$\therefore \frac{\partial W_r}{\partial b} = -2 V_o \frac{T_a}{\pi} \left\{ \frac{\partial}{\partial b} \left[ \int_0^b \cos^{-1} \left[ \frac{\cosh \left( \frac{\pi x}{ac} \right)}{\cosh \left( \frac{\pi b}{ac} \right)} \right] dx \right] \right\}$$

\* see Appendix(1.3)

$$\therefore \frac{\partial}{\partial b} \left[ \int_0^b f(x,b) dx \right] = f(b,b) + \int_0^b \frac{\partial f(x,b)}{\partial b} dx$$

$$\therefore \frac{\partial}{\partial b} \left\{ \int_0^b \cos^{-1} \left[ \frac{\cosh \left( \frac{\pi x}{ac} \right)}{\cosh \left( \frac{\pi b}{ac} \right)} \right] dx \right\} = \cos^{-1} \left[ \frac{\cosh \left( \frac{\pi b}{ac} \right)}{\cosh \left( \frac{\pi b}{ac} \right)} \right]$$

$$+ \tanh \left( \frac{\pi b}{ac} \right) \int_0^b \frac{\cosh \left( \frac{\pi x}{ac} \right) \frac{\pi}{ac} dx}{\sqrt{\cosh^2 \left( \frac{\pi b}{ac} \right) - \cosh^2 \left( \frac{\pi x}{ac} \right)}}$$

$$= \frac{\pi}{2} \tanh \left( \frac{\pi b}{ac} \right)$$

$$\frac{\partial u}{\partial b} = \frac{dW_r}{\partial b} + \frac{\partial W_s}{\partial b} = 0$$

$$\therefore \frac{\partial W_r}{\partial b} = -2 V_o \frac{Ta}{\pi} \left\{ \frac{\pi}{2} \tanh \left( \frac{\pi b}{ac} \right) \right\}$$

$$\frac{\partial W_s}{\partial b} = 2\gamma$$

$$\therefore 2\gamma = V_o Ta \tanh \left( \frac{\pi b}{ac} \right)$$

$$\therefore V_o^2 = \frac{2 \gamma AE}{a \tanh \left( \frac{\pi b}{ac} \right)} \quad (9)$$

$$\text{where } c = \left[ \frac{T_o h}{AE L_o} \right]^{\frac{1}{2}}$$

Equation (9) yields the relation between the critical tension and half the crack length for uncoated nets under biaxial tension exerted by fixed grips.

As before, Equation (9) can be used to give an approximate solution for the case of coated fabrics, but in this case  $c$  have a modified

value equals

$$\left[ \frac{T_0 h + G h^2}{A E L_0} \right]^{\frac{1}{2}}$$

It can be seen that in both the infinite boundary case and the fixed grips loading case, the value of the second derivative of the total energy system with respect to half the crack length "b" is negative. Which means that the system energy is a maximum at equilibrium, thus the equilibrium is said to be unstable. That is to say, if the applied boundary forces exceeds the critical level then spontaneous crack propagation will occur leading to the complete failure of the structural net.



### 2.6.3 Recommended test for calculating the fracture toughness value " $\gamma$ " and the shear modulus of coated fabric " $G$ "

For the general infinite boundary case the crack shape was given as an ellipse (2.3.2)

$$\frac{\phi^2}{\frac{Tb}{c}} + \frac{x^2}{b^2} = 1$$

$$\text{where } T = \frac{V_0}{AE} \text{ and } c = \left\{ \frac{T_0 h + G h^2}{AE L_0} \right\}^{\frac{1}{2}}$$

and the crack starts to propagate when

$$V_0 = \left\{ \frac{2\gamma}{\pi} AE \left[ \frac{T_0 h + G h^2}{AE L_0} \right]^{\frac{1}{2}} \right\}^{\frac{1}{2}} \cdot \frac{1}{(b)^{\frac{1}{2}}}$$

$$b \cdot V_0^2 = \frac{2\gamma}{\pi} AE \left\{ \frac{T_0 h + G h^2}{AE L_0} \right\}^{\frac{1}{2}}$$

substituting in the crack shape equation and taken  $X = 0$

$$\phi^2 = \frac{2\gamma}{\pi AE} \left\{ \frac{AE L_0}{T_0 h + G h^2} \right\}^{\frac{1}{2}} \cdot b$$

$$\phi^2 = \text{constant} \cdot b$$

similarly an equation giving the relation between the length and max width of the crack at failure can be obtained for the fixed grips case. But what is really important about the two equations mentioned above is that they yield a simple expression for the fracture toughness value " $\gamma$ " by solving them together i.e.

$$b \cdot V_0^2 \cdot \phi^2 = \left( \frac{2\gamma}{\pi} \right)^2 \cdot b$$

$$\therefore \gamma = \frac{\pi}{2} V_0 \cdot \phi$$

This equation means that the value of the fracture toughness " $\gamma$ " can simply be evaluated from a biaxial tear propagation test in which only the critical boundary tension and the corresponding max value for the crack opening needs to be determined, provided that in such a test the crack length must be relatively small to simulate infinite boundary conditions.

The same two equations can be used to yield a useful expression giving the value of the shear modulus for coated fabrics " $G$ " as follows

$$\frac{b \cdot V_o^2}{\phi^2} = \frac{(AE)^2}{b} \left\{ \frac{T_o h + Gh^2}{AE L_o} \right\}$$

and since  $h \approx L_o$

$$\left[ \frac{b \cdot V_o}{\phi} \right]^2 = AE (T_o + Gh)$$

$$\therefore G = \left[ \frac{b \cdot V_o}{\phi} \right]^2 \cdot \frac{1}{AEh} - \frac{T_o}{h}$$

but to use this expression another value needs to be calculated from the suggested test, and that is the crack length

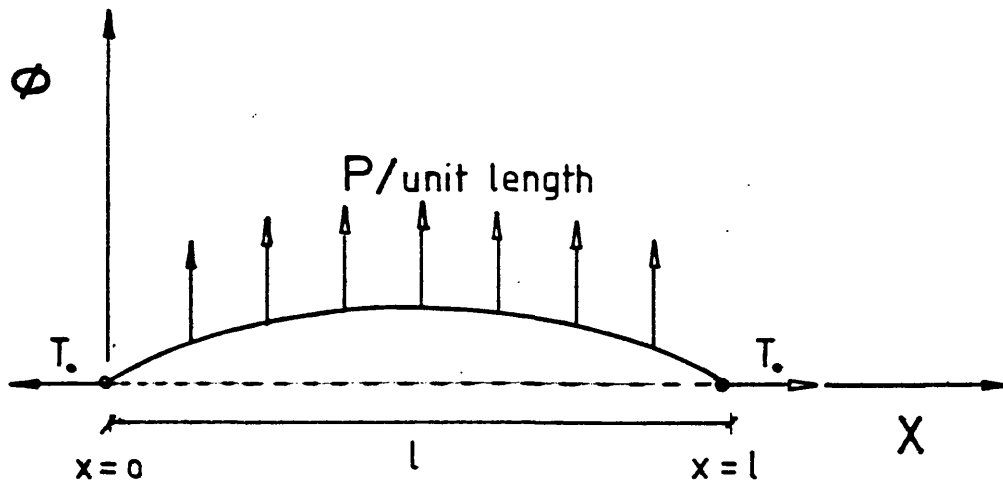


FIG (2-1)

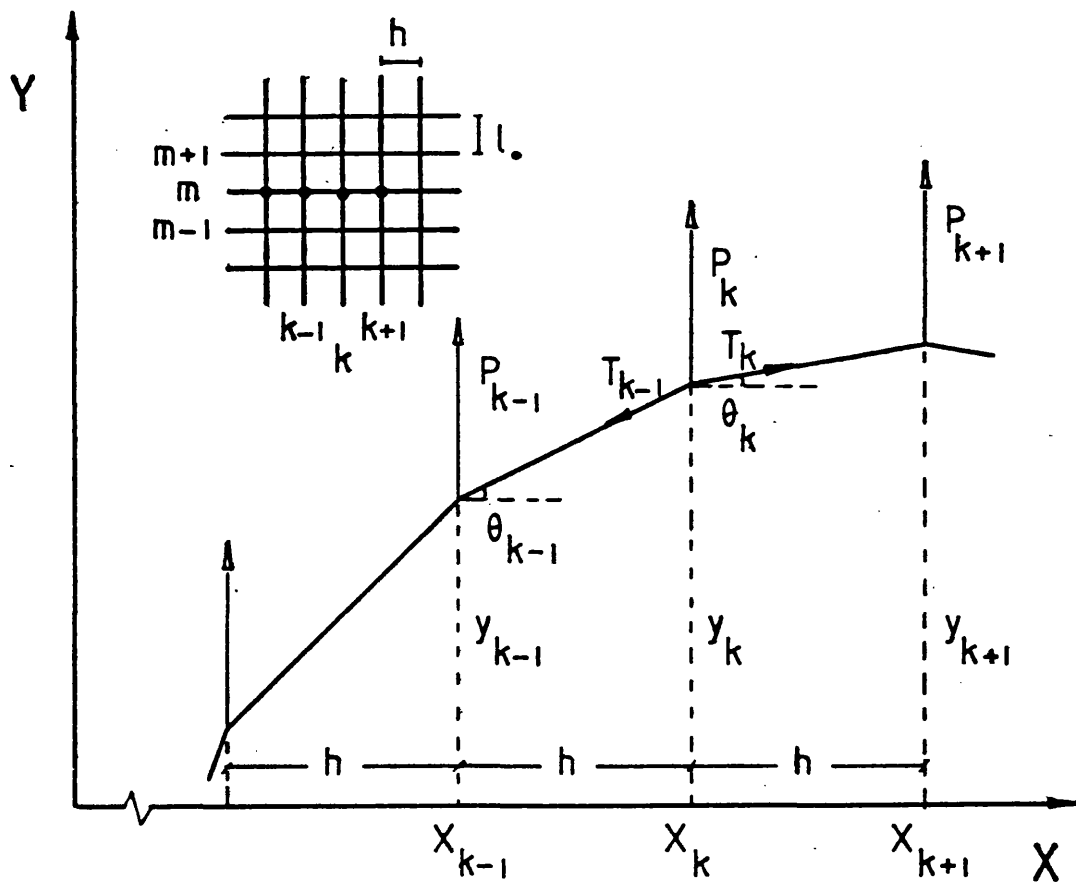


FIG (2-2)

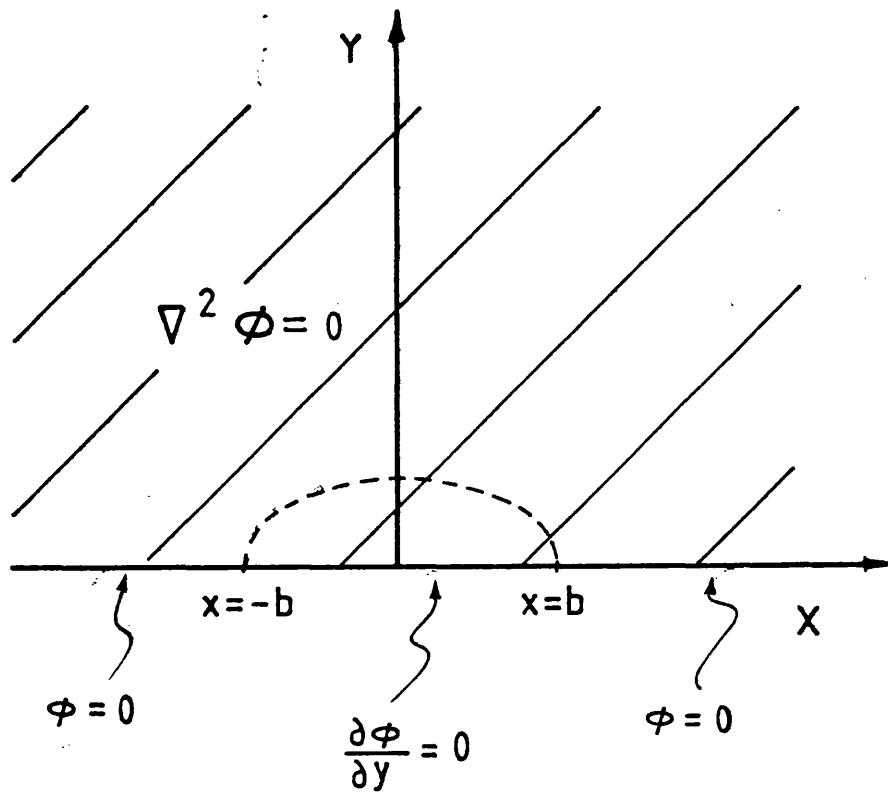
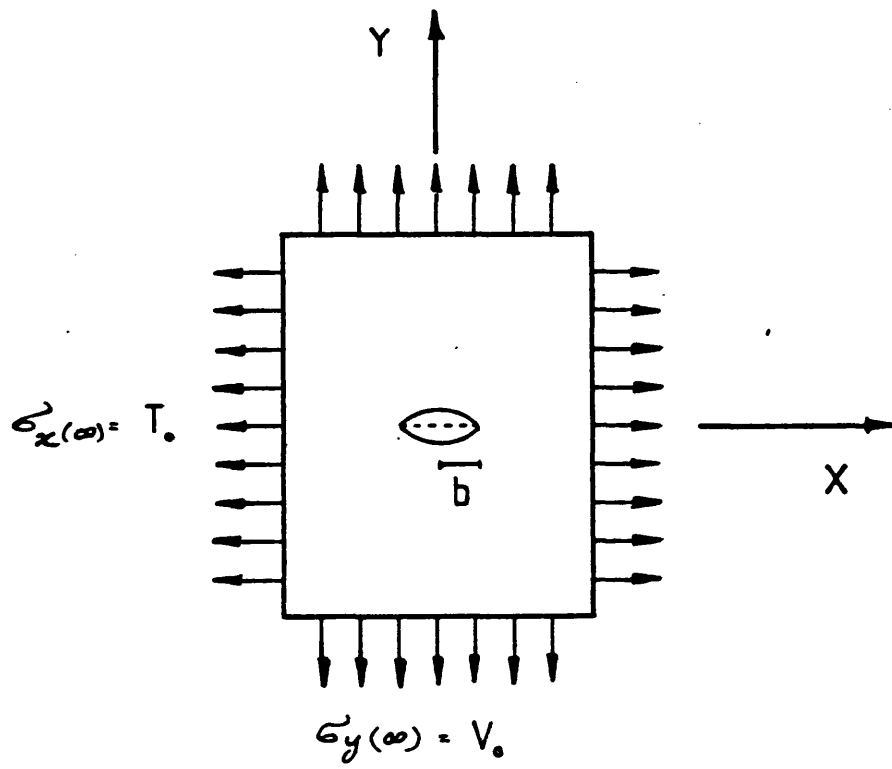
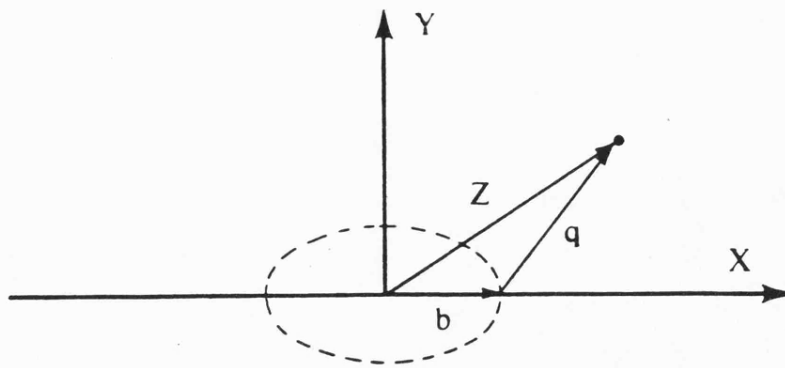


FIG ( 2.3 )



FIG(2.4)

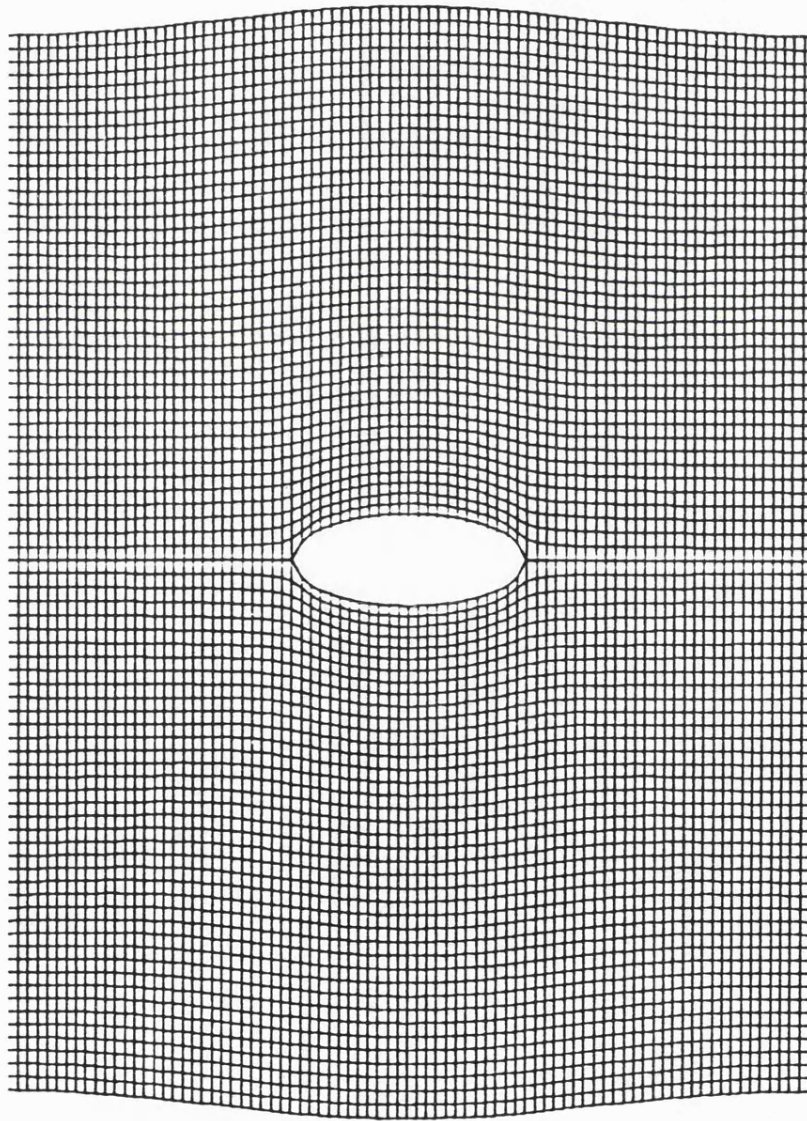


FIG (2.5)

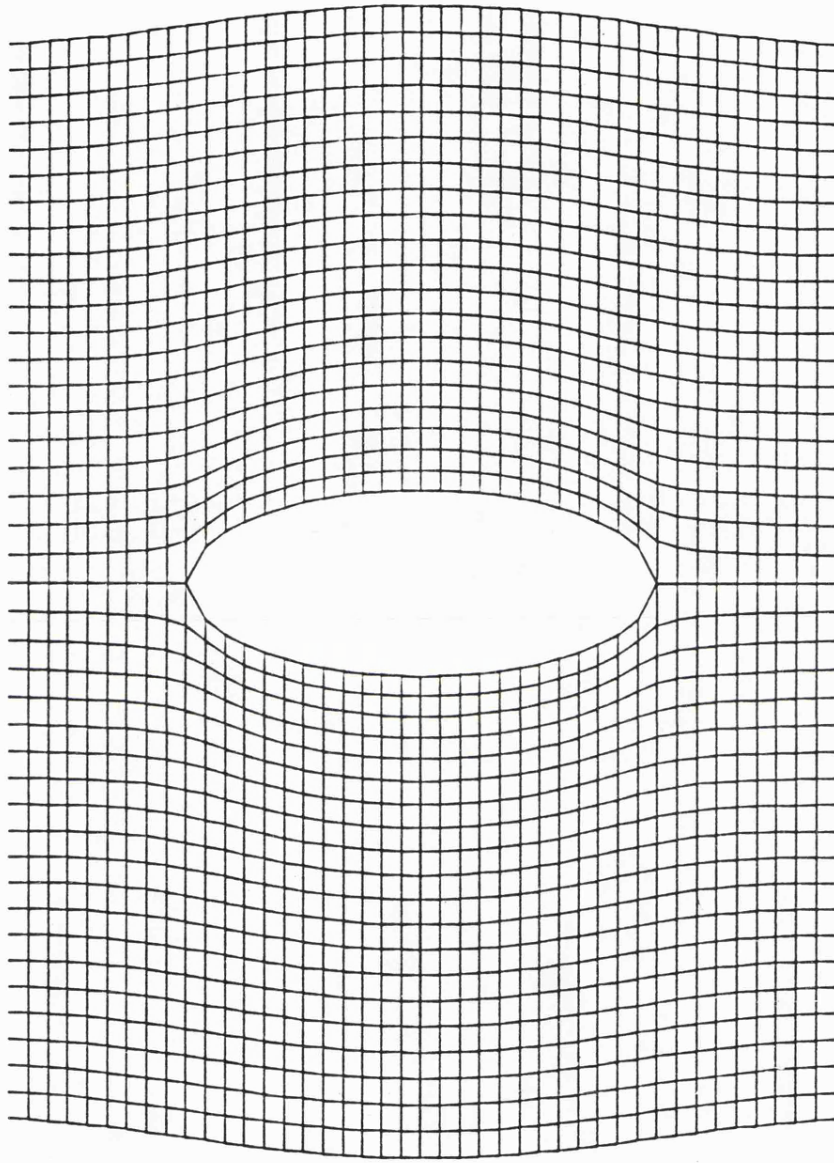
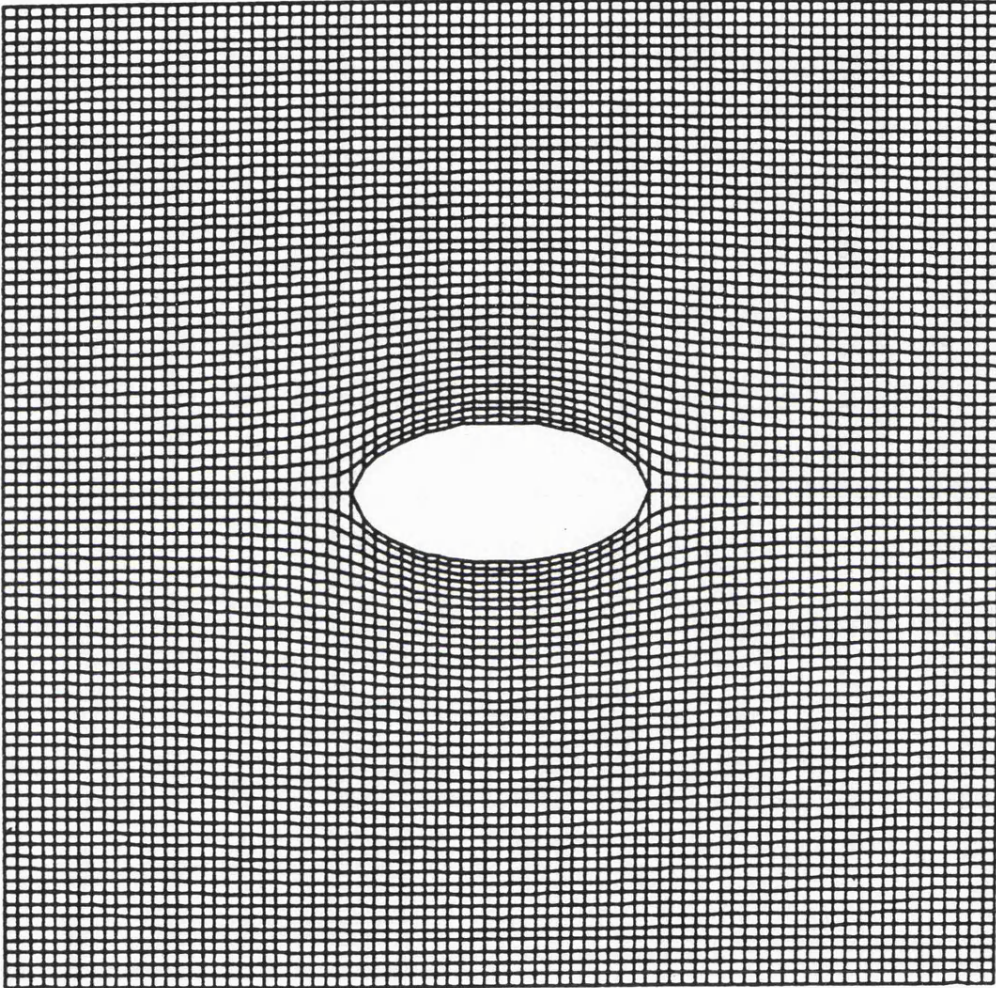


FIG (2.6)





FIG(2.7)

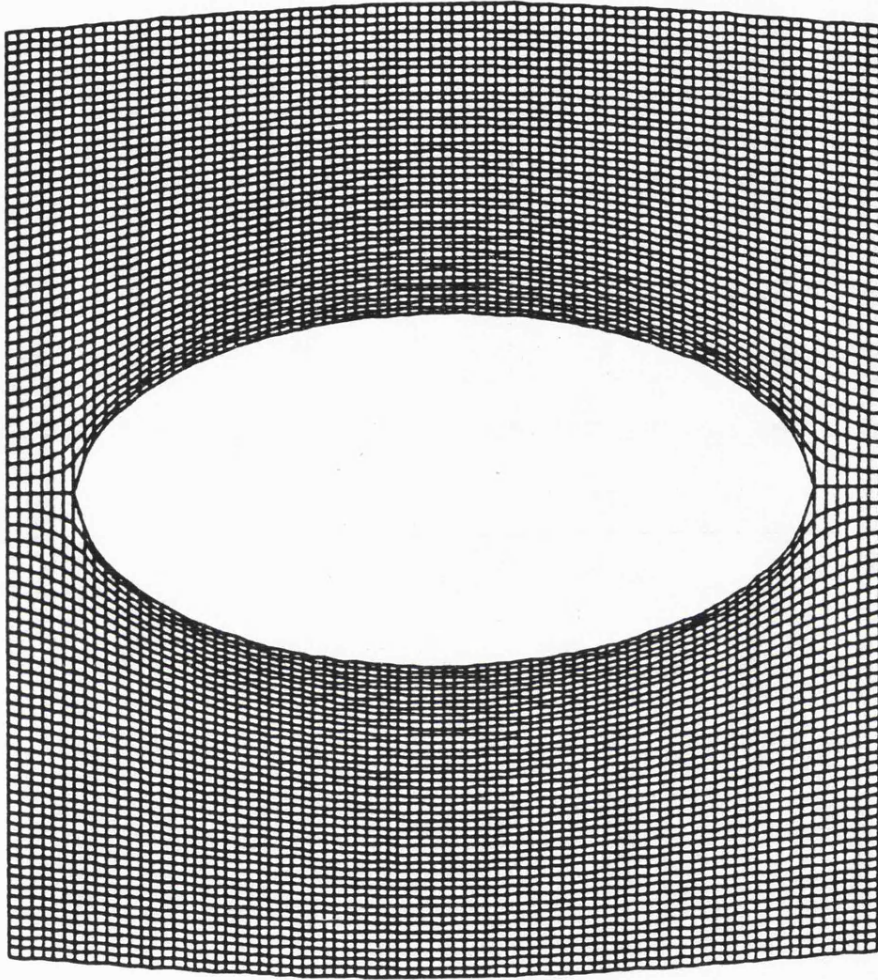
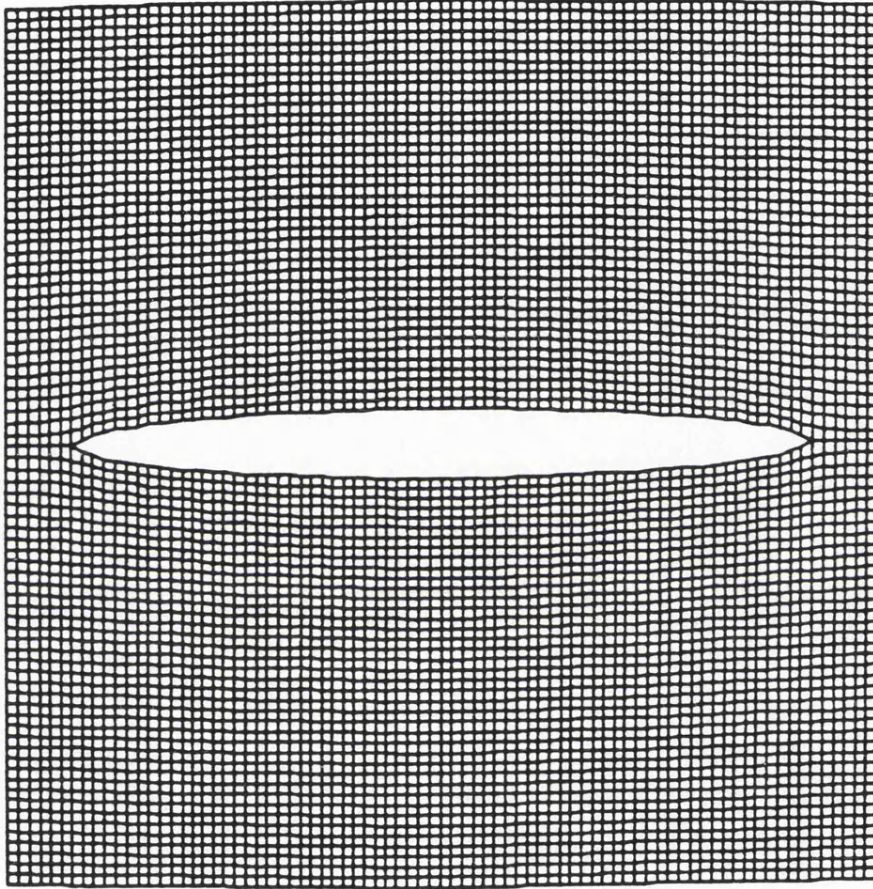
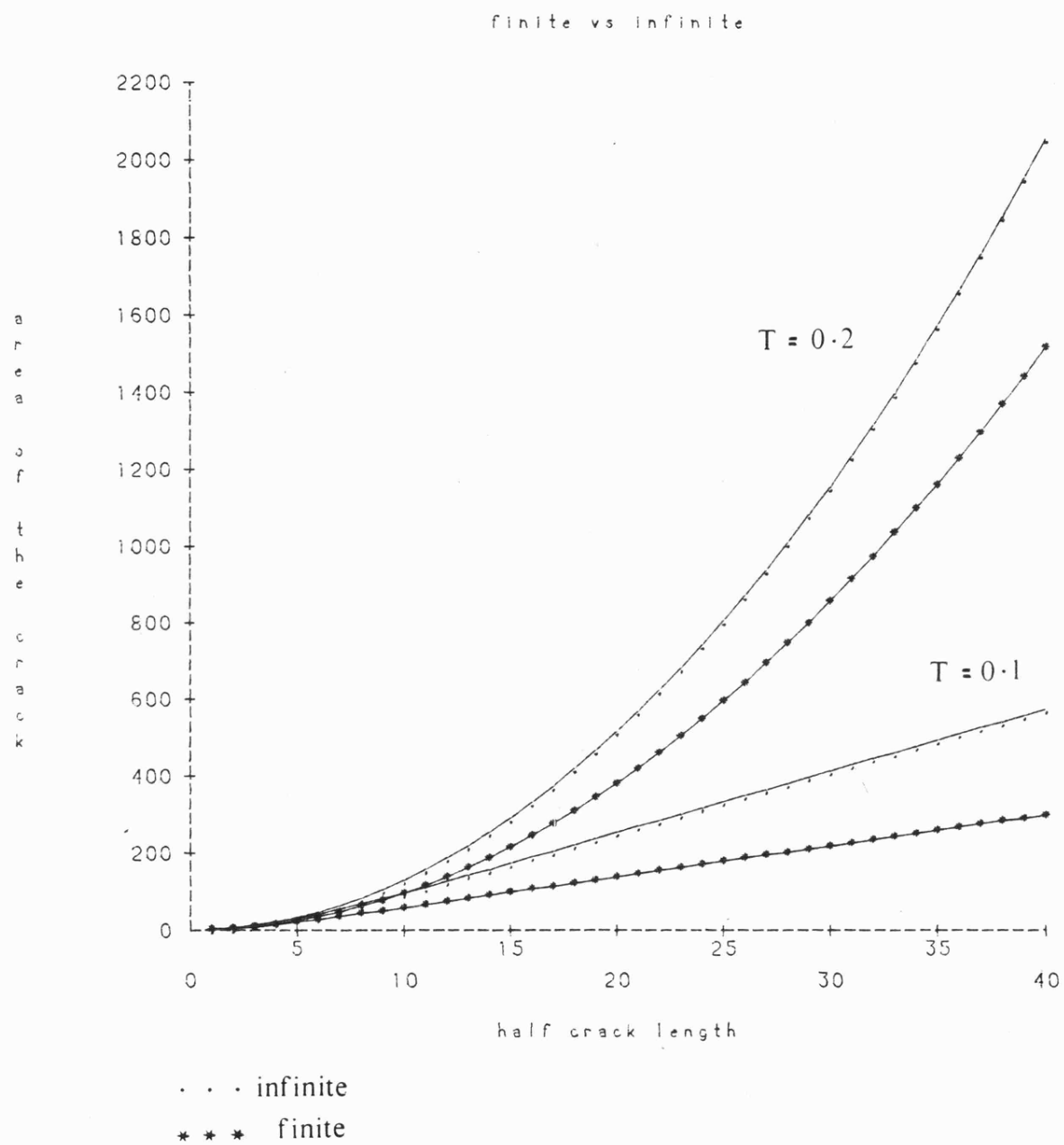


FIG (2.8)





FIG(2.9)



fig( 2.10)

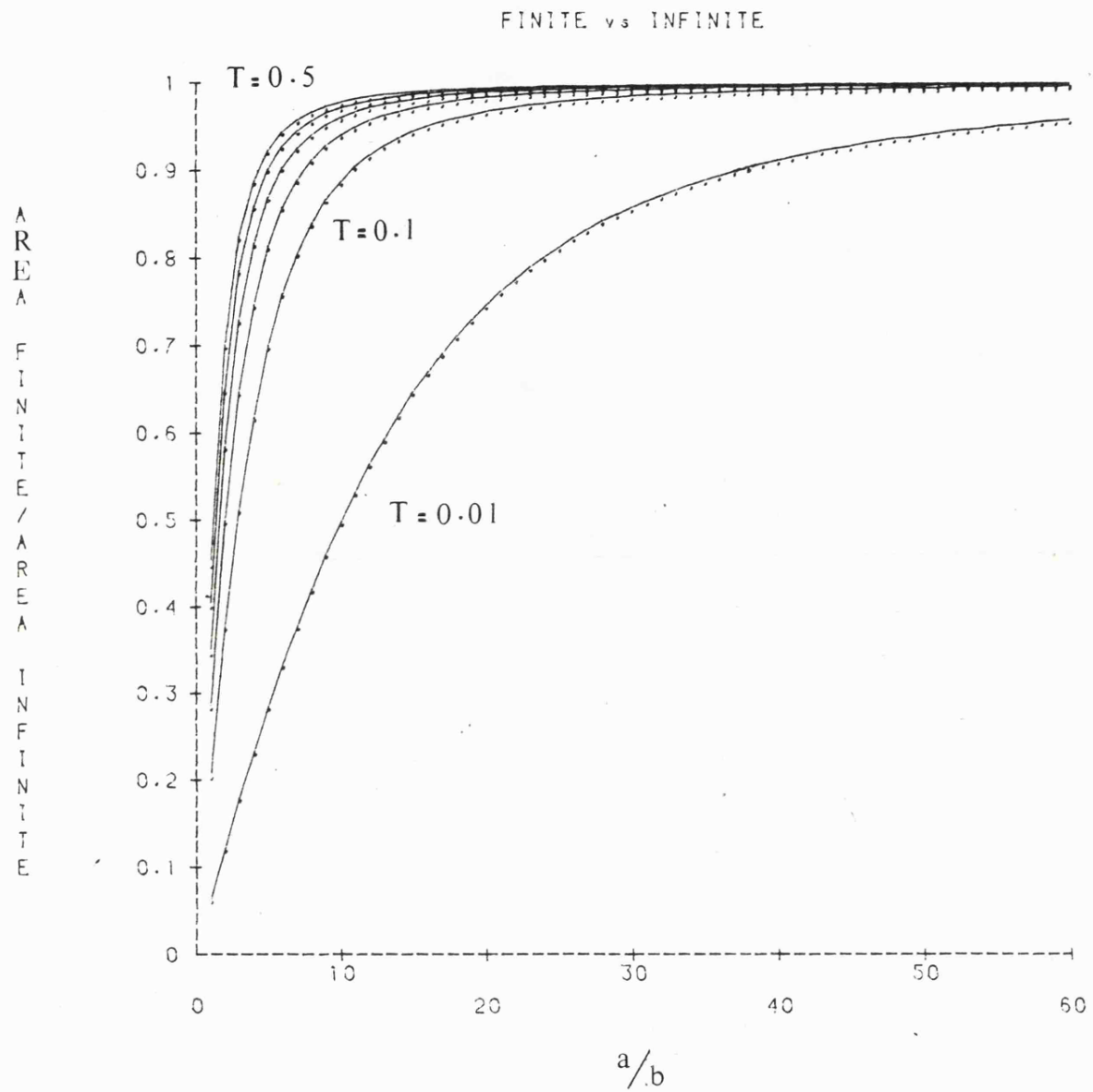
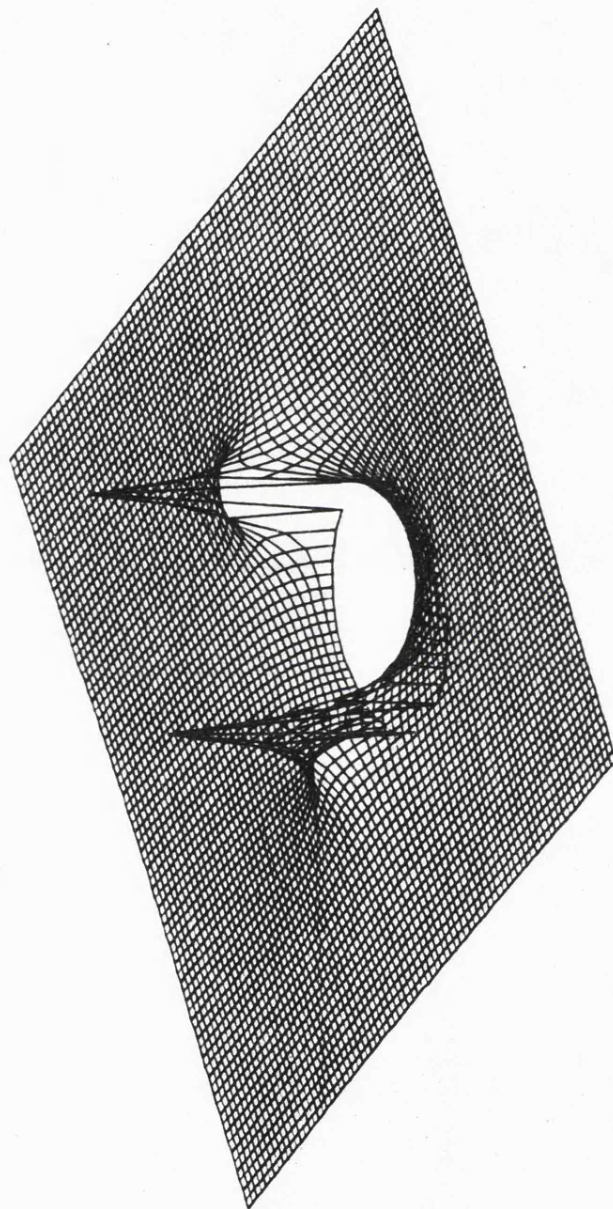
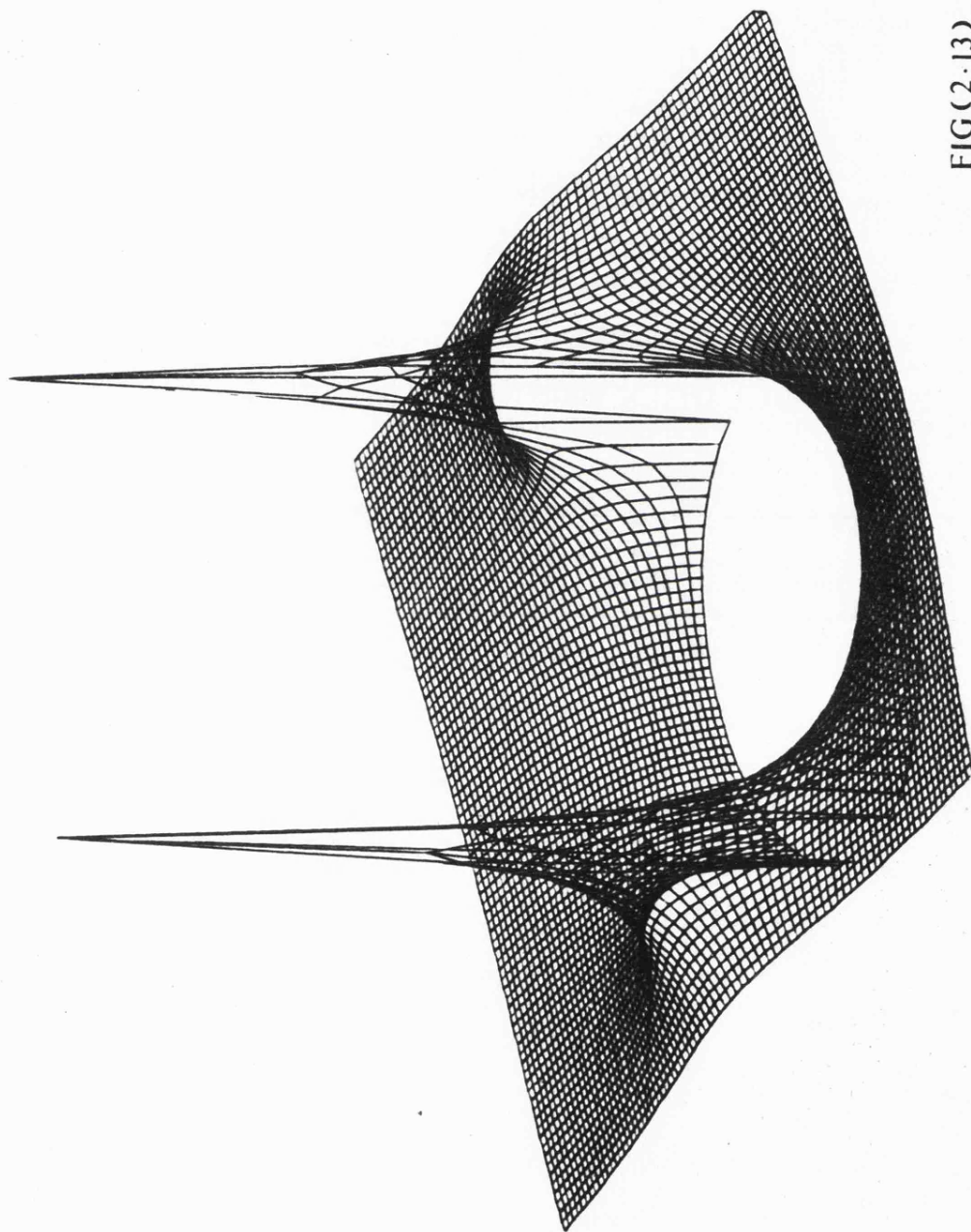


FIG (2-11)

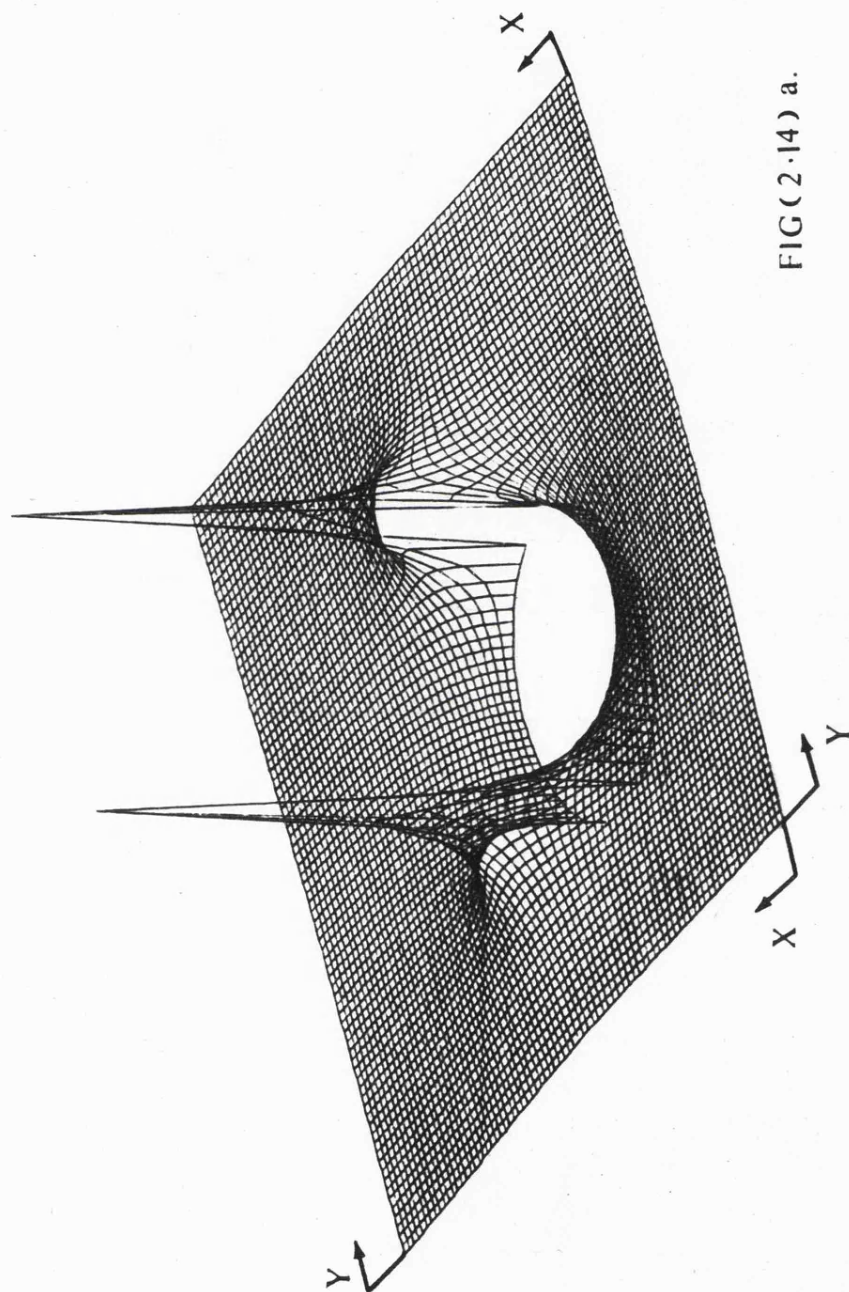


FIG(2.12 )



FIG(2-13)





FIG(2.14) a.

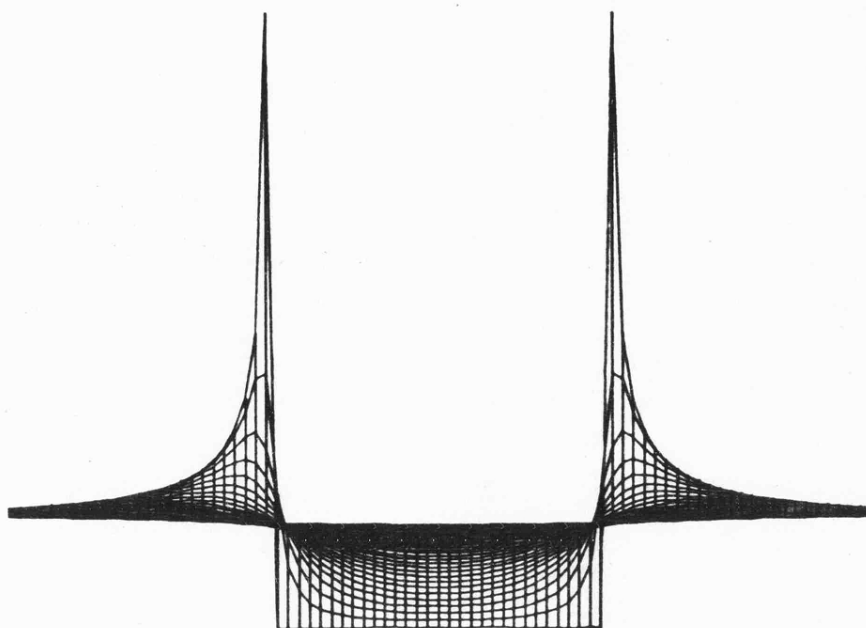


FIG (2.14)b. section X-X

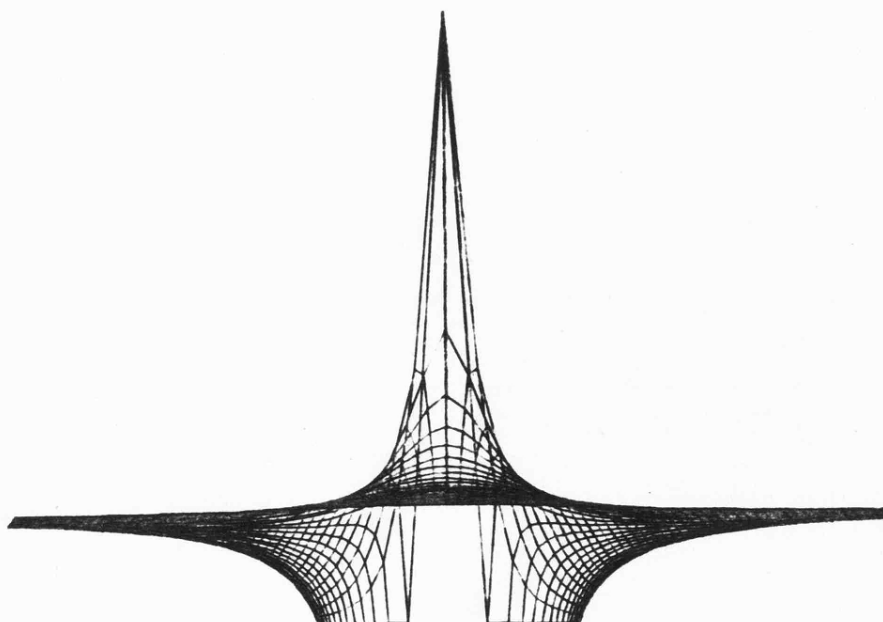


FIG (2.14)c. section Y-Y

### CHAPTER 3

DISCUSSION AND COMPARISON WITH  
PREVIOUS WORK



## CHAPTER 3

### DISCUSSION AND COMPARISON WITH PREVIOUS WORK

#### 3.1. Influence of Stress Fields Biaxiality on the Crack Propagation Behaviour

To appreciate the significance of the proposed solution, it would be better to try and cast some light on the boundary separating a structural net from a homogeneous material through investigating some atomistic aspects of crack propagation in brittle solids. After all in fracture, as in any thermodynamic process, the final answers should be sought at the atomic or molecular level, for it is the nature of the cohesive bonding between the constituent atoms in solids which ultimately determines the resistance to the propagation of the crack (21).

While an atomistic approach provides physical insight into the problem, it inevitably involves greater complication in analysis specially in crack systems with its added configurational complexity, so simplifying assumptions must be made in order to achieve some structural model of a solid which can be used in the analysis.

Figures (3.1), (3.2) illustrates two models which have been subjected to a lattice-static analysis (21). In the first model (24) one-dimensional, the crack is depicted as two semi-infinite chains consisting of point atoms linked horizontally by bendable elements and vertically by stretchable elements, the chains are subjected to opening forces applied vertically at the free ends.

The second model (25), two dimensional, comprise an infinite square lattice of atoms linked by stretchable and bendable elements, with the crack centred horizontally at the origin.

The crack is opened by a vertical wedging force or by vertical tensile forces distributed uniformly at infinity.

The analysis assumes the simplest of force laws for the linking

elements, i.e. that the elements are hooked up to a critical breaking point, since the dominant factor is the interplay between adjacent bonds at the crack plane rather than the nature of the force law itself.

Considering the first model and using the co-ordinate system in Fig. (3.3) for the  $j$ th atom to calculate the total energy of the crack system for the case of infinite boundary. The energy components are:

1. Work of external forces " $U_L$ "

$$U_L = -2Fu_o \quad (j = 0)$$

2. Shear strain energy in bendable elements " $W_s$ "

The bonds at atom " $j$ " are bent through an angle

$$\theta_j = \text{shear strain at } j = \theta_{j,j+1} - \theta_{j,j-1}$$

$$\approx \tan \theta_{j,j+1} - \tan \theta_{j,j-1} \quad (\text{small angle approximation})$$

$$= (u_{j+1} - u_j)/a_o - (u_j - u_{j-1})/a_o = (u_{j+1} - 2u_j + u_{j-1})/a_o$$

$$\therefore W_s = 2\left(\frac{1}{2} \alpha a_o^2 \theta_j^2\right) = \alpha(u_{j+1} - 2u_j + u_{j-1})^2$$

$$(1 \leq j \leq \infty)$$

where " $\alpha$ " is the shear stiffness constant.

3. Separation energy of stretchable elements

The bonds at atom " $j$ " are stretched through " $2u_j$ ", and the broken bonds are the ones who have exceeded some critical displacement " $2u_c$ ".

$$\text{Separation energy} = \frac{1}{2} \beta (2u_c)^2 \quad (1 \leq j < n)$$

$$= \frac{1}{2} \beta (2u_j)^2 \quad (n \leq j \leq \infty)$$

Where " $n$ " identifies the crack-tip bond and " $\beta$ " is the stiffness constant for stretching.

The total system energy (ignoring kinetic terms)

$$U = \alpha \sum_{j=1}^{\infty} (u_{j+1} - 2u_j + u_{j-1})^2 \\ + 2(n-1) \beta u_c^2 + 2\beta \sum_{j=n}^{\infty} u_j^2 - 2Fu_o$$

This equation incorporates the boundary conditions.

And for stable equilibrium

$$\frac{\partial U}{\partial u_j} = 0 \quad (0 \leq j \leq \infty)$$

which gives an infinite set of fourth-order, linear difference equations (the analogue of the differential equations of equilibrium for a linear elastic continuum). And it can be seen that the fourth-order terms are resulting from the shear strain energy, and that is why the governing eqm. equation for thin sheets of homogeneous isotropic material under plane stress is the biharmonic equation:

$$\nabla^4 \phi = 0$$

While in a structural net, with its shear-lag nature, the governing eqm. equation is the harmonic or Laplace's equation:

$$\nabla^2 \phi = 0$$

Now, observing the proposed solution for the infinite net cases (uncoated), which is given by:

$$V_o = \left[ \frac{2\gamma}{\pi} \left( \frac{AE h T_o}{L_o} \right)^{\frac{1}{2}} \right]^{\frac{1}{2}} \frac{1}{(b)^{\frac{1}{2}}}$$

in a biaxial stress field (i.e.  $T_o \neq 0$ ).

When  $T_o$  is not linearly related to  $V_o$  (i.e.  $T_o \neq \lambda V_o$ ) the equation becomes:

$$V_o = \frac{K}{(b)^{\frac{1}{2}}}$$

which is similar to that obtained for homogeneous isotropic materials under uniaxial tension uniformly distributed at infinity.

This should be expected, and is due to the influence of the biaxiality of the stress field.

Because once the value of " $T_o$ " exceeds zero, this means a reduction in the cable's (yarns) ability to rotate relative to each other to share the load, it is in effect an introduction of a shear resistance in the net, and the higher the  $T_o$  value, the higher the shear stiffness introduced. Once a shear stiffness, independent of  $V_o$ , is introduced in the net, the situation becomes similar to that of the atomistic model and so, it would be reasonable to expect a crack propagation behaviour similar to that of a homogeneous isotropic material.

When  $T_o$  is linearly related to  $V_o$  (i.e.  $\lambda = \text{constant}$ ) the equation relating the critical tension to half the crack length " $b$ " becomes:

$$V_o = \frac{K}{(b)^{2/3}}$$

### 3.2. Correlation Between Topping's Work (12) and the Proposed Solution for Coated Fabrics Subjected to a Biaxial Stress Field

The proposed solution given by Equation (8a) can be written in the form:

$$v_o^4 b^2 = \left(\frac{2\gamma}{\pi}\right)^2 AE [T_o + Gh]$$

which gives a straight line equation as shown in Fig. (3.4).

$$\text{where } m = \left(\frac{2\gamma}{\pi}\right)^2 AE$$

$$K = m.Gh$$

As mentioned earlier, Topping compared the following theories:

1. Modified Griffith theory.
2. Elementary fabric theory.
3. Hedgepeth's stress concentration factor.
4. Deaton's fracture mechanics approach.

Which predicts the burst strength of longitudinally slit pressurised fabric cylinders, with tests of warp cylinders having various diameters and lengths, and containing slits of various lengths and widths.

Topping came to the conclusion that, the only theory that fits the data very well, is the modified Griffith theory, requiring three empirical constants, and given in the form:

$$pr = \frac{40.6}{l^{0.65} \left(1 + 0.76 \frac{l}{r}\right)}$$

where  $pr$  = failure stress

$l$  = crack length

$r$  = cylinder's radius

and in which the term  $\left(1 + 0.76 \frac{l}{r}\right)$ , cylinder curvature factor, was introduced to account for the additional stress concentration due to the local effect of the pressure acting normal to the sheet in the region of the slit.

For a flat net this equation can be written as:

$$V_o = \frac{K}{b^{0.65}} \quad \text{where } b = \frac{l}{2}$$

which is almost identical to the proposed equation for uncoated fabrics (i.e. for  $G = 0$ ) given as;

$$V_o = \frac{K}{\{b\}^{2/3}} = \frac{K}{b^{0.666}}$$

but since Topping's experimental work was conducted on coated fabrics, this meant that, in order that the proposed relation, Fig. (3.4), be valid, plotting Topping's experimental results on the same axis as in Fig. (3.4) had to give a straight line relation which passes through or close to the origin, indicating that the coating had no or little effect on the tear propagation behaviour of the warp cylinders, thus explaining why as a result a relation almost identical to that predicted for uncoated fabrics was obtained.

Figure (3.5) shows the plotting of Topping's results, and it can be seen that the relation obtained is almost a straight line passing through the origin, thus confirming the validity of the proposed solution.

3.3. Comparison Between Racah's Experimental Work (15)  
and the Proposed Solution for Coated Fabrics  
Under a Uniaxial Stress Field

Experimental work was conducted by Racah to determine an empirical relation between the critical boundary tension and the crack length for PVC coated polyester fabrics subjected to a uniaxial stress field.

In interpreting his results Racah concluded that the required relation is given by:

$$V_o = \frac{K}{(b)^n} = \frac{5}{(b)^{0.44}} \quad (\text{warp direction})$$

$$V_o = \frac{4.8}{(b)^{0.39}} \quad (\text{weft direction})$$

The proposed relation in the present work gives the value of the exponent "n" in both directions to be  $n = 0.5$ , and in order to investigate the reason for this contradiction, Racah's results were examined thoroughly. The results are given in Table (3.1) while Table (3.2) shows a comparison between the value of the constant "K", in the warp direction, obtained by adopting an exponent value  $n = 0.44$  and  $n = 0.5$  and also a similar comparison for the weft direction.

The straight line relation:

$$\log(V_o) = -n \log(b) + \log(k)$$

was also plotted in Fig. (3.6) to investigate which value for the exponent "n" would give a better fit for the experimental results.

It is arguable which of the two exponent values should be considered to give a more accurate representation for the results.

Racah in interpreting his results calculated the value of the exponent "n" as the average value of the five test results, but it

can be argued that putting more emphasis in calculating the value of the exponent on the last three tests in which the length of the crack ranged between 4 cm  $\rightarrow$  10 cm would be more accurate, since the error accumulated in achieving these three results is less than in the other two.

The author tends to favour the later view, specially since these crack lengths were measured after the test by examining the torn specimen.



### 3.4. Comparison Between Minami's Work (9) and the Proposed Solution for Coated Fabrics Under a Uniaxial Stress Field

Minami's expression for the fracture toughness of coated fabrics

$$\gamma = \frac{\pi}{8 \sqrt{E_t G_t}} \left( 4b + \frac{1}{n_c} \right) V_o^2$$

gives the fracture toughness value " $\gamma$ " in terms of the critical tension " $V_o$ ", half the crack length " $b$ ", yarn count per unit length " $n_c$ ", shear modulus of coated fabric " $G_t$ " and Young's modulus of yarn " $E_t$ ".

When the distance between yarns  $\frac{1}{n_c} \ll b$  this expression becomes:

$$\gamma = \frac{\pi}{2} \frac{b V_o^2}{\sqrt{E_t G_t}}$$

Since Minami's expression was developed using Hedgepeth's influence function, which does not account for the effect of the finite boundaries, the proposed solution for the infinite boundary case was used to derive a corresponding expression for the fracture toughness as follows:

$$V_o = \left[ \frac{2\gamma}{\pi} c \right]^{\frac{1}{2}} \frac{1}{(b)^{\frac{1}{2}}}$$

$$\therefore \gamma = \frac{\pi}{2} \cdot \frac{b V_o^2}{c} \quad \text{where } c = \left[ \frac{AE}{L_o} h (T_o + Gh) \right]^{\frac{1}{2}}$$

for  $T_o = 0$

and in the case of a square mesh  $\therefore L_o = h$  and the fracture toughness value is given by:

$$\gamma = \frac{\pi}{2} \cdot \frac{b V_o^2}{\sqrt{AEGh}}$$

which is quite similar to that of Minami and where  $G$  : the shear modulus between yarns (depends on the method of coating, degree of coating penetration into the woven fabric structure, and the properties of the coating material), " $E$ " is Young's modulus for yarn,

and "A" is the cross-sectional area of the yarn.

As mentioned earlier, since the application of coating introduces shear stiffness independent of  $V_0$  and assumed to be constant in the net, both expressions show a crack propagation behaviour similar to that of a homogeneous material.

b [ mm ]	V <sub>o</sub> [ KN/m ]	
	warp	weft
8	40.0	31.1
12.5	34.7	26.6
20	28.8	23.4
31.5	23.1	19.3
50	18.0	14.8

TABLE (3.1)

b mm	Constant "K"			
	warp		weft	
	n = 0.44	n = 0.5	n = 0.39	n = 0.5
8	4.78	3.5777	4.7311	2.7817
12.5	5.046	3.8795	4.815	2.9739
20	5.15	4.0729	5.088	3.309
31.5	5.045	4.099	5.01	3.42
50	4.8174	4.025	4.60	3.31

TABLE (3.2)

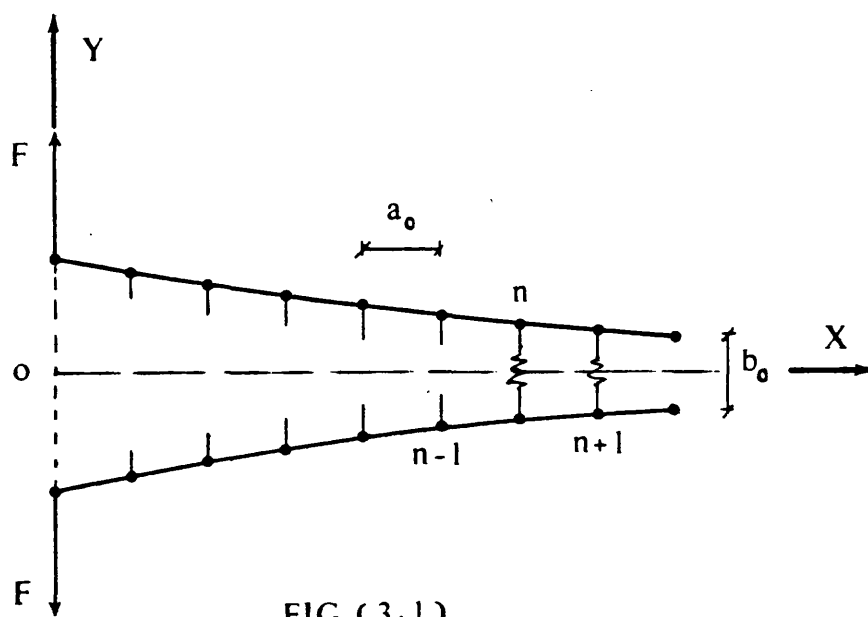


FIG (3.1)

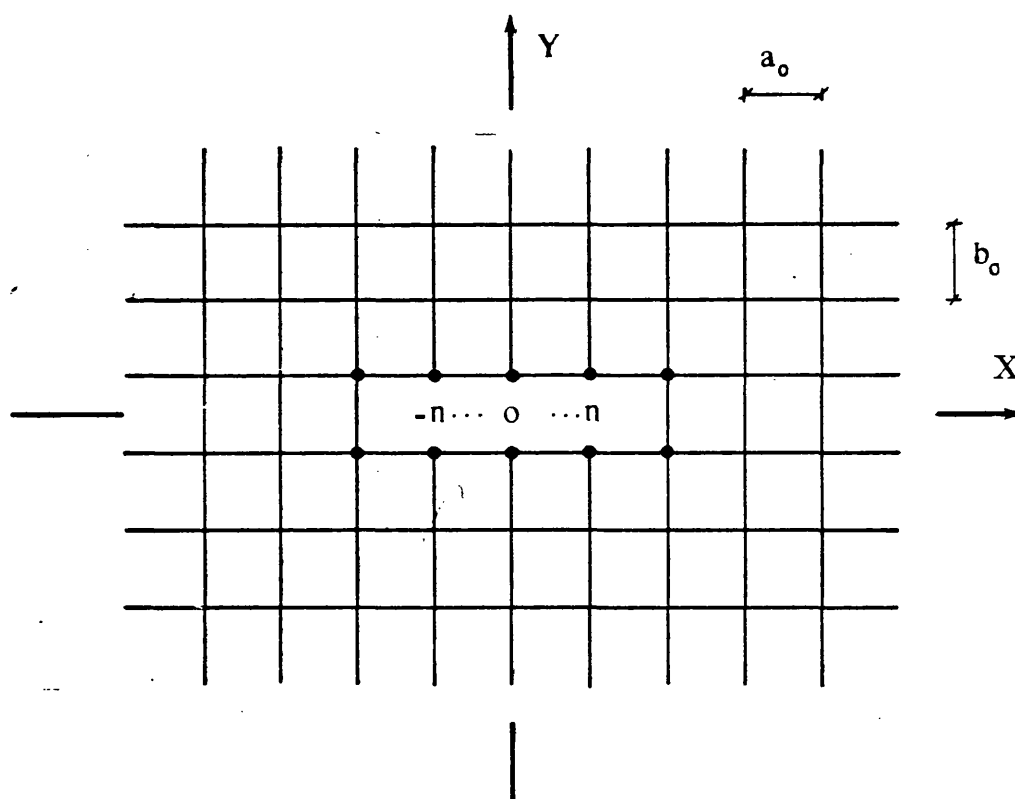
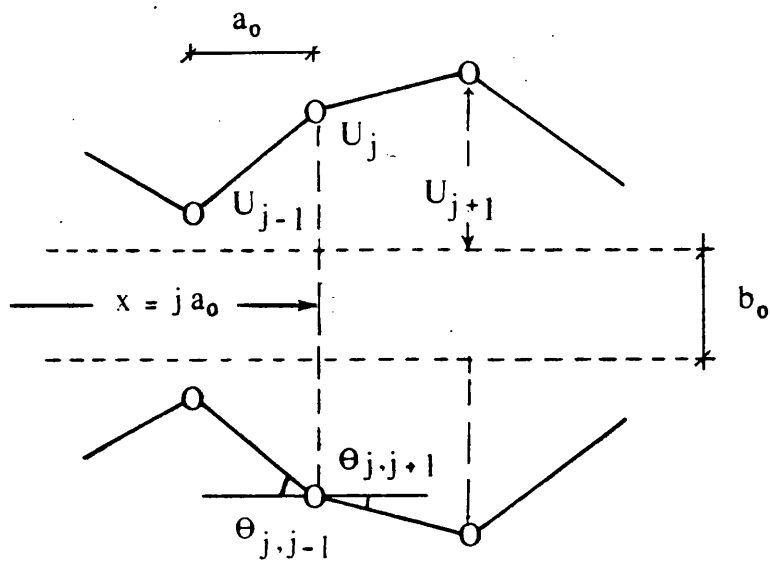


FIG (3.2)



FIG(3.3)

Coordinate system for atomistic models (21)

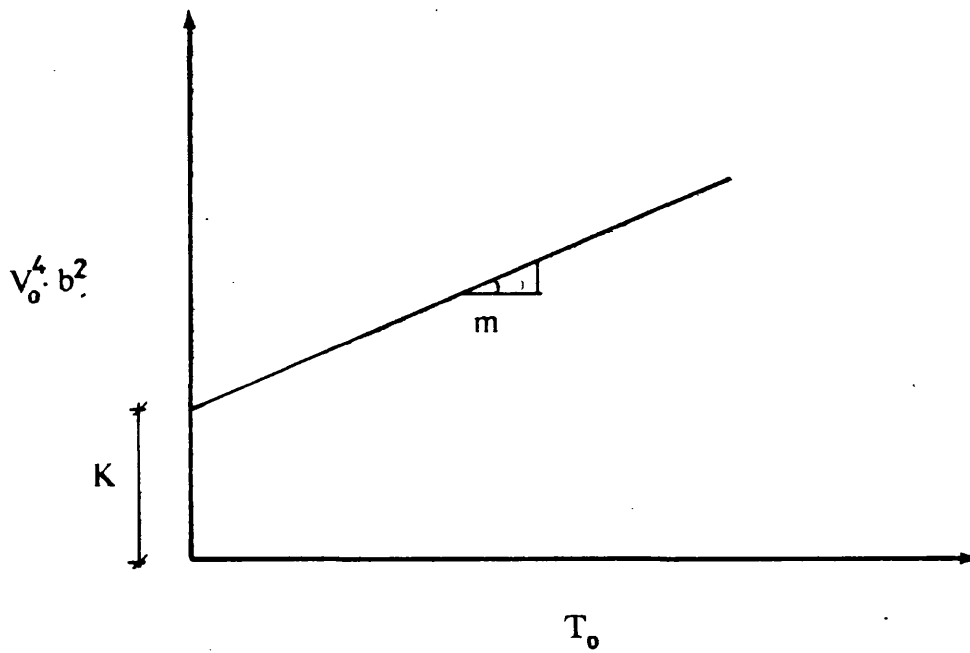
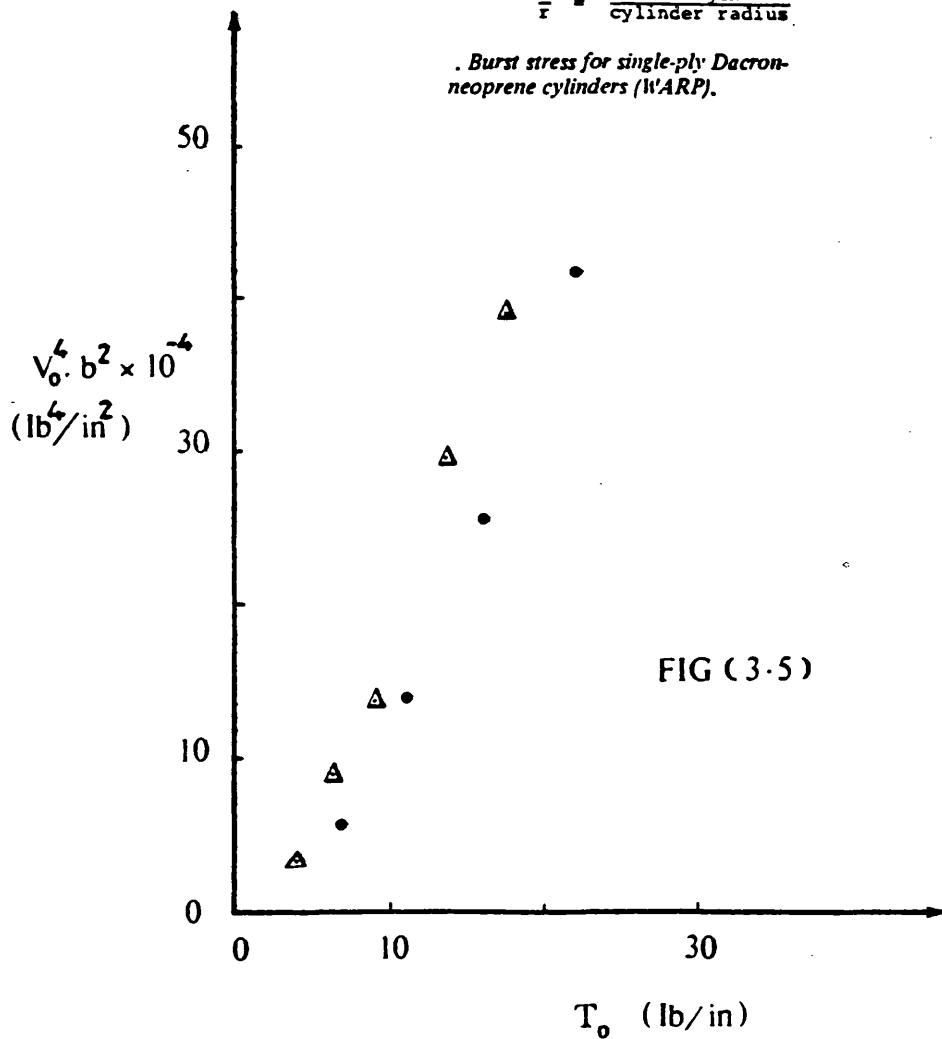
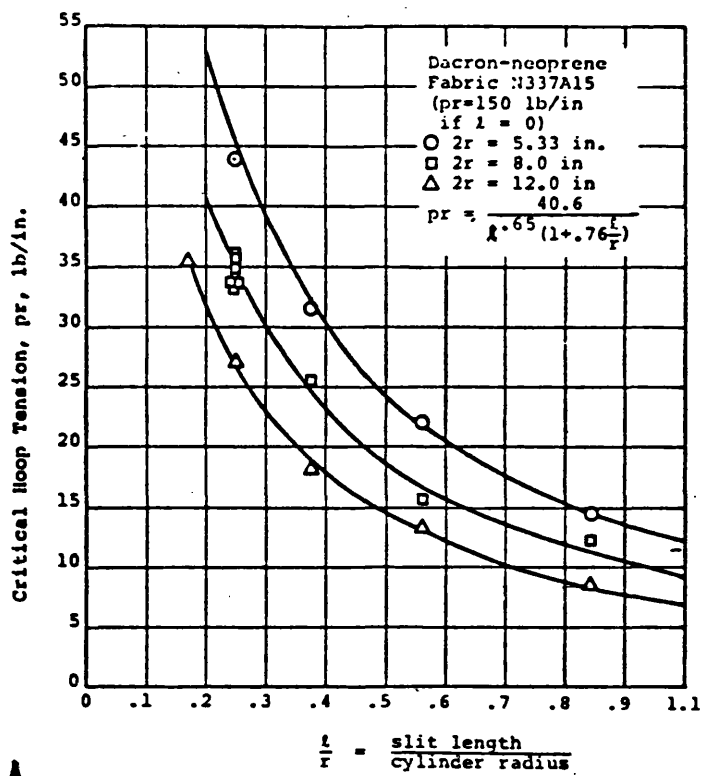
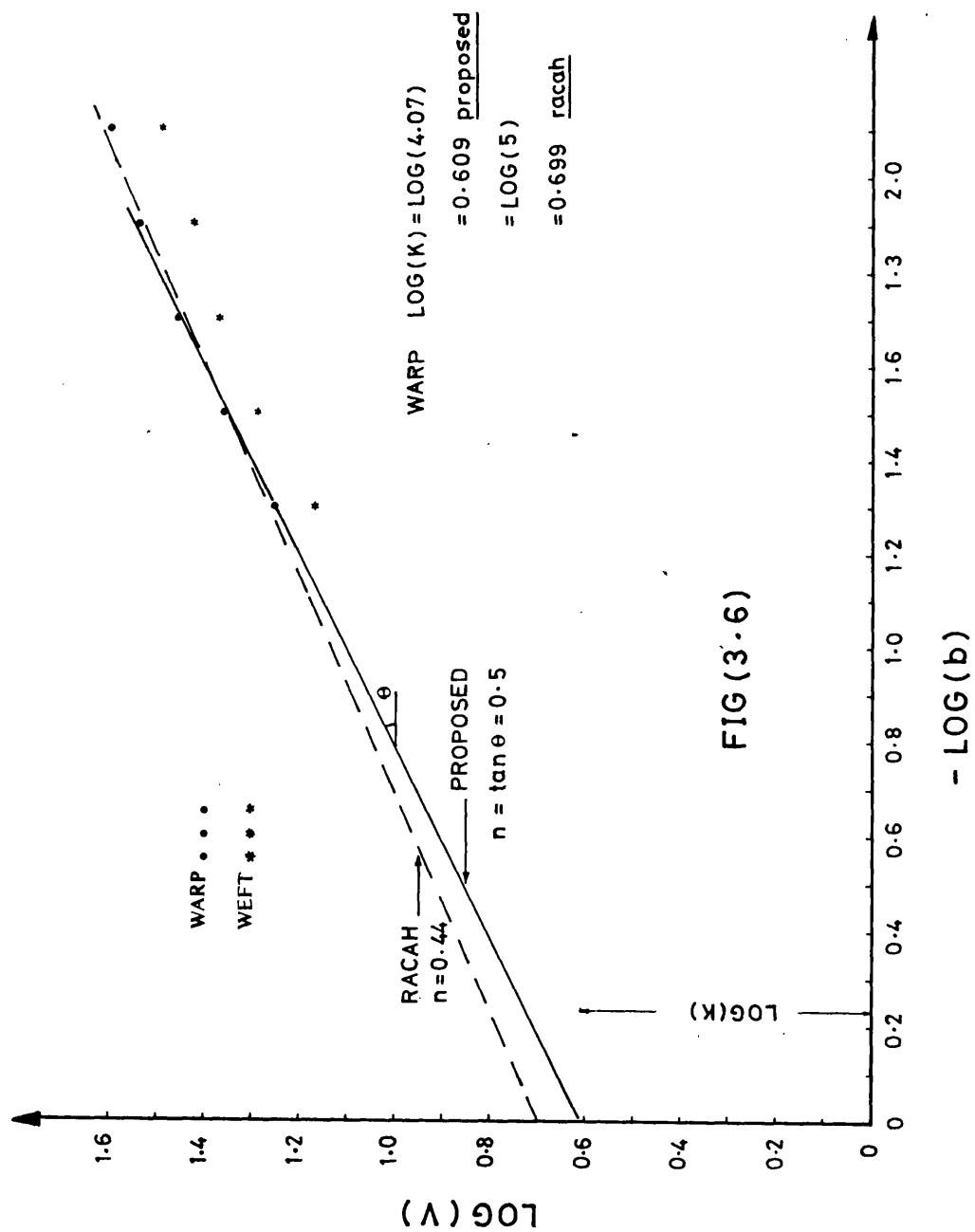


FIG (3.4)

Predicted relation for coated fabrics under biaxial stress.

The Critical Slit Length of Pressurized Coated Fabric Cylinders (12)







## CHAPTER 4

### DISCRETE ANALYSIS APPROACH TO CRACK PROPAGATION OF STRUCTURAL NETS

CHAPTER 4DISCRETE ANALYSIS APPROACH TO CRACK  
PROPAGATION OF STRUCTURAL NETS4.1. Introduction

Structural nets are characterised by the fact that for a given loading condition, the internal forces and the resulting geometry necessary to maintain equilibrium are interdependent.

This property means that the usual assumption of infinitesimal deformations no longer holds, thus the principle of superposition loses its validity and the equations governing its deflection behaviour becomes non-linear.

From the point of view of analysis, a structural net is treated mainly in two ways:

- (1) As a continuous system (i.e. membrane without shear stiffness).

Where a continuous mathematical function is developed to represent the surface, and the unknown displacements are calculated by solving the differential equations of equilibrium. This approach was illustrated in deriving at the proposed solution.

- (2) As a discrete system (i.e. an assembly of pin-jointed members interconnected at a finite number of nodal points).

In this system, the loads are assumed to be concentrated at the nodal points, and at each node equilibrium between external and internal forces and compatibility of displacements must be achieved.

Due to the mathematical complexity of the equations governing the deflection behaviour of structural nets, usually after setting the problem and its governing equations, using either approach, iterative techniques are adopted to solve these equations and determine the final shape.

Treating networks as a discrete system is generally preferred, because it can be used for almost any net configurations and edge conditions, and it enables the designer to take into account the effects of material non-linearity, and even allows the use of more than one type of cables in forming the network, if he so wishes.

The discrete approach is particularly suitable for investigating some of the aspects associated with crack propagation in structural nets, such as the slipping of joints due to the concentration of stresses at the crack tip region.

Computer programs adopting the latter approach were developed to give further evaluation to the theoretical solution proposed, and to explore other aspects of the crack propagation phenomenon.

#### 4.2. Discrete Analysis Method

The method considered herein makes the following assumptions:

- (1) The cable net is replaced by line segments.
- (2) The line segments have negligible bending stiffness.
- (3) Loads are applied at the nodes only.
- (4) The edge elements of the networks are either edge cables or fixed cable ends.

The method of analysis is an explicit one, i.e. it does not require the formation of an overall stiffness matrix and equilibrium and compatibility conditions are treated separately.

Large displacements of the cable net are considered and the effect of the change in both the net geometry and the material properties may be taken into account when formulating the static equilibrium equations.

The procedure of analysis can best be explained by considering a single unstrained cable element in three dimensions, defined by the cartesian co-ordinates of its two ends, (1) and (2) as shown in Fig. (4.1), i.e.  $(x_1, y_1, z_1)$  and  $(x_2, y_2, z_2)$  respectively. When this element is strained under the effect of axial force, the co-ordinates of the two ends (1) and (2) become  $(x_1 + u_1, y_1 + v_1, z_1 + w_1)$  and  $(x_2 + u_2, y_2 + v_2, z_2 + w_2)$  respectively, and a force "S" is introduced in the cable.

$$S = AE \cdot \frac{\Delta}{L_0} \quad (9)$$

where A : cross-sectional area of the cable

E : modulus of elasticity

$\Delta$  : change in length

$L_0$  : original length of the cable

and the projections of the cable centre line on the principle axes

$$x = x_o \pm (u_1 - u_2)$$

$$y = y_o \pm (v_1 - v_2)$$

$$z = z_o \pm (w_1 - w_2)$$

The subscript o indicates the initial value of the projections.

The length of the deformed member is:

$$L = \sqrt{x^2 + y^2 + z^2}$$

$$\text{The strain} = \frac{L - L_o}{L_o} = \frac{\Delta}{L_o}$$

Considering an assembly of such cables forming a net and fixed at the boundaries and in a state of equilibrium, such a net has the capacity to resist both in and out of plane loads, and when subjected to a load (P) the position of the interior nodes will change to achieve another equilibrium state.

Taking the components of the load (P) in the x, y and z directions as ( $P_x$ ), ( $P_y$ ) and ( $P_z$ ) respectively, and the components of the force in the strand (S) in the x, y and z directions as ( $S_x$ ), ( $S_y$ ) and ( $S_z$ ) respectively. At each node three equations of equilibrium can be set up relating the cable forces to the load components.

For "n" cables meeting at a node, the equilibrium equations at this node are:

$$\sum_{i=1}^{i=n} S_{x_i} - P_x = 0$$

$$\sum_{i=1}^{i=n} S_{y_i} - P_y = 0$$

$$\sum_{i=1}^n S_{z_i} - P_z = 0$$

These governing equations are non-linear algebraic equations, each in terms of the unknown displacements of the deflected nodes.

For a regular network where the strands are intersecting at more than one point, setting up the equilibrium equations at each deflected node for the whole net will lead to a number of simultaneous non-linear equations equal to the number of nodal points multiplied by the number of degrees of displacement freedom per node, which must be solved to obtain the deformed shape.

As mentioned earlier, the method allows, the effect of the change in both the modulus of elasticity and the cross-sectional area of the cables to be taken into account when formulating the equilibrium equations.

This aim is accomplished by means of an algebraic expression which simulates the elongation behaviour of the cables, determined by testing. This expression could then be used to represent the relation between the value of (AE) for the cables and the corresponding value of the cable strain ( $\epsilon$ ), so that the value of (AE) for each cable in the net at each stage of the solution can be expressed in the equilibrium equations in terms of the unknown displacements of the deflected nodes in the x, y and z directions. Hence equation (9) becomes a function of only the strain ( $\epsilon$ ).

$$S = f(\epsilon) = f\left(\frac{\Delta}{L_0}\right)$$

Thus when setting up the governing equilibrium equations, it will contain only the unknown displacements.

The method solves the non-linear load/displacement equations by treating fictitious nodal propping forces, which are a measure of the difference between the true and assumed loading patterns, as

residuals to be liquidated by relaxation.

The scheme is characterised by the advantage that for any geometrical configurations there is no need to determine the initial shape of the suspended system, which may require extensive trial and error computations. The numerical scheme adopted for solving the governing equations is GAUSS-Seidel's iterative technique.

For further information concerning the method of analysis and its application to structural nets, consult References (26), (27). The computer program used to execute the analysis of the various networks considered in this investigation is given in Appendix (2).

#### 4.3. Discrete Analysis of Nets Subjected to Biaxial Tension

Although the discrete method of analysis developed is well capable of accounting for the effects of material non-linearity, linear elastic material behaviour was adopted in order to use the results obtained from this discrete analysis to evaluate the reliability of the proposed theoretical solution for nets with finite boundary.

##### 4.3.1. Evaluating the reliability of the theoretical solution proposed

The procedure adopted to achieve this aim can be summarised as follows:-

- (1) A hypothetical material properties were chosen to use in the analysis.
- (2) For a certain net configuration, the discrete method was deployed to calculate the value of the critical boundary tension necessary to produce the chosen tensile breaking force at the crack tip cables, i.e. the tension necessary to start propagating the crack. Then the fracture toughness of the net is evaluated by substituting in the proposed expression.

To investigate whether or not the calculated value of the fracture toughness, for this structural net, is unique and independent of the net size or the crack length, the discrete analysis was repeated while varying the size of the net and the crack length and for each case the corresponding value for the fracture toughness, as predicted by the proposed expression, was determined.

##### (1) Material properties of the cables

Assuming linear elastic properties and that the cables are hookean up to the critical breaking point, (i.e. the plastic zone is sufficiently small enough to be neglected). The value of the



extensional stiffness of the cables, given as force units for simplicity,

$$AE = 7 \text{ force units}$$

In deriving the theoretical expression, the horizontal movement parallel to the crack was considered to be negligible. The value of this movement increases with the increase in the maximum strain value at failure.

Although even for light fabrics the maximum strain at failure is less than 20%, it seemed appropriate to adopt in the discrete analysis a high value for the maximum strain to show that even at such high strain levels the assumption made was justified.

The value of the tensile breaking force chosen

$$f_y = 3.89 \text{ force units}$$

assumed to be the force in the crack tip cables at which the crack starts to propagate. This meant that the value of the maximum strain in the nets studied is about 55%.

## (2) Evaluating the fracture toughness for a given net configuration

Consider the structural net shown in Fig. (4.2) which comprise a number of horizontal linking elements ( $nhL$ ) intersecting a number of vertical linking elements ( $nvL$ ) at a finite number of nodal points to form a square net with a crack centred horizontally, as shown, the number of broken cables ( $nc$ ) is one, i.e.  $nc = 1$ .

Simulating the loading configurations adopted in the mathematical model, Fig. (2.2) i.e.

- (1) A constant force ( $F$ ) parallel to the crack is applied at each nodal point along the two edge cables which are normal to the crack length.
- (2) The crack is opened by an outward constant displacement of the other two edges, resulting from a vertical wedging force (fixed grips loading) equals ( $F \times nvL$ ).

Then using the discrete analysis method to calculate the value of the boundary force (F) necessary to produce a force in the crack tip cables equal to the tensile breaking force, it was found that  $F = 3$  force units per cable.

The final equilibrium shape is shown in Fig. (4.3). substituting in the proposed expression to evaluate the value of the fracture toughness

$$\gamma = \frac{a V_0^2}{2AE} \tanh \left( \frac{\pi b}{ac} \right)$$

$$\text{where } c = \left( \frac{T_o h}{AEL_o} \right)^{\frac{1}{2}} = \left[ \frac{3/7 \times 10}{7/10 \times 7} \right]^{\frac{1}{2}} = 0.935$$

$$\therefore \gamma = \frac{(25 \times 7)}{2} \cdot \frac{3}{7} \cdot \frac{3}{10} \tanh \left[ \frac{\pi \times 10}{(25 \times 7) \times 0.935} \right]$$

$$= \underline{2.133} \text{ force units}$$

#### Effect of net size on the value of " $\gamma$ "

First to investigate the effect of the net size on the value of the fracture toughness, the two nets shown in Figs. (4.4), (4.5), were analysed to find the value of the critical boundary tension, using similar loading configurations, required to start propagating the crack.

The value of the critical force for net (2) and net (3) was found to be "3.02" and "3.08" force units, and the final equilibrium shapes are shown in Figs. (4.6), (4.7) respectively, which means that:

#### for net (2)

$$c = \left[ \frac{(3.02/7) \times 10.02}{(7/10.02) \times 7} \right]^{\frac{1}{2}} = 0.94$$

$$\therefore \gamma = \frac{(17 \times 7)}{2} \times \frac{3.02}{7} \times \frac{3.02}{10.02} \tanh \left[ \frac{\pi \times 10.2}{(17 \times 7) \times 0.94} \right]$$

$$= \underline{2.121} \text{ force units}$$

for net (3)

$$c = \left[ \frac{(3.08/7) \times 10.08}{(7/10.08) \times 7} \right]^{\frac{1}{2}} = 0.955$$

$$\therefore \gamma = \frac{(9 \times 7)}{2} \times \frac{3.08}{7} \times \frac{3.08}{10.08} \tanh \left[ \frac{\pi \times 10.08}{(9 \times 7) \times 0.955} \right]$$

$$= \underline{2.05} \text{ force units}$$

Comparing the values obtained for " $\gamma$ ", it becomes obvious that the size of the net does not influence the fracture toughness value.

#### Effect of the crack length on the value of " $\gamma$ "

To assess the effect of the crack length on the fracture toughness, net (1) was analysed varying the number of broken cables ( $n_c = 1 \rightarrow 5$ ), and the value of the critical boundary force in each case and the corresponding fracture toughness value were determined.

The final equilibrium shapes are shown in Figs. (4.8)  $\rightarrow$  (4.11) and the results obtained are given in Table (4.1).

The relation between the fracture toughness and the crack length is plotted in Fig. (4.12). As should be expected, it can be seen that with the increase in the number of broken cables ( $n_c$ ), the membrane analogy becomes more evident, and so the proposed expression for the fracture toughness becomes more accurate and assumes a constant value.

#### 4.3.2. Practical applications

##### \* Recommended test

Now having affirmed the reliability of the proposed expression for the fracture toughness and its applicability to networks, with its discrete nature, this meant that a test apparatus which is designed to simulate the same boundary conditions adopted in deriving the proposed expression could then be used to determine the value of

the fracture toughness for light nets such as woven fabrics with plain weave, and such a test would free the designer from any restrictions concerning the size of the specimen tested and/or the length of the crack initiated, and would involve calculating only one value for the critical tension necessary to start propagating a crack in the net under consideration. Thus knowing the extensional stiffness for the linking elements (AE) and the net spacing in both directions, the value of the fracture toughness is determined by substituting in the proposed expression.

The test is specially suitable for light fabrics and gains more creditability from examining the stress-strain curves for light fabrics, reported in previous works published (9), (14), (15), (28), which showed a roughly linear and brittle behaviour, thus considerably narrowing the gap between theory and practice, a fact that was confirmed by the excellent correlation between the proposed theoretical solution, for infinite boundary, and Topping's experimental work, as shown earlier.

#### Approximate evaluation of " $\gamma$ " using the Inglis analysis

As for other types of structural nets for which such test apparatus may not be practical, as in the case of heavy network, the need for an approximate evaluation for the fracture toughness could be satisfied to a certain extent, assuming hookean cables up to the breaking point, by making full use of the foresight offered from the Inglis analysis (20), that is, in an elastic field the intensity of the field is governed by the outer boundary conditions, i.e., applied loading configurations, while the distribution of the field is governed by the inner boundary conditions. i.e., stress free crack surfaces, particularly in the vicinity of the crack tip.

This meant that any variation in the value of the cable's extensional stiffness (AE) or the cables spacing ( $L_0$ ) for a given net should not affect the value of the critical boundary force per cable.

In other words the net should behave as an isotropic material and the stress concentration factor should remain constant (i.e., independent of the material properties), particularly at the vicinity of the crack tip.

To check how accurate this statement is for structural nets and to have a better understanding of the way in which the stresses are redistributed in a net as a result of changing the material properties of the cables. The discrete analysis method was used to re-analyse net (2), maintaining the same applied loading configurations but for an extensional stiffness value (AE) double the previous one (i.e.  $AE = 14.0$  force units). Figure (4.13) shows the final equilibrium shape. Then comparing the force in each cable with its corresponding value, i.e. for  $AE = 7.0$ , it was found that increasing the extensional stiffness of the cables lead to a reduction in the tensile force in the cables along line C-C, having a maximum of 15.6% in cable (1) and gradually reaching a minimum of 7% at cable (8). In addition, there was a less significant force increase of around 2.7% in cables (9), (10), an increase which vanished rapidly away from the crack. The value of the crack tip cable force in both cases was identical, while everywhere else the values of the cables tension remained almost unchanged.

A similar analysis procedure to investigate the effect of a change in the net spacing ( $L_0$ ) was not necessary, since such a change is the equivalent to a change in the net scale. This showed, beyond any shadow of doubt, that, for this loading configurations at least, the stress concentration factor is independent of the net spacing or material properties. i.e. The relation between the critical tension per cable at the boundary and the crack tip stress is linear for a given net configuration. Further investigations along these lines for different net sizes with various crack lengths confirmed this fact.

This independence of the stress concentration factor means that the need for an equation which gives an approximate evaluation of the

fracture toughness without having to do any experimental work can be satisfied, since the only unknown parameter in the proposed expression is the value of the critical boundary tension which can be expressed for a standard net in terms of its stress concentration factor and the tensile breaking force of the cables. i.e. The fracture toughness would be given in terms of the material properties and the net spacing only.

$$\therefore \gamma = \frac{a}{2} \frac{V_o^2}{AE} \tanh \left[ \frac{\pi b}{ac} \right]$$

$$\text{where } c = \left( \frac{T_o h}{AE L_o} \right)^{\frac{1}{2}}$$

$$\therefore V_o = \text{boundary force per cable (vll direction)/h}$$

$$\therefore V_o = \frac{F}{h}, \quad T_o = \frac{F}{L_o}$$

$$\therefore \text{substituting for net (1) (nc = 4)}$$

$$\text{with } a = 25 L_o$$

$$b = 2.5 h$$

$$E = K f_y = \frac{2.03}{3.89} f_y = 0.5219 f_y$$

$$\therefore \gamma = 3.404 \left[ \frac{f_y^2}{AE + 0.5219 f_y} \right] \tanh \left[ 0.4349 \left( \frac{AE}{f_y} \right)^{\frac{1}{2}} \right] \quad (10)$$

and this equation should give an approximate value for the fracture toughness, for nets with four or more broken cables, without having to do any crack propagation tests.

Similarly for net (1) (nc = 5)

$$b = 3h, \quad F = \frac{1.85}{3.89} f_y = 0.476 f_y$$

$$\therefore \gamma = 2.832 \left[ \frac{f_y^2}{AE + 0.476 f_y} \right] \tanh \left[ 0.5464 \left( \frac{AE}{f_y} \right)^{\frac{1}{2}} \right] \quad (11)$$

Theoretically either of these equations, or any other equations developed similarly, should give the same result. This was checked and confirmed, specially for relatively small strains, by plotting the value of the fracture toughness obtained using these two

equations for different strain levels, as shown in Fig. (4.14). What is also interesting about these equations is that they show clearly that the net spacing has no effect whatsoever on the value of the fracture toughness, and that its value is solely determined by the material properties of the cables.

The other advantage gained from the Inglis result, is that the independence of the stress concentration factor can be used to investigate how the accuracy of the proposed expression may be affected if there is a change in the value of the maximum strain in the net, without having to repeat the discrete analysis for these new strain levels.

For net (1), new values for the fracture toughness were calculated using the same stress concentration factors and the same value for the tensile breaking force and an increased value of the cables extensional stiffness ( $AE = 14$  force units), thus reducing the maximum strain in the net from 55% to 28%.

The new values for the fracture toughness are given in Table (4.2). Examining the results shown in Tables (4.1), (4.2), indicates that, as expected, the decrease in the value of the maximum strain improved the accuracy of the proposed fracture toughness expression for less than three cables broken.

So, for the case of heavy nets, or even light nets, equations similar to Equation (10) and (11) can be used to evaluate " $\gamma$ " reasonably accurate for nets with four or more cables broken. As for the case when three or less cables are broken, thus there are two options available, either to develop a similar equation for each case or to use Equations (10), (11), since in practice such a small number of broken cables could hardly be of interest, except for high tensile strength cable networks and at which case the strains are very small, so the accuracy of the proposed expressions is considerably improved for less than three cables broken.

#### 4.3.3. Discussion and comparison with previous work

##### \* Hedgepeth's stress concentration factor (10)

The emergence of the stress concentration concept in the discrete analysis of structural nets in the fixed grips loading case emphasised the need for a more rigorous examination of Hedgepeth's stress concentration factor, in order to investigate its relevance and verify the results obtained using this method.

Hedgepeth (10), using small deflection elasticity theory, presented a theoretical analysis of the stress distribution in a sheet of parallel purely tension-carrying filaments imbedded in a purely shear-carrying matrix containing a crack transverse to the filament direction, and subjected to a uniaxial uniformly distributed loading at infinity. He used an influence function technique to solve a partial-differential-difference equation, and concluded that if the crack transverses "m" cut filaments, then the stress concentration factor at the crack tip filaments was given by:

$$K_n = \frac{4 \ 6 \ 8 \ \dots (2m + 2)}{3 \ 5 \ 7 \ \dots (2m + 1)}$$

Topping (12), as mentioned earlier, using Stirling's approximation for large values of "m", transformed the stress concentration expression into

$$K_n \approx \frac{(\pi m)^{\frac{1}{2}} (m + 1)}{2m + 1} \xrightarrow{m \rightarrow \infty} \frac{(\pi m)^{\frac{1}{2}}}{2}$$

and when he compared the experimental values of the burst strength of longitudinally slit pressurised fabric cylinders with Hedgepeth's predicted values, he found that the latter are only 2/3 of the experimental values.

The argument suggesting that this may be attributed to an unsatisfied infinite boundary conditions is really not founded, because if that was the case then for relatively small cracks the predicted Hedgepeth values should be expected to show some tendency



toward the correct values, which is not the case as can be seen from Figs. (4.15a,b,c). Besides, similar results were reported in K<sub>o</sub> (14) experimental work. He tested flat coated nylon fabrics using a closed-looped, servo-controlled hydraulic load frame, and found that the test specimens showed lower levels of stress concentrations than that predicted by Hedgepeth's theory. Yet when Zender and Deaton (28) compared Hedgepeth's theory with uniaxial tests of Dacron cords in aurethane matrix, they found that the results were in favourable agreement with the theoretical values but became increasingly conservative with the increasing number of threads cut.

All these facts and observations can be simply explained on the light of the theoretical solution proposed in this thesis as follows.

#### (1) Topping's work and Hedgepeth's theory

Hedgepeth's theory can be written in terms of the slit length " $l$ ", since  $m = cl$ , as

$$f_y = \frac{2 F_y}{(\pi cl)^2}$$

and for a given fabric,  $c$  and  $F_y$  are constants, so it can be seen that Hedgepeth's theory reduces to Griffith's original theory, and in other words it reduces to a relation similar to that proposed in the present work for the case of a coated fabric with infinite boundary under uniaxial stress field. But in Topping's experimental work the stress field was biaxial, and on the light of the present work it can be understood why. As a result of the transverse tension, the burst strengths predicted by Hedgepeth's theory were less than the experimental values, and the fact that the predicted values were about 2/3 of the experimental values for all specimens, does show consistency with the relation proposed in Fig. (3.4).

(2) Zender and Deaton's work (28) and Hedgepeth's theory

When Zender and Deaton compared Hedgepeth's theory with uniaxial tests, of Dacron cords in a urethane matrix, they were comparing the experimental results with a similar relation to the one proposed in the present work for coated fabrics subjected to a uniaxial stress field, thus confirming its validity.

The reason they found Hedgepeth's theory becoming increasingly conservative with the increasing number of threads cut, can be explained by the fact that as the crack length increased the assumption of infinite boundary conditions became increasingly less satisfied and that the Hedgepeth theory, unlike the proposed relation, neglected the non-linear geometric effects. Because the theory assumed small-deflections and this means that the geometry of the linking elements remains basically unchanged during the loading process, and that infinitesimal strain approximations can be used. This really is not an accurate representation, specially for large numbers of threads cut, as shown from the discrete analysis results, and even though the strains may be small, large displacements in structural nets arise mainly as a result of large rotations rather than high strains, and the Hedgepeth model does not allow for such rotations.

#### 4.4. Discrete Analysis for Nets Subjected to Uniaxial Tension

Having deployed the discrete analysis method to confirm the validity of the mathematical solution developed for structural nets under biaxial tension, the work was extended to investigate, using the same discrete method, some aspects of crack propagation in uncoated nets subjected to uniaxial tension, and for which no similar mathematical treatment is available. In order to have a clearer picture and a better understanding of the effect which such a change in loading conditions have on the crack propagation behaviour, the investigation was conducted on the same net configurations. Net (1), adopting the same hypothetical cable material, was studied for various crack lengths ( $n_c = 1 \rightarrow 5$ ) to determine the necessary uniaxial force, fixed grips loading, required to start propagating a crack. The final equilibrium shapes are shown in Figs. (4.16) to (4.20).

In general the stress distribution in all cases showed that the lack of any shear stiffness lead to the slackening of the transverse cables except at the vicinity of the crack, i.e. at the crack level and the adjacent two or three cable lines, while everywhere else the applied uniaxial force is almost solely resisted by the initially vertical cables.

It was interesting to find that for a given net the concept of a stress concentration factor relating the value of the boundary force to that of the crack tip cables is very suspect and inconsistent specially for increasingly large marginal differences between boundary force values, contrary to that in a biaxial stress field. This is probably due to the fact, that as the value of boundary force increases the contribution of the transverse cables in carrying load increases in both number and magnitude, thus altering the stress distribution in the net.

Fig. (4.21) shows the relation obtained between the initial crack length ( $b_0$ ) and the critical boundary force per cable, and it was found that, for net (1) in the range of crack lengths studied, that this relation could be expressed as:

$$F = \frac{6.20}{(b)^{0.4}}$$

i.e.  $F (b)^{0.4} = \text{constant}$ .

Table(4.3) shows a comparison between the values of the critical boundary force per cable, for various numbers of broken cables under both biaxial and uniaxial stress fields. It can also be seen, contrary to what is usually assumed, that after a certain crack length the biaxial stress field becomes more detrimental to structural nets.

#### 4.4.1. The effect of the net length and width

The influence of the width and length of the net, compared with the crack length, on the value of the uniaxial boundary force were also investigated.

First, to assess the influence of the net width, net (3) was analysed having a constant crack length ( $n_c = 5$ ) for various widths ( $n_v L = 7 \rightarrow 25$ ). The results, plotted in Fig. (4.22), indicates that for a given crack length as the net width decreases, the uniaxial force per cable required to start propagating the crack increases slightly and gradually to a maximum value, which occurs when there is only one cable, at each crack tip, resisting the applied force. When this last cable is broken, the required force drops sharply to zero. This behaviour is different from that reported by Racah (15), who indicated a gradual decrease in the value of the boundary force until it reaches zero.

To evaluate the effect of the net length, a similar analysis was conducted on net (1), with five cables broken, while varying the net length ( $n_h L = 4 \rightarrow 26$ ). The results are plotted in Fig. (4.23) and it shows that for the same crack length any slight change in the length of the net drastically alters the value of the uniaxial boundary force required. This effect is similar to what Racah found experimentally for coated fabrics.

$V_0$  : Force per cable

nc	$V_0$ (force unit)	$\gamma$ (force unit)
1	3.0	2.133
2	2.52	2.537
3	2.21	2.782
4	2.03	2.996
5	1.85	3.02

Table (4.1)

nc	$V_0$ (force unit)	$\gamma$ (force unit)
1	3.0	1.754
2	2.52	2.005
3	2.21	2.1084
4	2.03	2.178
5	1.85	2.096

Table (4.2)

nc	$V_O$ (force units)	
	Uniaxial	Biaxial
1	2.85	3.0
2	2.37	2.52
3	2.15	2.21
4	2.03	2.01
5	1.975	1.85

Table (4.3)



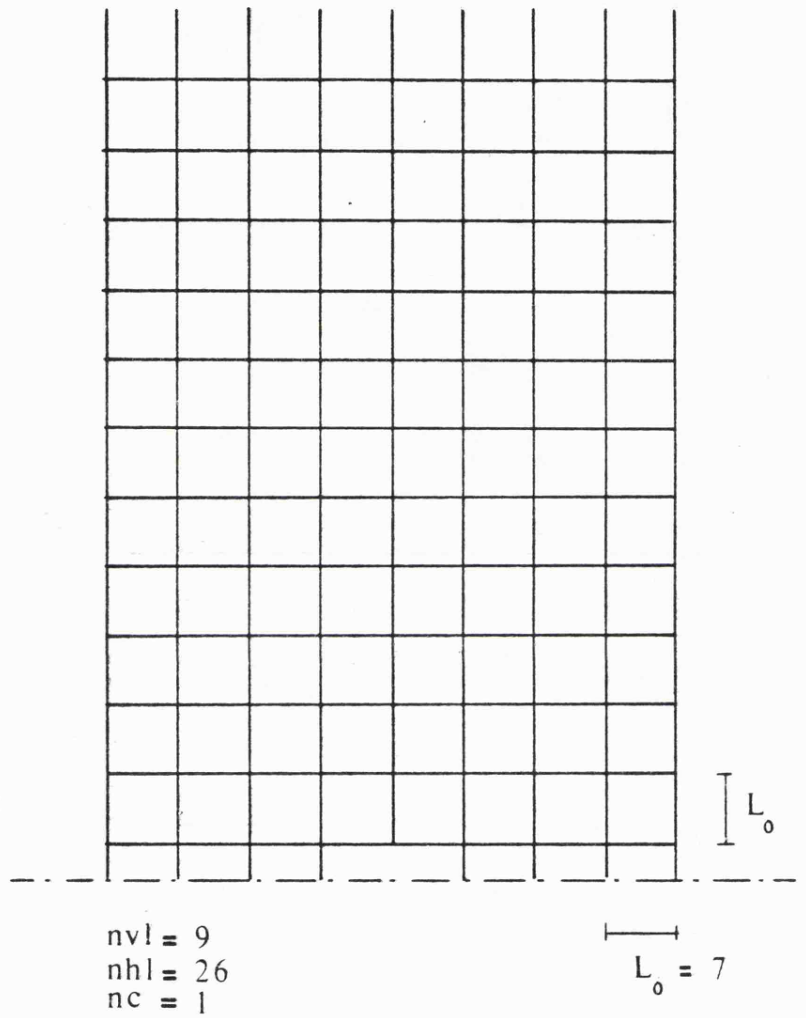


FIG (4.2)



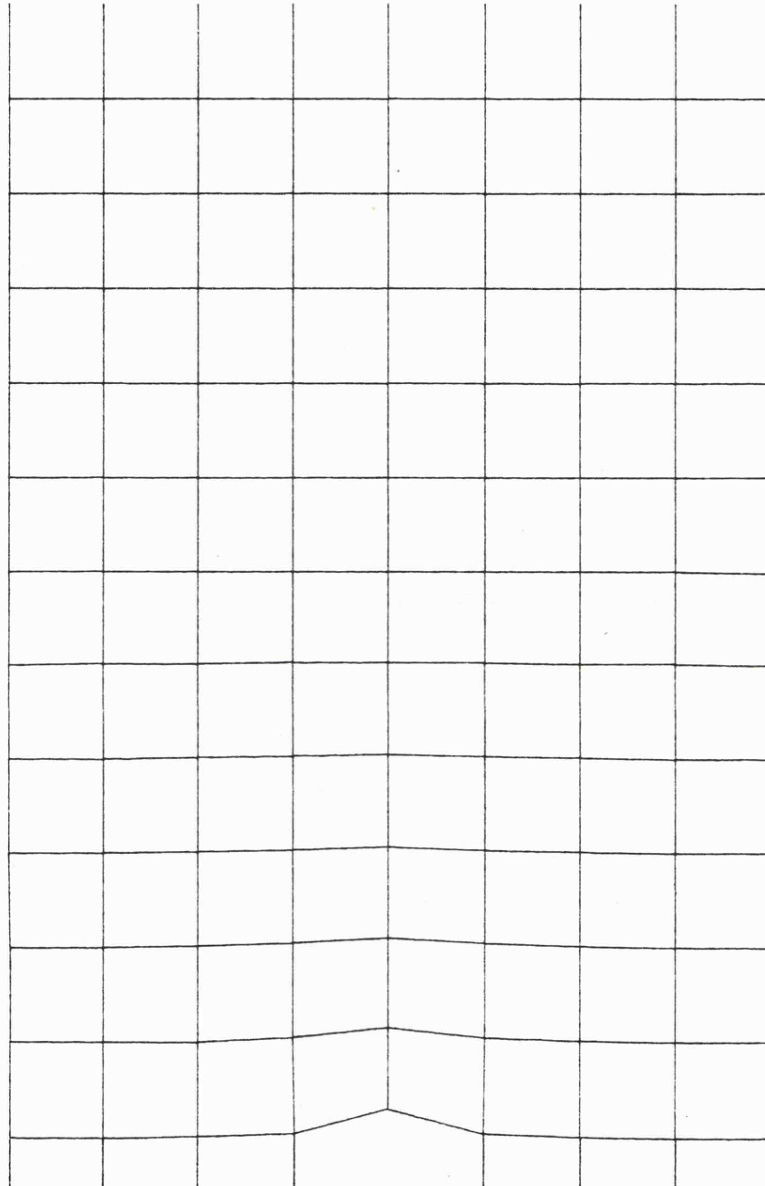
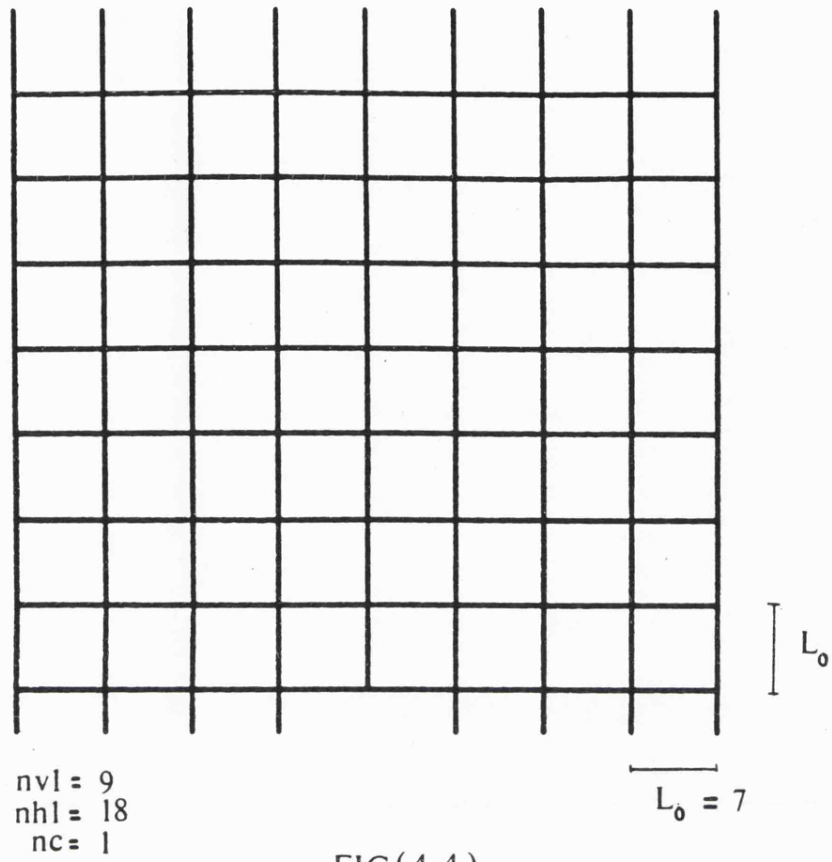
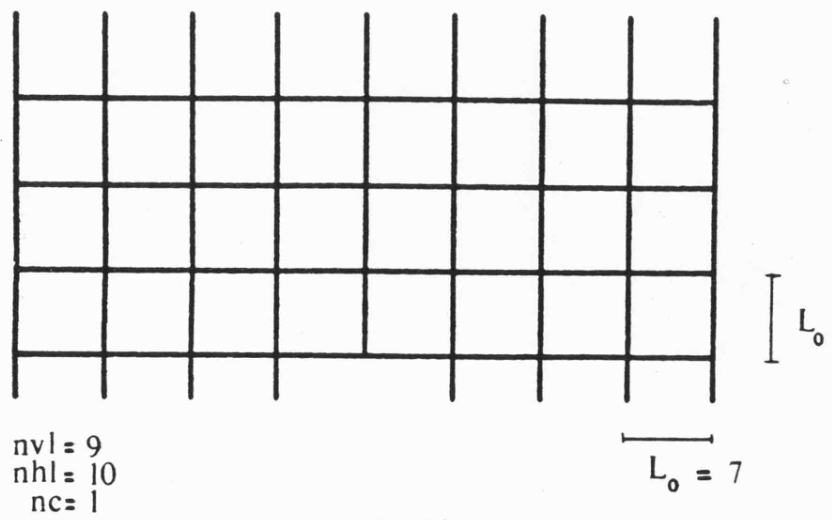


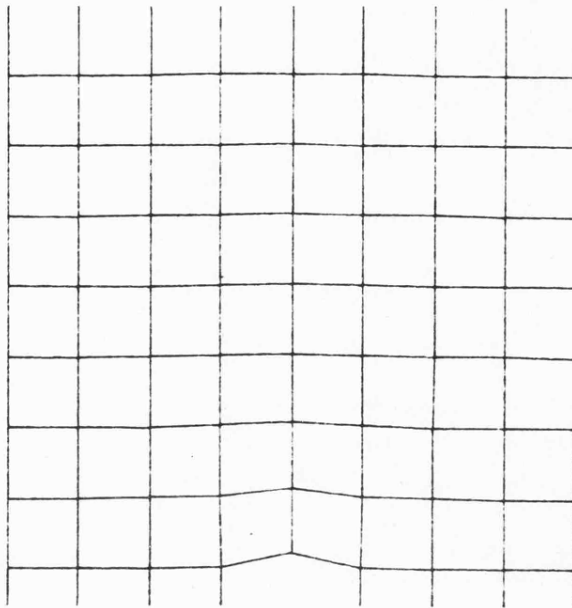
FIG (4 . 3 )



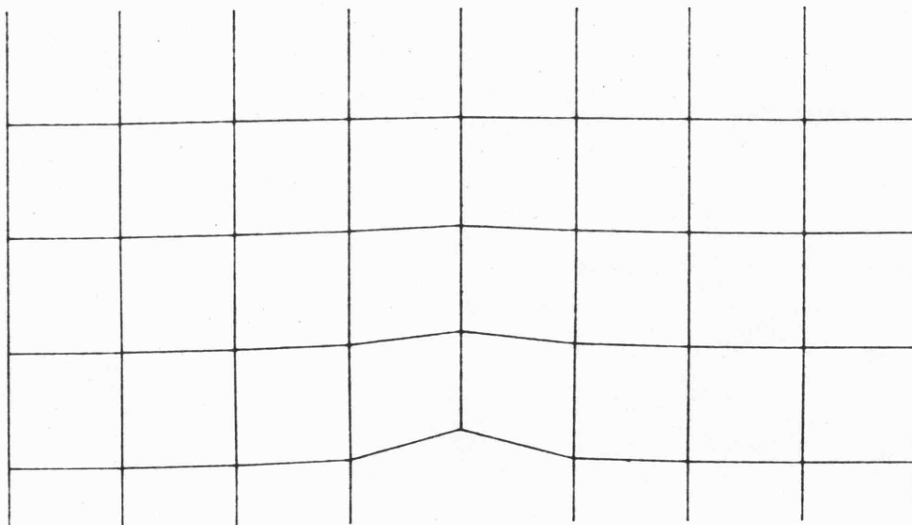
FIG(4.4)



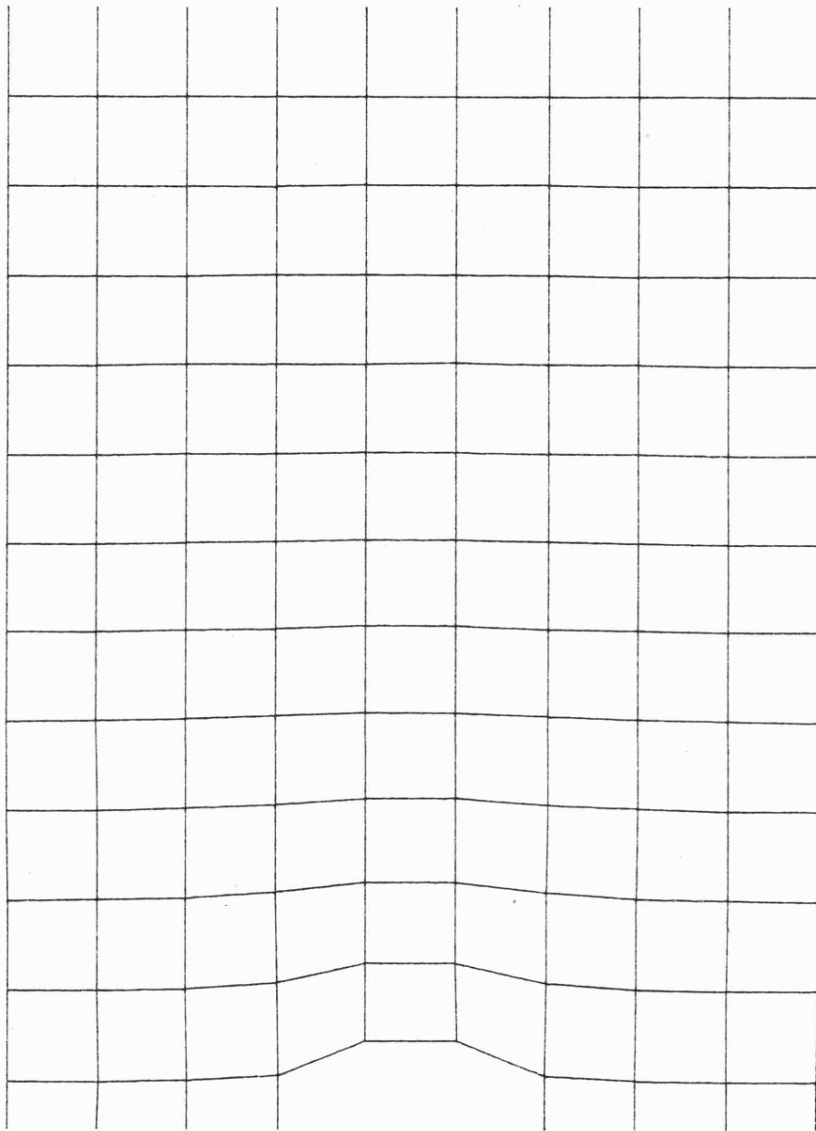
FIG(4.5)



FIG(4.6)



FIG(4.7)



FIG(4.8)

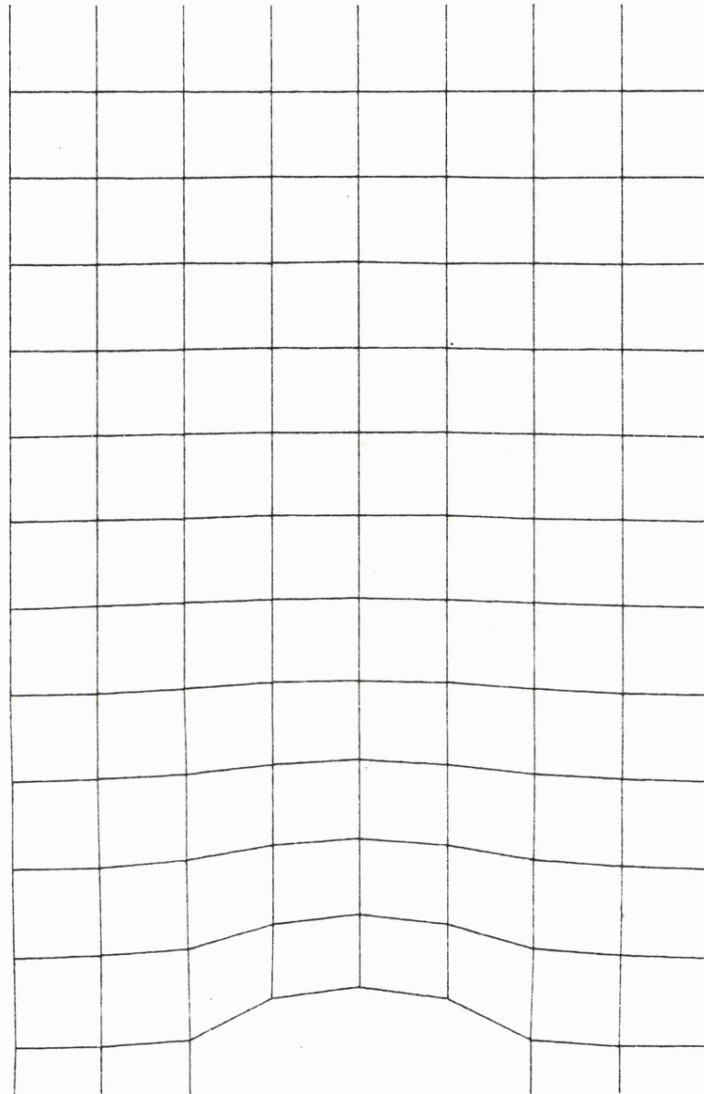


FIG ( 4 . 9 )

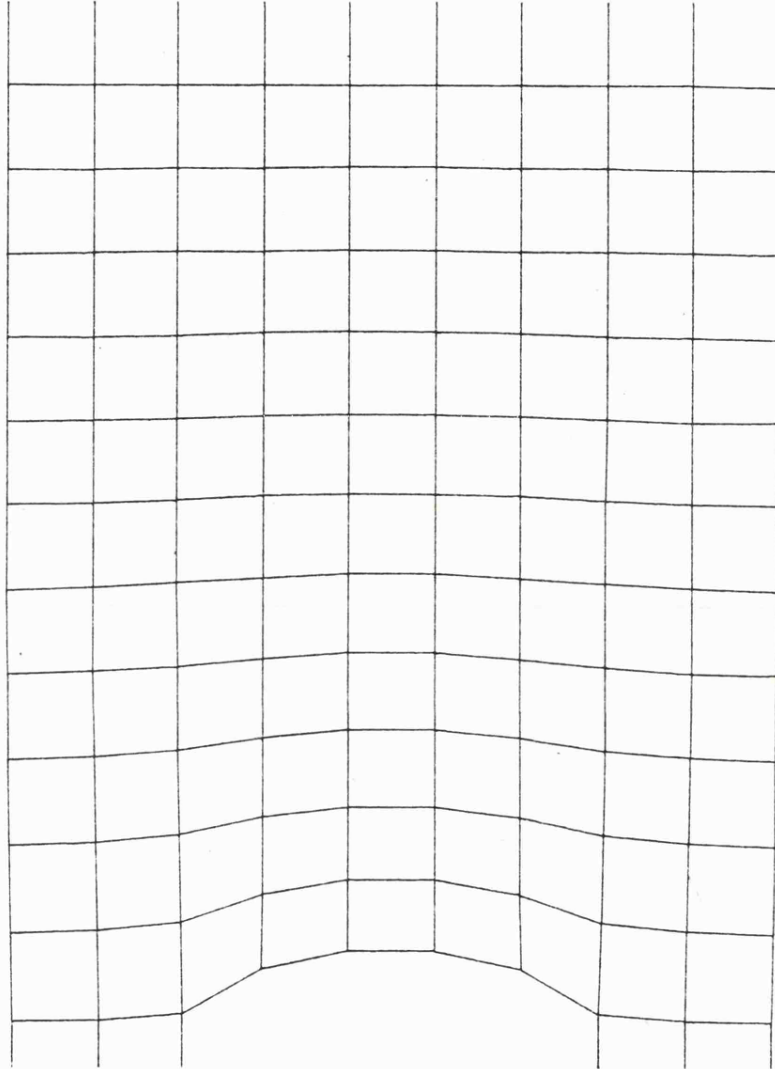


FIG (4·10)

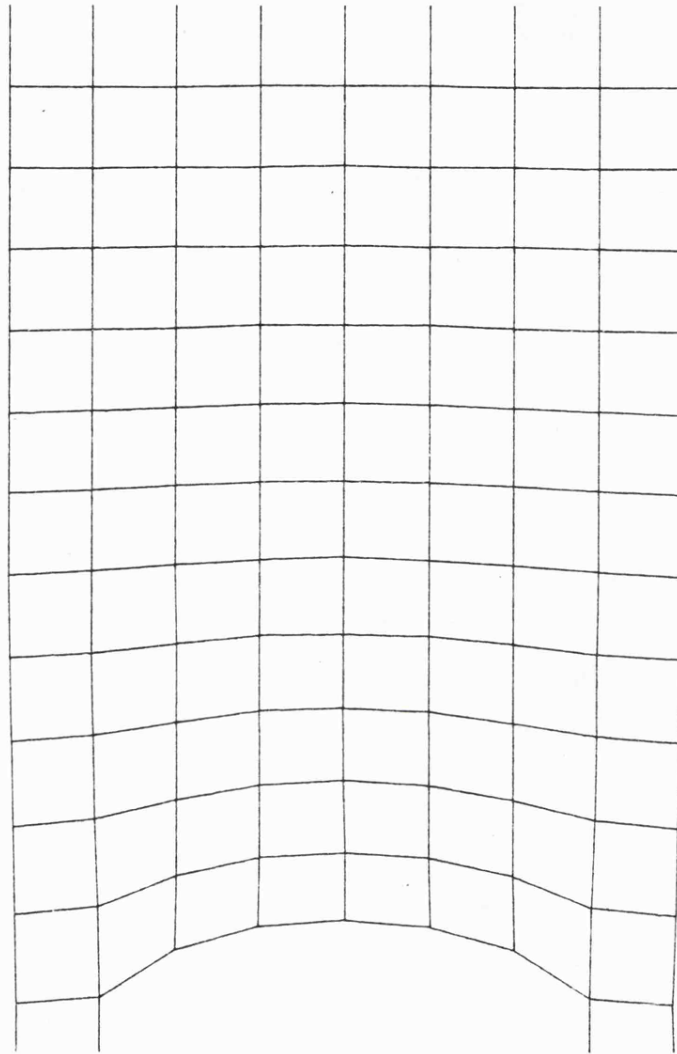
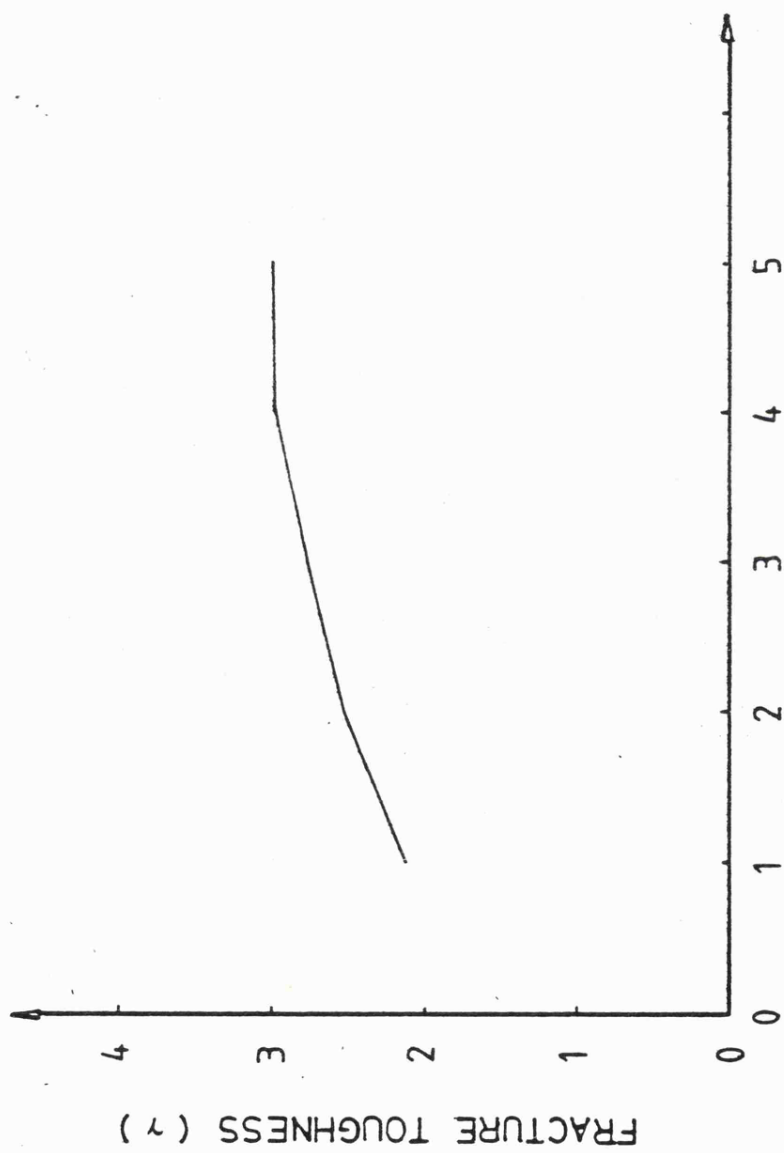


FIG (4.11)



FIG(4.12) NO. OF BROKEN CABLES (nc)



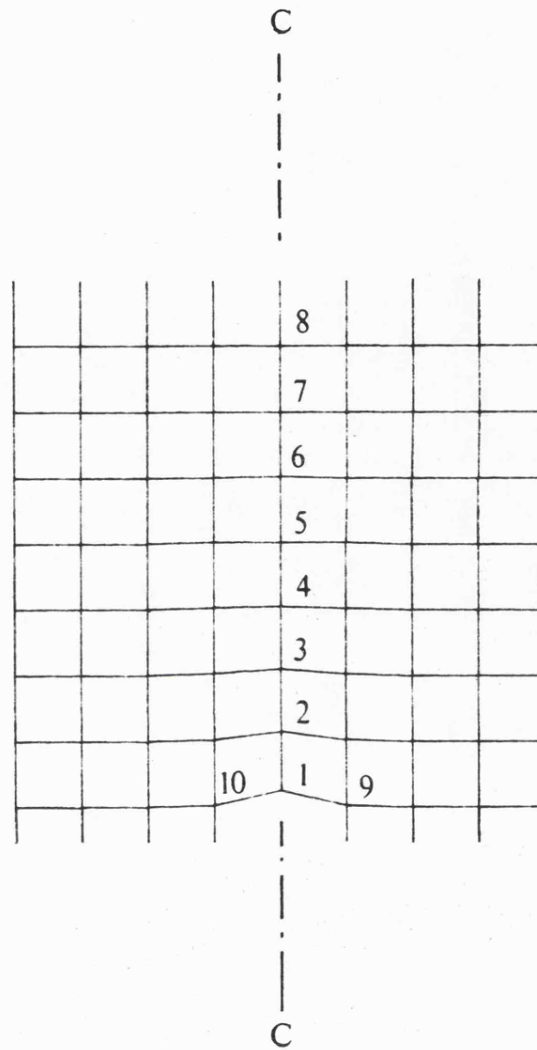


FIG (4.13)

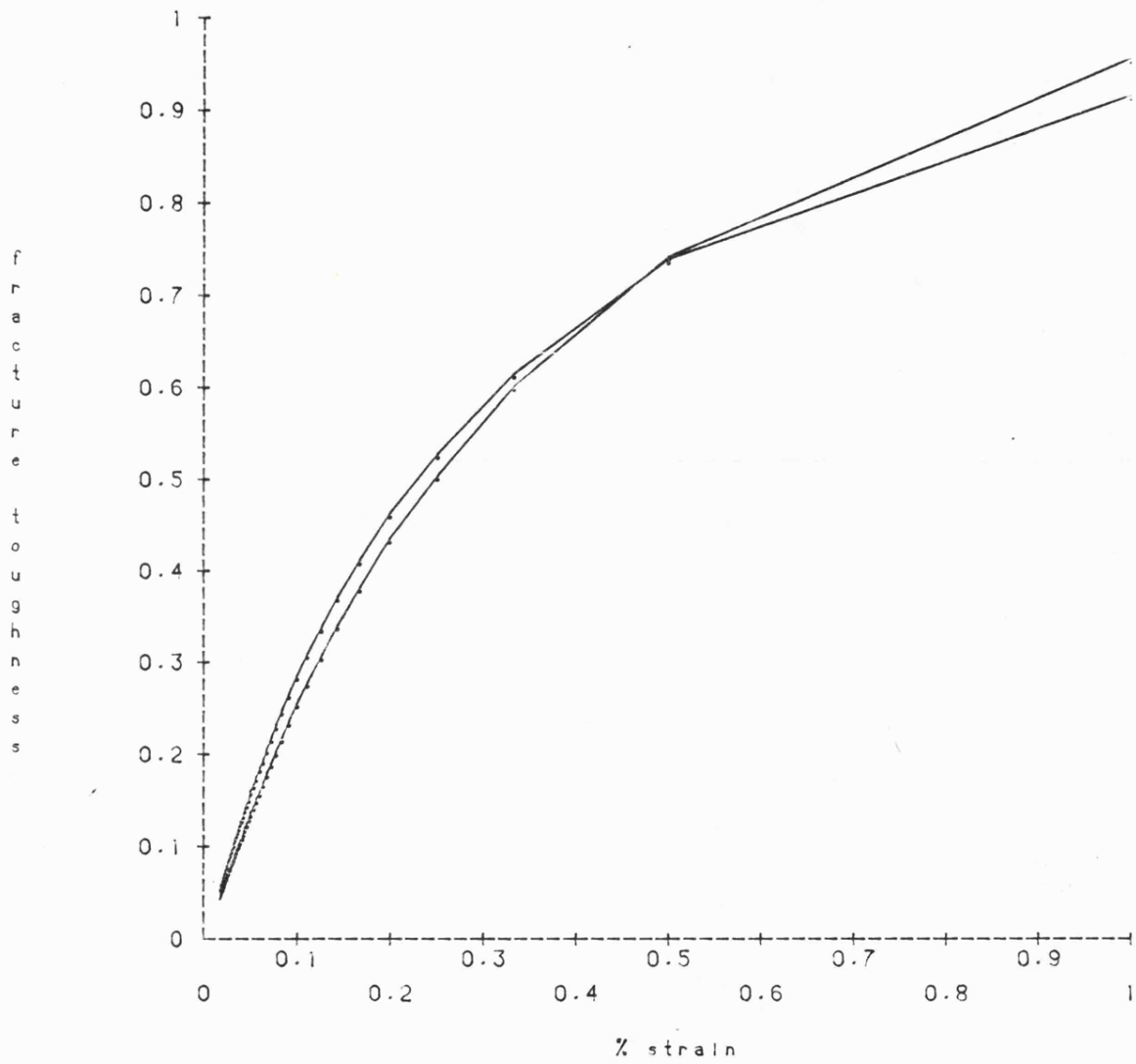
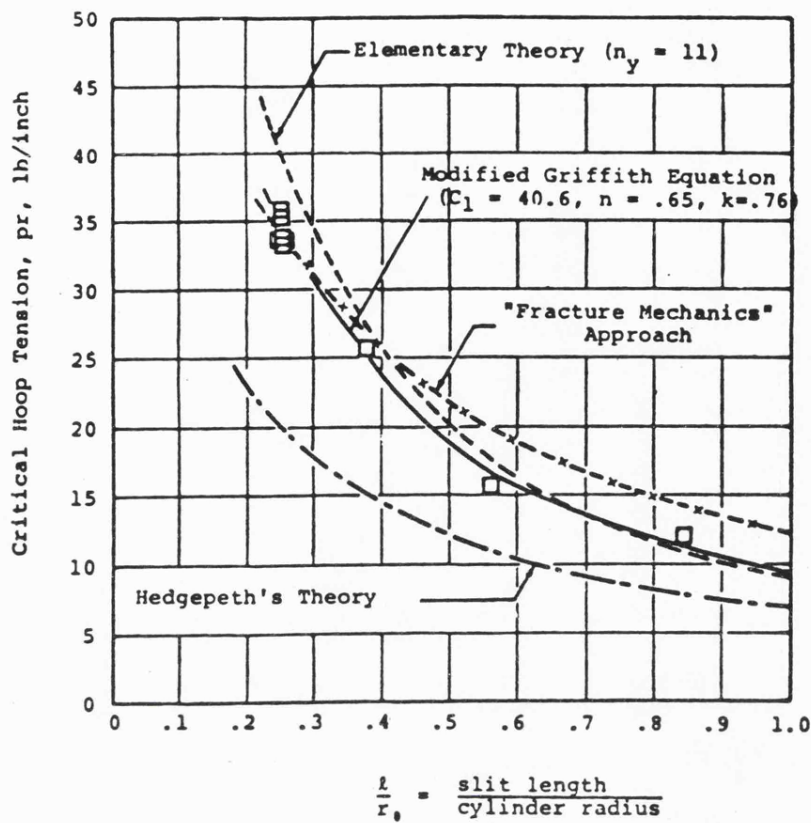


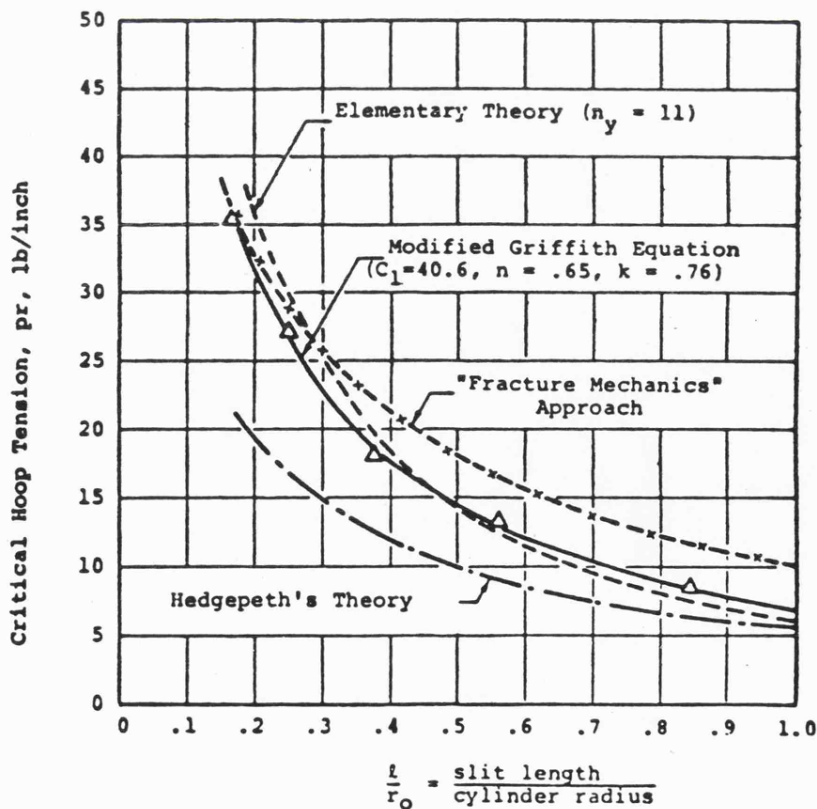
FIG (4.14)



a. Burst strength of an 8-inch diameter

Dacron-Neoprene  
Fabric N337A15

Data Points  $\Delta$   
 $k = 0.76$  for all theories

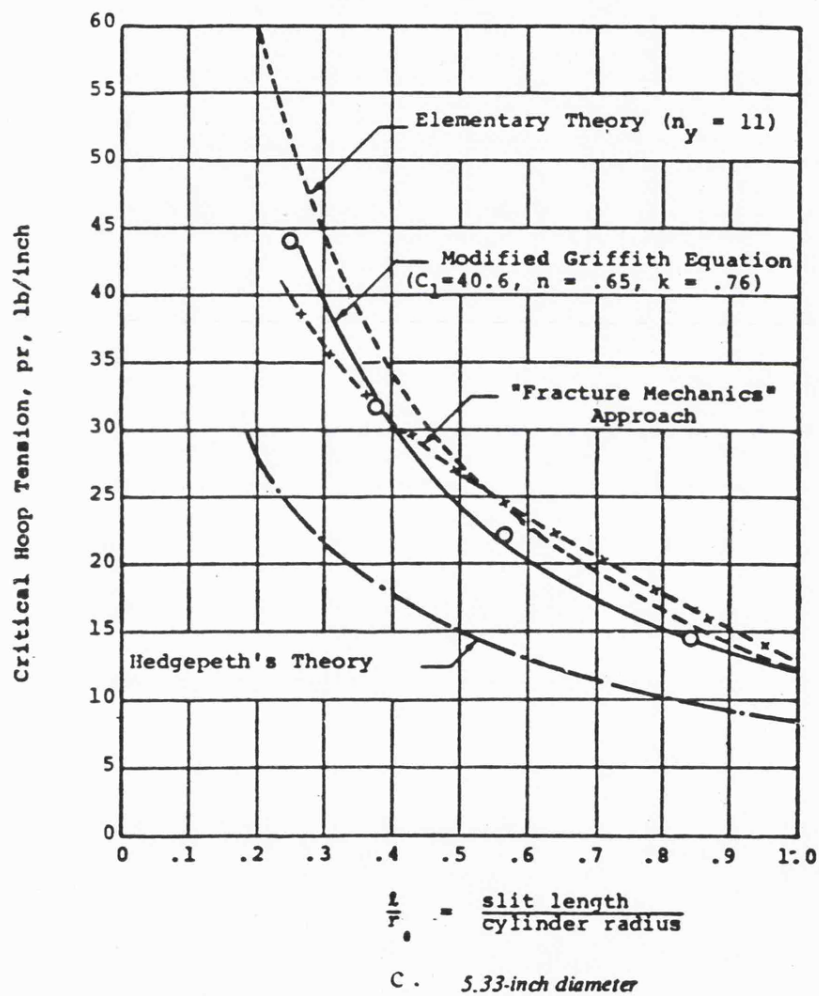


fig(4.15)

b. Burst strength of a 12-inch diameter  
Slit cylinder - test vs theory.

Dacron-Neoprene  
Fabric N337A15

Data Points O  
 $k = 0.76$  for all theories



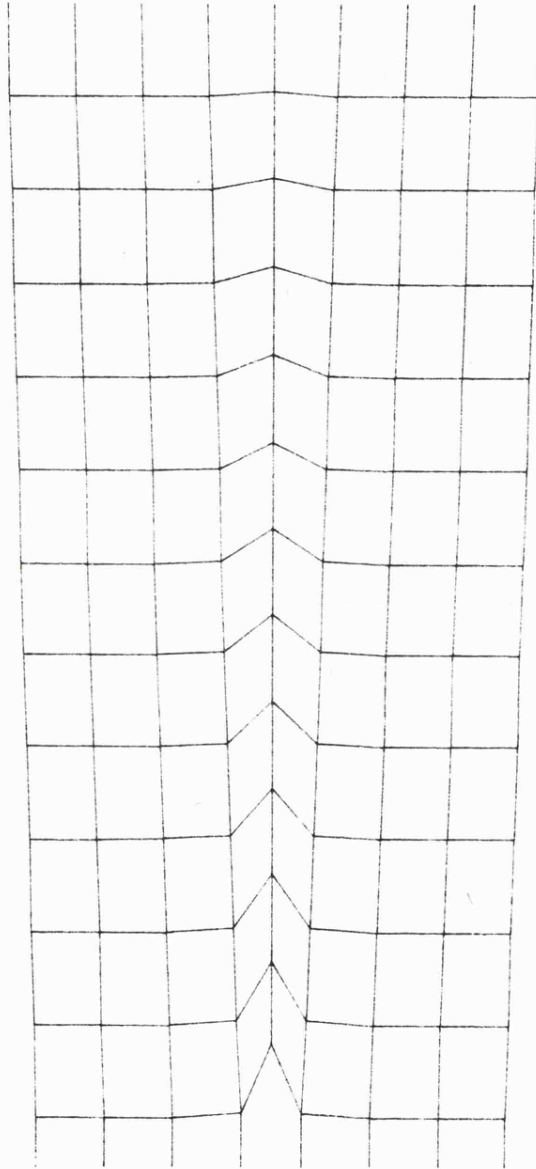


FIG (4.16)

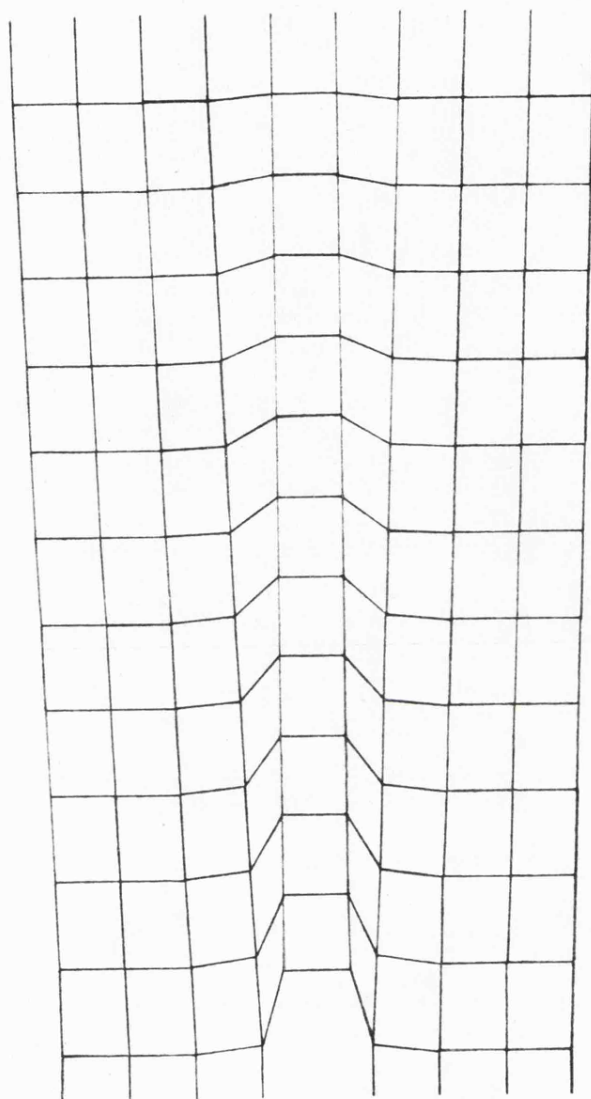


FIG (4.17)

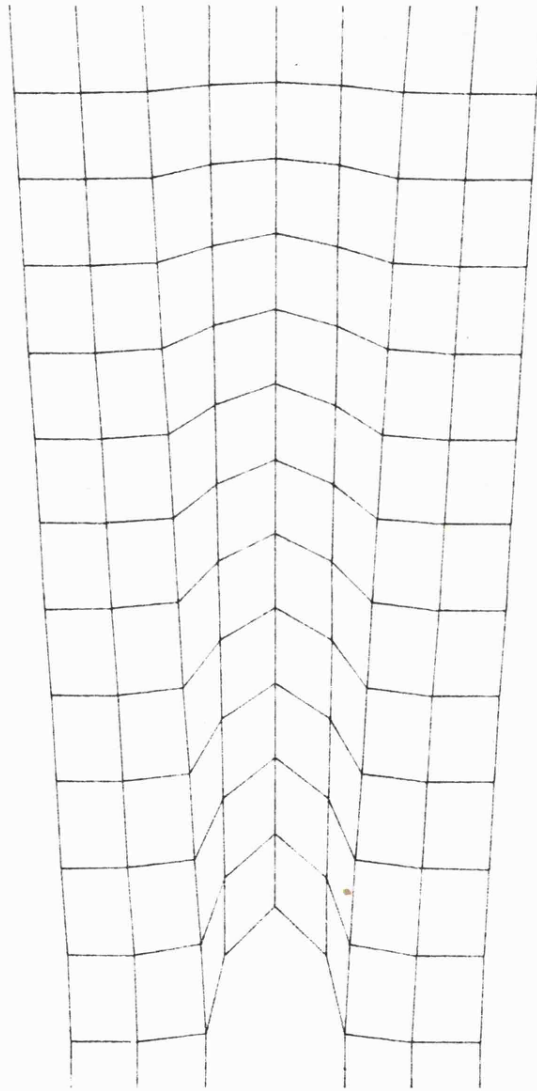


FIG (4.18)

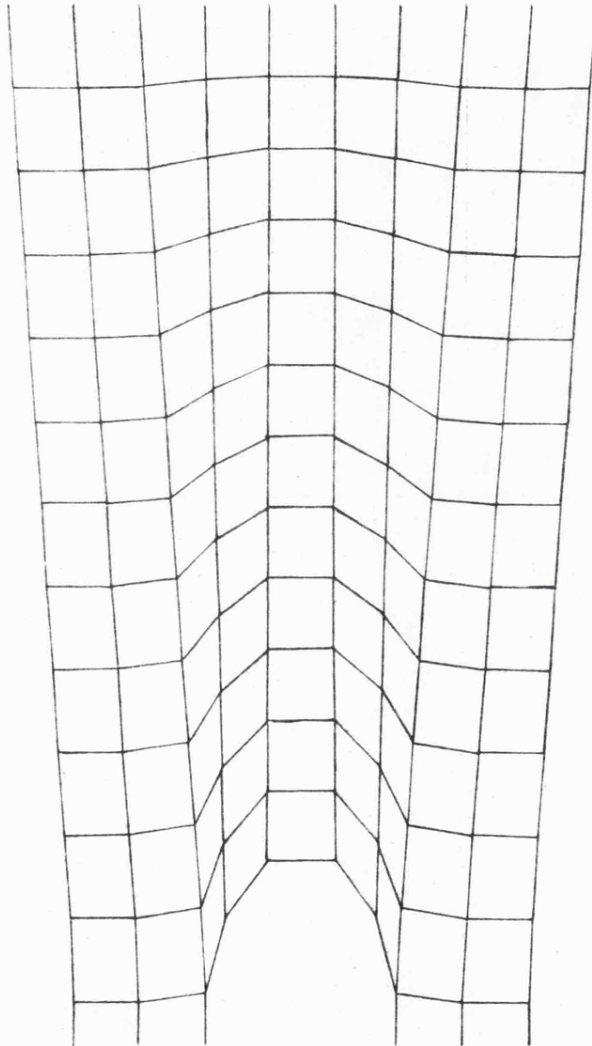


FIG (4.19)



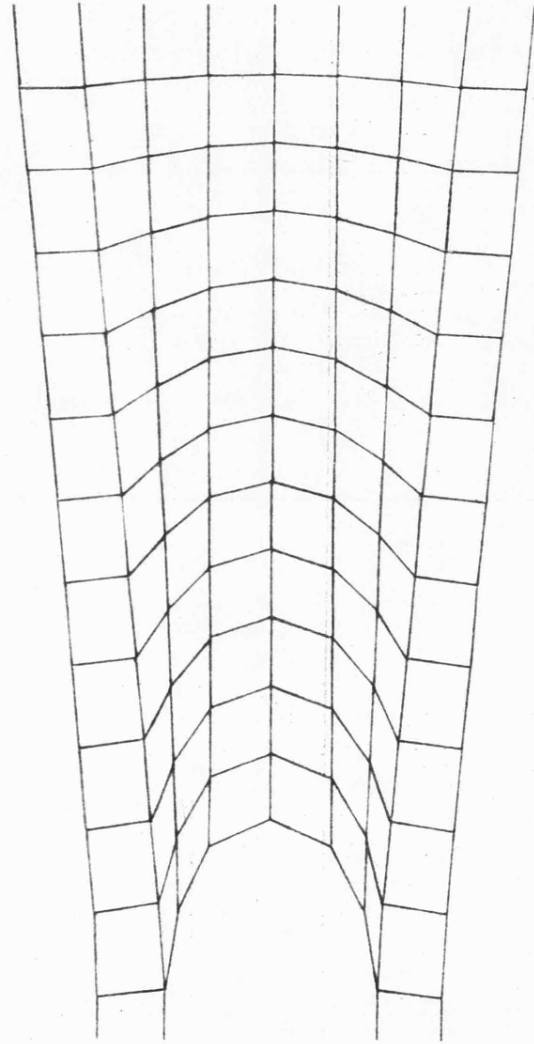
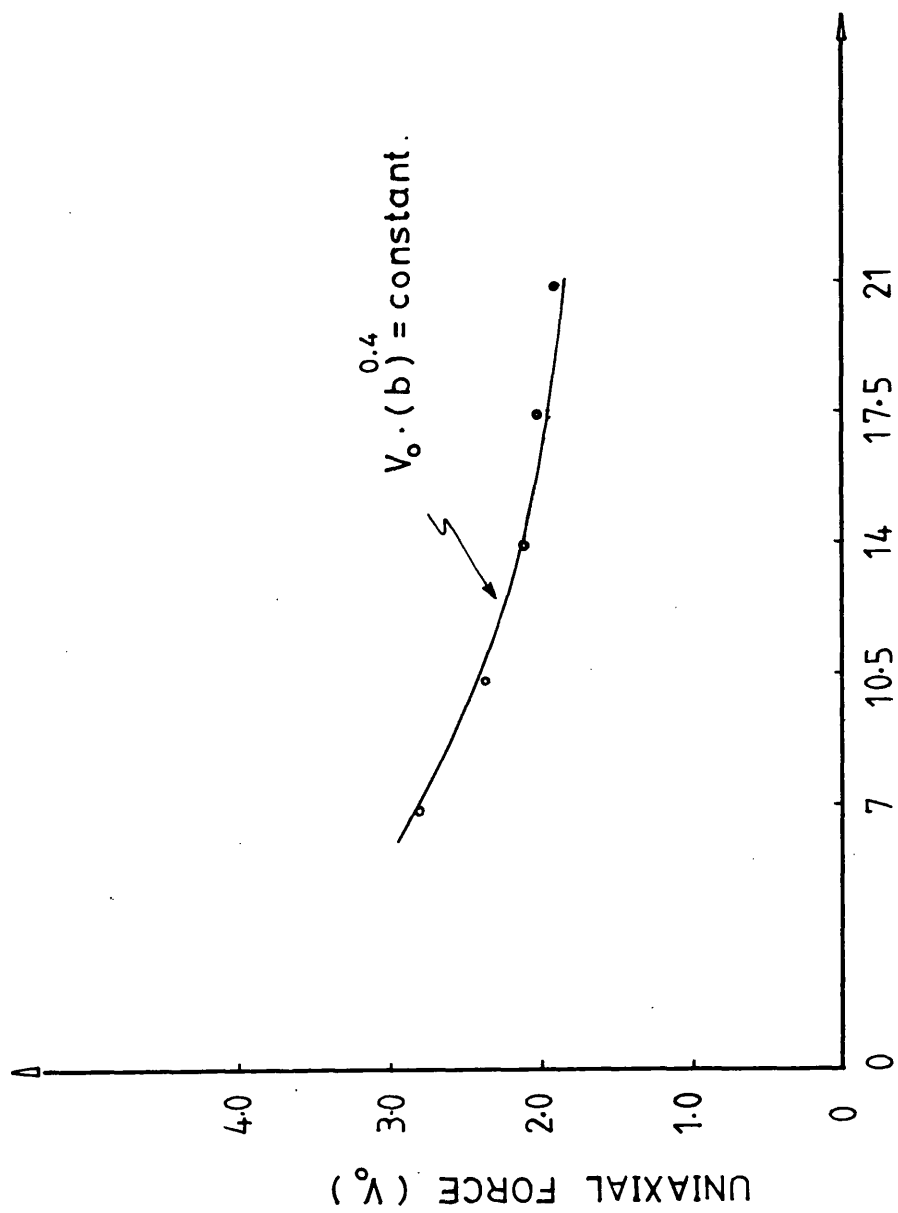
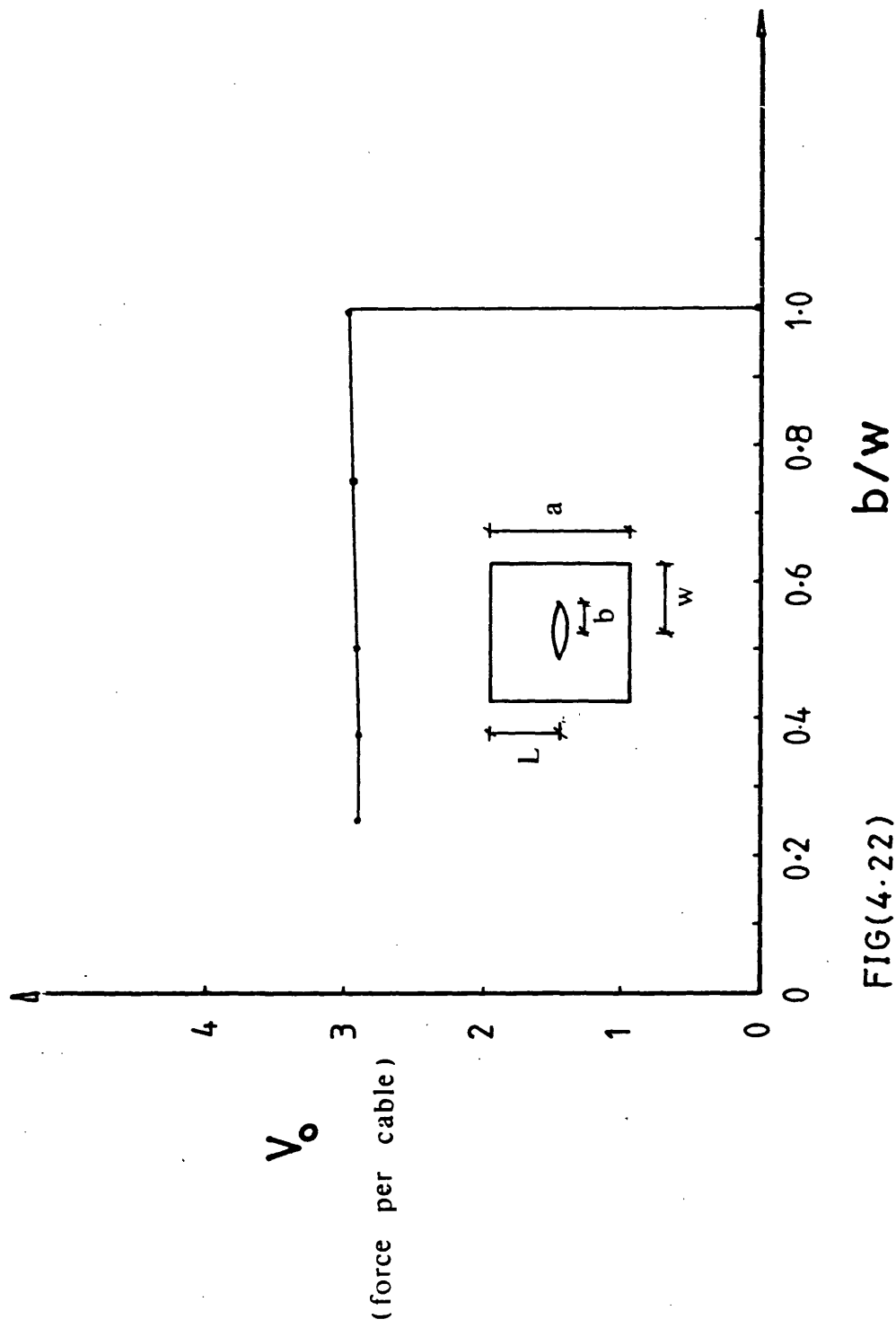


FIG ( 4 · 20 )



FIG(4.21) HALF THE CRACK LENGTH ( b )



FIG(4.22)

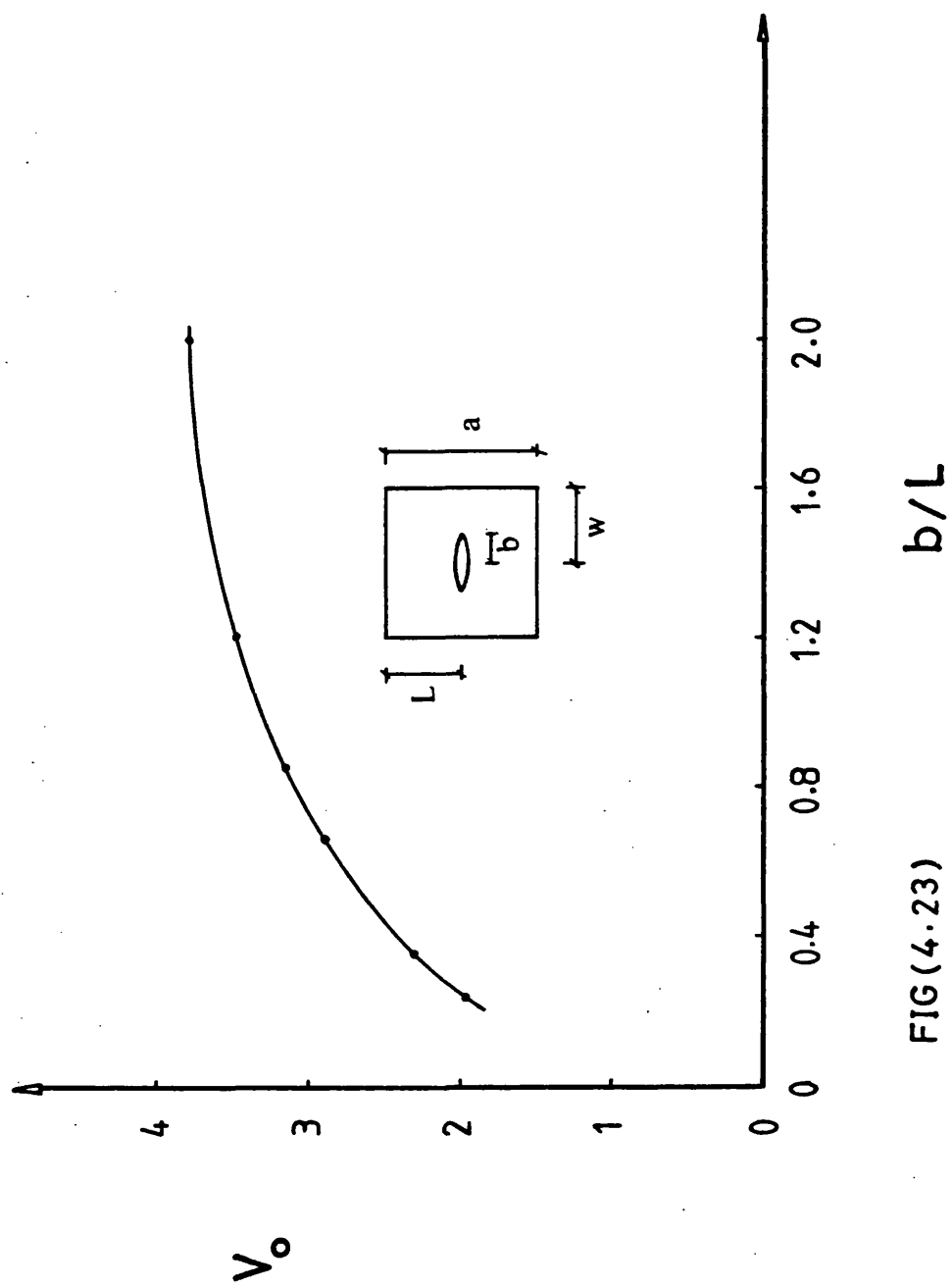


FIG (4.23)

 $b/L$

## CHAPTER 5

THE EFFECT OF JOINT SLIPPING ON  
THE CRACK PROPAGATION BEHAVIOUR  
OF STRUCTURAL NETS

## CHAPTER 5

### THE EFFECT OF JOINT SLIPPING ON THE CRACK PROPAGATION BEHAVIOUR OF STRUCTURAL NETS

#### 5.1. Introduction

In cable networks, the net is held together by friction grips or clamps applied at the nodal points. Fig. (5.1) shows typical clamp arrangements (31).

Ideally, the stresses in a structural net should be evenly distributed, but in situations where a stress concentration region occurs in the net and if as a result, the difference between the cable's tensile force on both sides of a clamp exceeds the value of the friction force, then the clamp will slide along the cable releasing the excess force until an equilibrium state is achieved. So, joint slipping simply means relaxing the high stresses in one cable by sharing it with other adjoining cables.

The relevance of joint slipping to the problem of crack propagation in structural nets is quite obvious, and with the presence of a high stress concentration region around the crack tip, an efficient design of the clamps allowing a controlled amount of joint slipping at high levels of stress concentration could mean the difference between a crack propagating or not. Also, since experimental work (7) showed that in some cases coating of woven fabric nets had a detrimental effect on its resistance to crack propagation, it is important to have a better understanding of the consequence of joint slipping, to be able to assess how much of this detrimental effect is attributed to the prevention of the slipping by coating.

## 5.2. Factors Affecting the Value of the Slipping Force

A biaxial stress field, the fixed grips loading case, was adopted in studying the effect of joint slipping on the crack propagation behaviour. As a result of the discrete analysis work conducted in the previous chapter for a biaxial stress field, the main factors which affect the value of the maximum slipping force at the crack tip region could be summarised as follows.

### (1) The boundary force

As the value of the boundary force increases, both the crack tip force and the slipping force increase, and while the value of the crack tip force was found to be proportional to the value of the initial boundary force per cable, the slipping force increased rather more rapidly. i.e. The ratio of the slipping force to the crack tip force increased.

nc	Initial Boundary Force Per cable (force units)	Crack Tip Force	Maximum Slipping Force
1	3.0	3.89	0.72
2	2.52	3.89	0.95
3	2.21	3.89	1.09
4	2.03	3.89	1.15
5	1.85	3.89	1.17

TABLE (5.1)

(2) The crack length

From the discrete analysis of net (1), for various crack lengths, Table (5.1) shows that as the crack length increases the value of the slipping force increases, though with a slowing rate.

(3) The extensional stiffness of the cables

For a given net configuration, maintaining the same number of broken cables and the same boundary force, an increase in the value of the cable's extensional stiffness leads to a reduction in the value of the slipping force.

(4) Net length

Comparing the value of the maximum slipping force obtained from the discrete analysis of net (1) and net (3), with one cable broken, showed a 2% increase as a result of reducing the net length, i.e. an increase in the net length means that the boundary force required to achieve the same crack tip force is reduced. This reduction results in a decrease in the value of the maximum slipping force.



### 5.3. Method of Evaluation

The procedure adopted to evaluate the effect of joint slipping on the crack propagation behaviour is as follows.

1. For a given material properties and net configuration, the discrete analysis method (Appendix (3)) is deployed to calculate the stress distribution and the final equilibrium shape for the net under the effect of a biaxial field (fixed grips loading) without allowing joint slipping.
2. A computer program was developed to check that for the equilibrium state obtained, the maximum slipping force at every nodal point is less than a specified value for the friction force. When this is true, then the equilibrium state achieved is valid and final. But, if the value of the slipping force at any node exceeds the specified limit this means that the node will slip, and an iterative technique is then used to calculate the amount of slipping necessary to obtain a state of equilibrium at this node, such that the value of the slipping force equals the specified limit.
3. Then the discrete analysis method is deployed again to calculate the new stress distribution and equilibrium shape.
4. The process is repeated until an equilibrium state is achieved which satisfies the following two conditions:
  - (i) At the nodal points which did not slip, the value of the slipping force should be less or equal to the specified value of the friction force.
  - (ii) At nodal points where slipping occurred, the value of the slipping force must be equal to the specified value of the friction force.
5. The effect of joint slipping is evaluated by comparing the stress distribution in the two equilibrium states obtained with and without joint slipping, and specially the value of the crack tip force.

#### 5.4. Presentation of the Work Done

The work done to evaluate the effect of joint slipping on the crack propagation behaviour is presented under three main headings.

- (i) Description of the net configurations studied for joint slipping and the procedure adopted.
- (ii) Presentation of some analysis samples to illustrate the different joint slipping patterns encountered.
- (iii) Detailed results and an overall assessment of the effect of joint slipping on the crack propagation behaviour.

##### 5.4.1. Description of net configurations studied and the procedure adopted

The effect of the different factors on the value of the slipping force, outlined earlier, offered some guide lines concerning the choice of the cable properties and the net configurations to put more emphasis on joint slipping. e.g. Choosing low extensional stiffness and smaller net length increases the slipping force value. So, the value of the cable's extensional stiffness used was  $AE = 7$  force units, and for different friction force values, the joint slipping analysis was carried out on the net configuration shown in Fig. (5.2), for various crack lengths.

In all cases studied the net was subjected to a biaxial stress field (fixed grips loading case) created by:

- (i) A constant force (3 force units) parallel to the crack is applied at each nodal point along the two edge cables which are normal to the crack.
- (ii) An outward constant displacement of the other two edges, resulting from a vertical wedging force (3 force units  $\times nvL$ ).

The analysis procedure adopted could be summarised as follows;

(i) Assigning a value for the friction force

First for one cable broken, the discrete analysis method was used to calculate the stress distribution at equilibrium without allowing joint slipping, and the value of the maximum slipping force, located at the crack tip region, was determined. This value was taken to represent the specified friction force at the nodal points.

(ii) Calculating joint slipping

Allowing joint slipping, the net was analysed for various crack length ( $n_c = 2 \rightarrow 5$ ), and in each case the amount of joint slipping necessary to achieve equilibrium was calculated and also the final equilibrium shape.

The whole procedure was similarly repeated for two, three and four central cables broken, i.e. for each case the corresponding friction force value, similarly assumed, was then used in net analysis allowing joint slipping, for various crack lengths.

#### 5.4.2. Different joint slipping patterns encountered

Fig. (5.3) shows a rough plotting for the expected relation between the crack tip cable force and the crack length for the different cases analysed for joint slipping, and is only intended to serve as a general layout to give the joint slipping pattern encountered in each case. Each point in the graph represents a case studied, and the number indicated on each point refers to the joint slipping pattern encountered in this case.

The two joint slipping patterns encountered in the analysis are shown in Fig. (5.4).

Pattern 1

Typical of the joint slipping behaviour for the majority of the cases studied, in which the slipping of one joint (A) at the crack tip was sufficient to achieve an equilibrium state which satisfies the following conditions.

- 1 The final slipping force across joint (A) equals the specified friction force value.
- 2 Everywhere else in the net, the slipping force is less than or equal to the specified value for the friction force.

Pattern 2

As joint (A) slipped to relax the stress concentration at the crack tip, the tensile force in cable (A-B) increased to such an extent that the slipping force across joint (B) exceeded the specified value for the friction force, thus causing joint (B) to slip.

After the slipping of joints (A) and (B) an equilibrium state was achieved such that:

- (i) The final slipping force across joint (A) equalled that across joint (B) and both were equal to the specified value for the friction force.
- (ii) The slipping force everywhere else was less than the specified value.

The effect of the two joint slipping patterns can be best appreciated by examining some of the cases studied, in which the net was analysed with five cables broken, for different friction force values,

For this crack length, plotting on the same axes the final equilibrium shapes obtained for the two extreme border cases, i.e.:-

- (i) The case in which joint slipping was not allowed.
- (ii) The case in which slipping was allowed, the friction force specified was minimum and the second slipping pattern was encountered.

As shown in Fig. (5.5) indicates a significant change in the net geometry at the crack tip region due to slipping.

To examine this change further and to assess the impact of the transition from the first slipping pattern to the second, the value of the cable forces along section  $x - x$  were compared for the following cases:

- (i) The two extreme cases, mentioned above.
- (ii) The case prior to that, in which the second slipping pattern was obtained.

The comparison is shown in Fig. (5.6).

#### 5.4.3. Detailed results

The results obtained for the joint slipping investigation are given in Table (5.2).

Where  $S_A$  : amount of slipping in joint (A)

$S_B$  : amount of slipping in joint (B)

and since the original length of the cables

$$L_0 = 7 \text{ length units}$$

then for a given value of joint slipping  $S_A = K$

This means that the final length of the crack tip cable became:

$$L = 7 + 2 \cdot K$$

and plotting the results in Fig. (5.7) shows the significant effect of joint slipping on the value of the crack tip force in the cases studied. Thus a similar influence on the crack propagation behaviour should be expected.

It is interesting to observe that once joint slipping occurs and an equilibrium state is achieved, increasing the length of the crack even considerably had little effect on the value of the final crack tip force.

Friction Force Specified (force units)	nc	Slipping Pattern	Amount of Slip "S" (length units)	Final Crack Tip Force (force units)
1.5437	1	0	-	3.8018
	2	0	-	4.3146
	3	0	-	4.628
	4	0	-	4.8126
	5	0	-	4.918
1.467	1	0	-	3.8018
	2	0	-	4.3146
	3	0	-	4.628
	4	0	-	4.8126
	5	1	$S_A = 0.11$	4.8496
1.3311	1	0	-	3.8018
	2	0	-	4.3146
	3	0	-	4.628
	4	1	$S_A = 0.18$	4.7039
	5	1	$S_A = 0.30$	4.7354
1.098	1	0	-	3.8018
	2	0	-	4.3146
	3	1	$S_A = 0.34$	4.4413
	4	1	$S_A = 0.52$	4.5132
	5	1	$S_A = 0.60$	4.5635
0.7037	1	0	-	3.8018
	2	1	$S_A = 0.62$	4.0192
	3	1	$S_A = 0.93$	4.1427
	4	2	$S_A = 1.08$	4.2369
			$S_B = 0.01$	
	5	2	$S_A = 1.20$	4.2420
			$S_B = 0.10$	

TABLE (5.2)

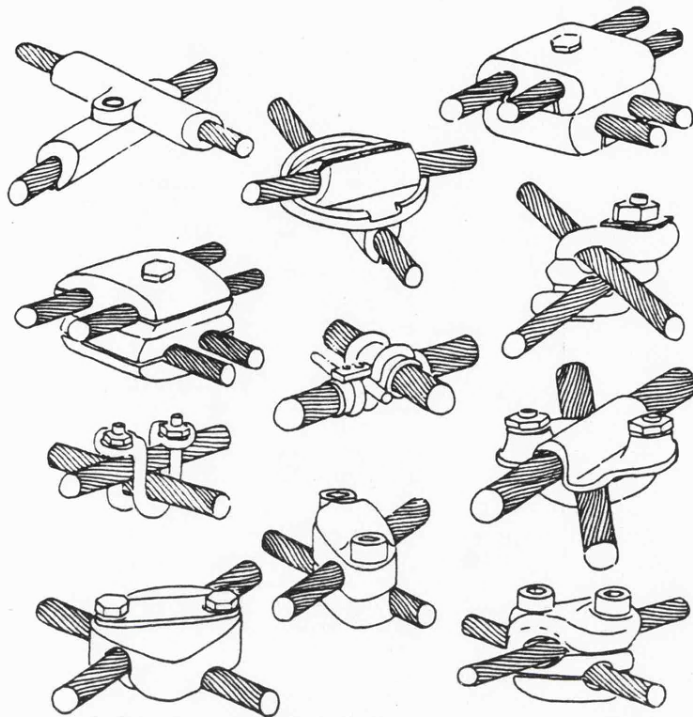
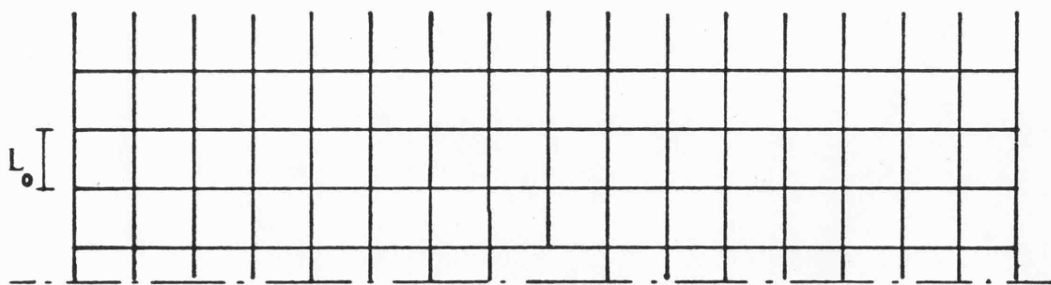


FIG (5.1)

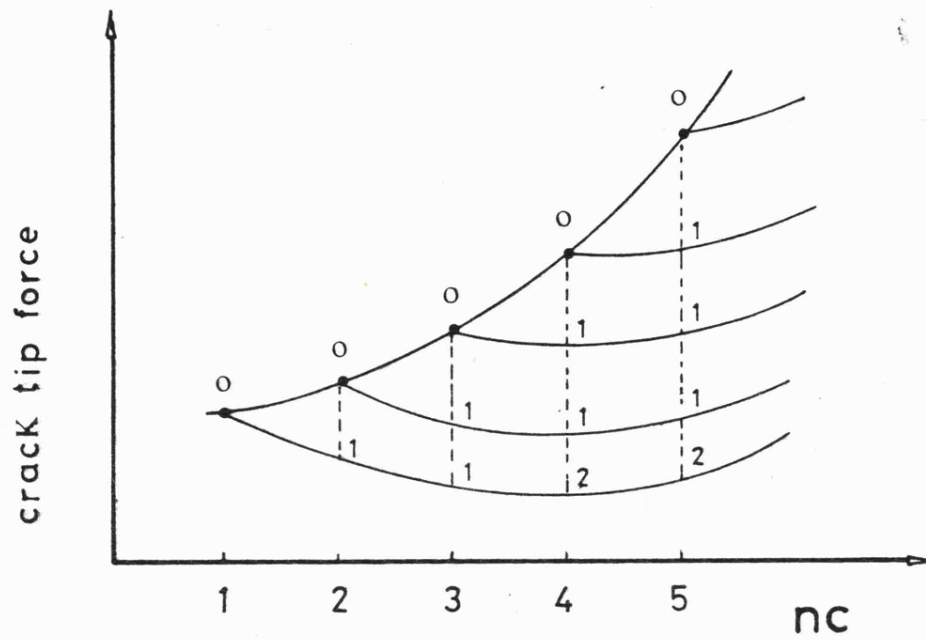


$nhl = 10$   
 $nvl = 17$   
 $nc = 1$

$L_0 = 7$

FIG (5.2)





0 : NO SLIPPING ALLOWED

FIG (5.3) 1 : SLIPPING PATTERN (1)

2 : SLIPPING PATTERN (2)

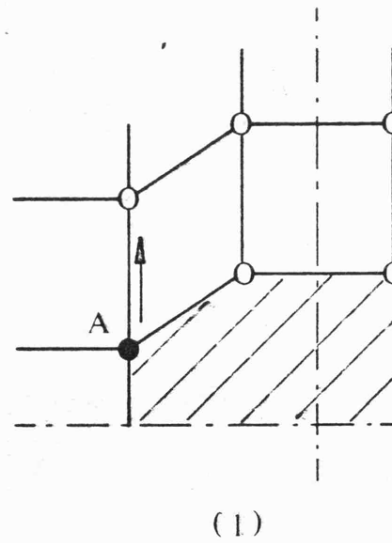
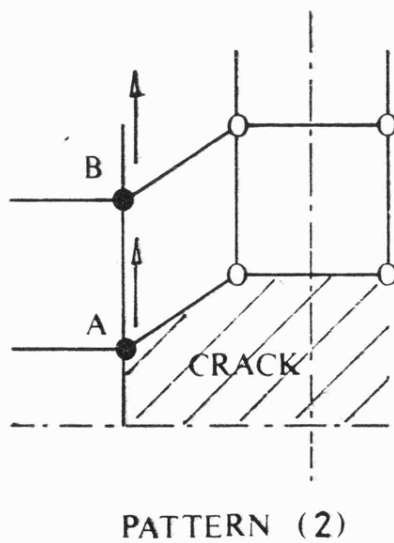


FIG (5.4)

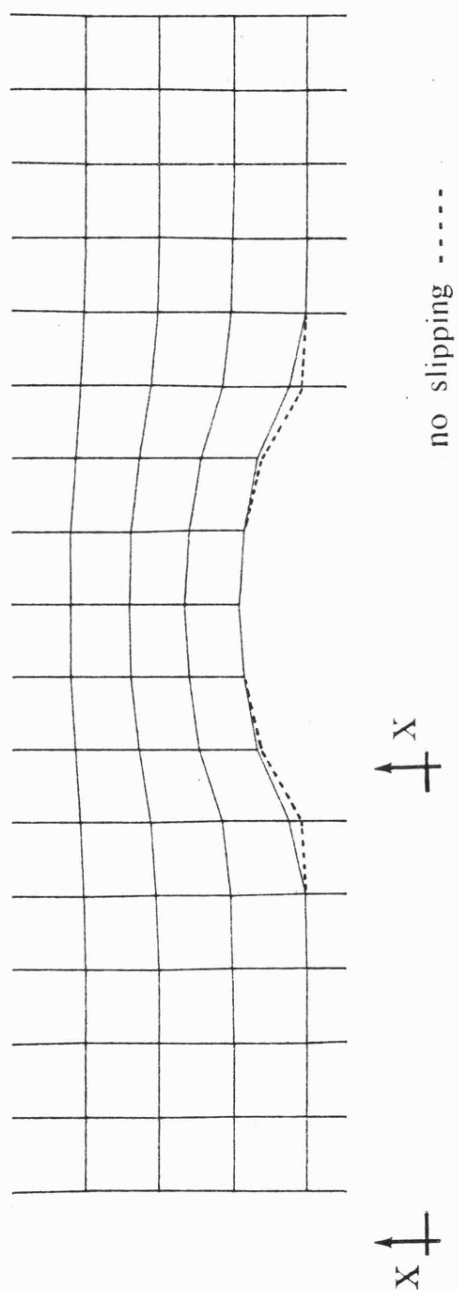
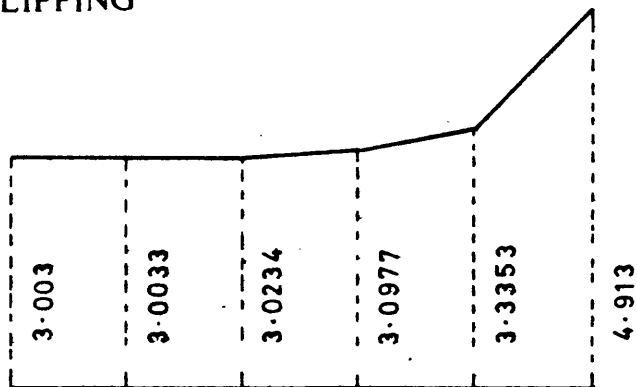


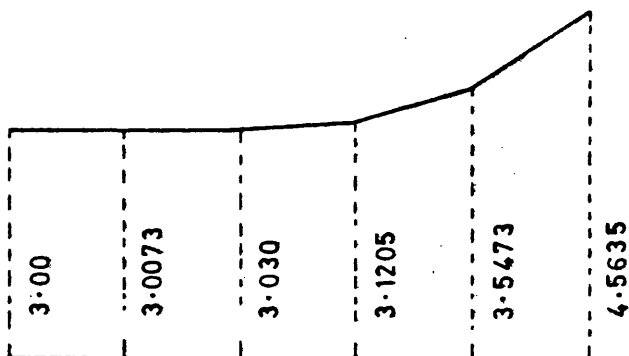
FIG (5.5)

## ★ NO SLIPPING



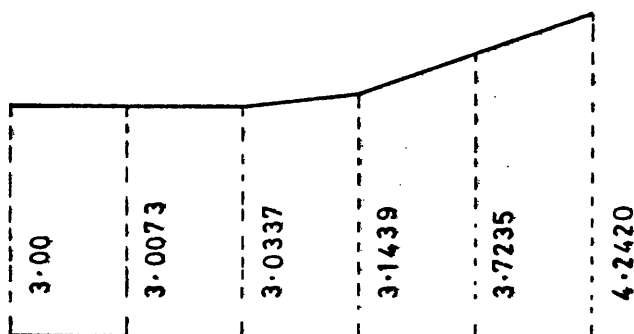
MAX SLIPPING FORCE = 1.5437

## ★ PATTERN (1)



MAX SLIPPING FORCE = 1.093

## ★ PATTERN (2)



MAX SLIPPING FORCE = 0.7037

FIG(5.6) FORCE ALONG X-X

effect of joint slipping

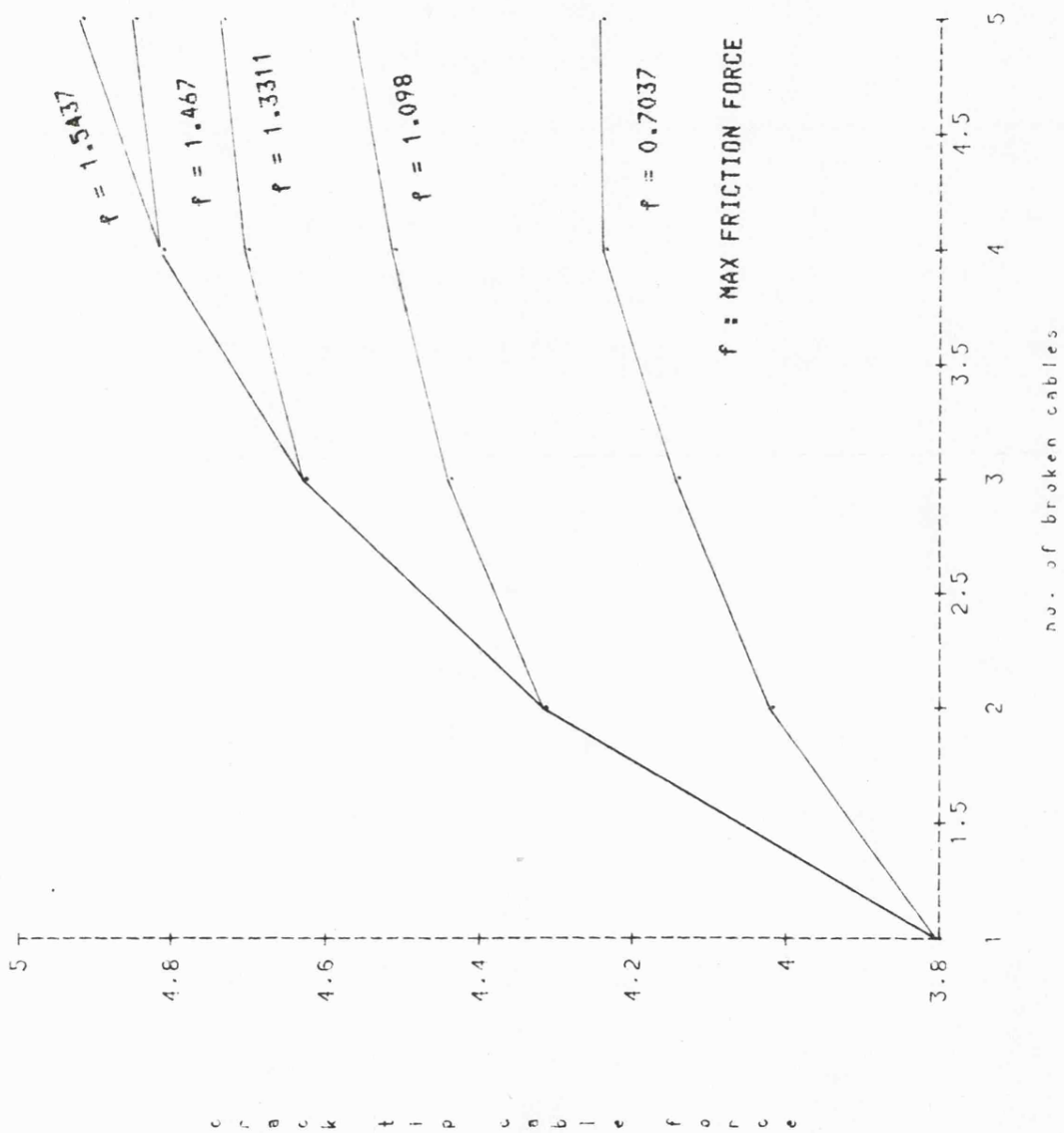


FIG ( 5.7 )

## CHAPTER 6

### EXPERIMENTAL INVESTIGATION OF TEAR PROPAGATION IN COATED FABRICS

## CHAPTER 6

### Experimental investigation of tear propagation in coated fabrics

#### 6.1 Introduction

Experimental work was conducted to investigate the tear propagation behaviour of coated fabrics in order to provide a further experimental evaluation of the validity of the proposed solution, and in particular the relation between the uniaxial and biaxial strength of coated fabrics.

#### 6.2 Properties of coated fabric used

A filamentary material with a light coating on the surface was desired in which the following conditions are satisfied.

- (i) a plain weave base fabric
- (ii) the yarn count per unit length and the tensile strength of the fabric in both the warp and weft directions should be as equal as possible.
- (iii) the fabric had to have an essentially elastic behaviour to failure.
- (v) to simulate infinite boundary conditions, a critical balance between the specimen size and the yarn count per unit length must be achieved and since the freedom of choice regarding the specimen size was some what restricted, the chosen fabric had to have a high value for the yarn count per unit length.

These requirements were necessary to satisfy the theoretical limitations and the supposition that the yarns at the crack tip in the filamentary sheet will fail at their individual yarn strength (28).

The tensile strength of the fabric had to be within a certain limit in order to be able to obtain as much information as possible using the laboratory facilities available, specially since the tensile boundary force had to be introduced by gravity loads.

### Technical aspects of the base textile employed in the fabric tested

- (1) The fiber is continuous filament high tensile nylon 6.6
- (2) The fabric is woven from 30 denier yarns having 7.5 twists per inch and is a plain weave fabric.
- (3) The sett is 115 warp threads per inch by 102 weft threads per inch.
- (4) The fabric weight is nominally 0.9 oz/yd<sup>2</sup> (30 g/m<sup>2</sup>).
- (5) Typical tensile strength of the fabric is:  
     Warp direction - 38 lbs/inch  
     Weft direction - 32 lbs/inch

Fig (6.1) shows a typical stress - strain curve for the coated fabric.

### 6.3 Shape of the specimens

#### (i) Uniaxial test specimen

Fig (6.2) show the specimen dimensions which was used in the uniaxial tests.

#### (ii) Biaxial test specimen

Before starting any tear propagation tests, it was vital to ensure that any measured value for the biaxial strength of the specimen did represent, at least to a reasonable extent, the true biaxial strength of the fabric. Reinhardt (30) investigated this problem and designed a suitable specimen shape, using which he managed to achieve a biaxial strength equal to the uniaxial strength of the fabric.

Adopting a specimen shape similar to Reinhardt's slitted cross-shaped specimen as shown in fig (6.4a), a biaxial strength of only about 45 percent of the uniaxial value was achieved, then fracture started in the corner of the square field and ran along the edge.

The reason for this failure could be explained by the fact that, although the overall size of the fabric specimen in both cases was roughly the same, the yarn count per unit length in the Reinhardt specimen was at least one order of magnitude smaller than that for the tested specimen.

This means that the Reinhardt specimen is effectively much smaller and the effect of the cuts in the strips and the corners which both act as stress intensifiers, is greatly reduced. Other modifications for the specimen shape were examined in an attempt to improve the method of biaxial testing. e.g. rounding the corners of the specimen as shown in fig (6.4b) increased the value of the biaxial strength slightly, then fracture occurred along the clamp edge. But the best result obtained was a biaxial strength of 85 per cent of the uniaxial, achieved using the specimen shown in fig (6.4c).

Although avoiding sharp corners in the specimen shape slightly altered the distribution of stresses, especially at the free edges, a state of uniform biaxial stress was achieved in the square field. This specimen shape was then adopted for the tear propagation tests.

#### 6.4 Method of Testing

The tear propagation behaviour for the fabric specimens was investigated under the effect of both uniaxial and biaxial stress fields. The boundary force acting at the clamps was introduced by gravity loads through a system of pulleys, then using a sharp blade the crack was initiated gradually perpendicular to the warp direction, until sudden failure occurred.

For each test the chosen value for the gravity loads and the corresponding crack length were recorded.

#### 6.5 Results and discussion

##### 6.5.1 Biaxial tests

The tear propagation behaviour was studied for various degrees of field biaxiality. The gravity loads applied at the boundary were chosen in such a way that the resulting crack length required to achieve the sudden and complete failure of the



specimen satisfies the following two conditions

- (i) the crack length must be small ( $b \leq 1$  cm) compared with the specimen dimensions to ensure the simulation of infinite boundary conditions.
- (ii) in the same time the crack length had to be large enough to minimize the possibility of any errors in the measurements.

Figs (6.5) and (6.6) show a fabric specimen with a central slit under biaxial stress field conditions during the tear propagation tests.

The theoretical solution for the infinite boundary case predicts an elliptic crack shape, and the close examination of the crack shown in figs (6.5) and (6.6) does support this prediction especially since only an elliptic crack would still remain as an ellipse after being projected on another plane, whatever the angle of this projection, a fact illustrated in particular by fig (6.5). With increasing crack length the simulated infinite boundary conditions gradually change into that of the finite boundary case as shown in figs (6.7) and (6.8), and it is interesting to compare the crack shape shown in fig (6.8) with that predicted by the proposed solution for the fixed grips case shown in fig (6.9) plotted adopting the same values for the crack length and the max crack opening.

Figs (6.10) and (6.11) show the specimen after the tear propagation test, and the fact that very little plastic deformation occurred can be concluded from the shape and the smoothness of the tear.

The experimental results of the tear propagation tests are given in table (6.1) and plotting the results as shown in fig (6.12) does support the validity of the predicted relation, fig (3.4), between the uniaxial and biaxial strength of coated fabrics.

#### 6.5.2 Uniaxial tests

Tear propagation behaviour of coated fabrics under uniaxial stress field was investigated. Tests were conducted to determine the relation between the crack propagation strength and the length of the crack. Figs (6.13) and (6.14) show a specimen with central slit subjected to uniaxial stresses during the test.

The results obtained are given in table (6.2). examining the experimental values does support the validity of the predicted equation (8a) and offers support to the author's view with relation to the discussion of Racah's work mentioned in 3.3.

The results indicates that the crack propagation strength is inversely proportional to the square root of the crack length provided that the crack length does not exceed half the width of the specimen.

$\lambda = \frac{T_o}{V_o}$	$T_o$ (kgf/cm)	$V_o$ (kgf/cm)	$b$ (cm)	$V_o^4 \cdot b^2$ (kgf <sup>4</sup> /cm <sup>2</sup> )
0.336	$\frac{10.09}{15} = 0.67$	$\frac{30}{15} = 2.0$	0.875	12.25
0.427	$\frac{12.818}{15} = 0.85$	$\frac{30}{15} = 2.0$	0.85	11.56
0.50	$\frac{15}{15} = 1.0$	$\frac{30}{15} = 2.0$	1.0	16
0.50	$\frac{22.5}{15} = 1.5$	$\frac{45}{15} = 3.0$	0.40	12.96
0.50	$\frac{30}{15} = 2.0$	$\frac{60}{15} = 4.0$	0.25	16
0.666	$\frac{24}{15} = 1.6$	$\frac{36}{15} = 2.4$	0.70	16.25
0.759	$\frac{30}{15} = 2.0$	$\frac{39.5}{15} = 2.63$	0.575	15.82
1.0	$\frac{30}{15} = 2.0$	2.0	1.05	17.64
1.0	$\frac{36}{15} = 2.40$	2.40	0.675	15.12
1.0	$\frac{42.818}{15} = 2.85$	2.85	0.50	16.49
1.0	$\frac{45}{15} = 3.0$	3.0	0.50	20.25
1.0	$\frac{60}{15} = 4.0$	4.0	0.30	23.04
1.405	$\frac{55.5}{15} = 3.70$	$\frac{39.5}{15} = 2.63$	0.70	23.44

Table (6.1)

$v_o$ (kgf/cm)	b (cm)	$v_o^2 \cdot b$ (kgf <sup>2</sup> /cm)
$\frac{60}{15} = 4.0$	0.275	4.40
$\frac{45}{15} = 3.0$	0.50	4.50
$\frac{30}{15} = 2.0$	1.10	4.40
$\frac{19.77}{15} = 1.318$	2.50	4.34
$\frac{15}{15} = 1.0$	4.10	4.10
$\frac{6}{15} = 0.40$	6.25	1.0

Table (6.2)

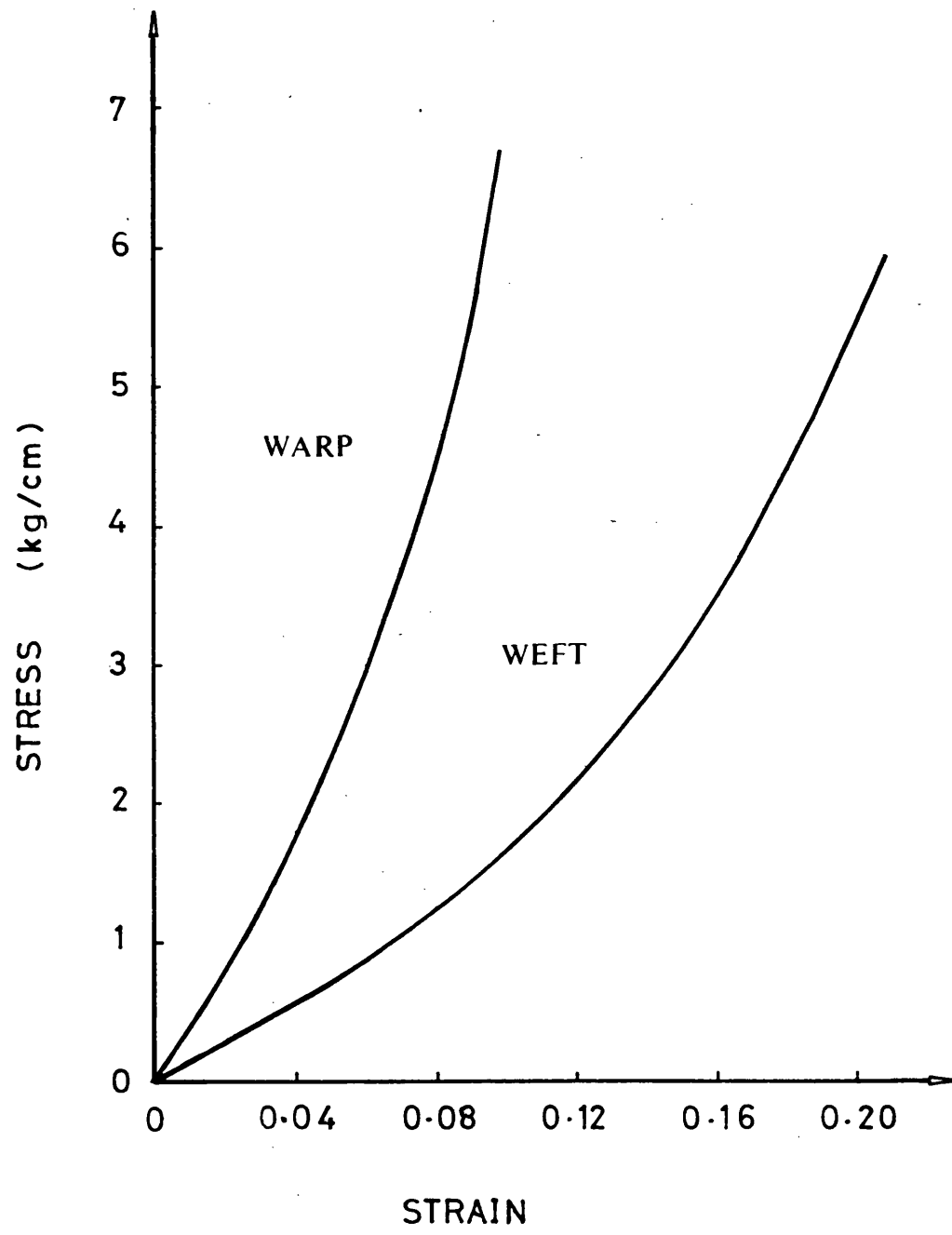


FIG ( 6.1)

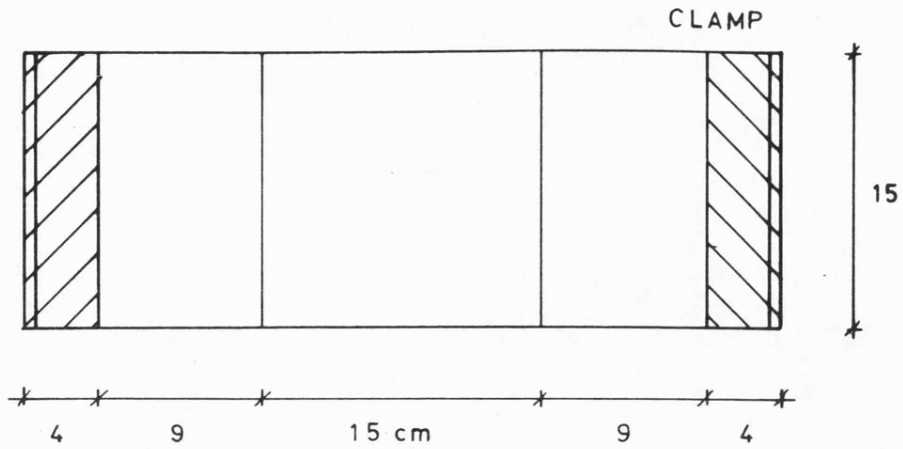


FIG (6·2) UNIA XIAL SPECIMEN

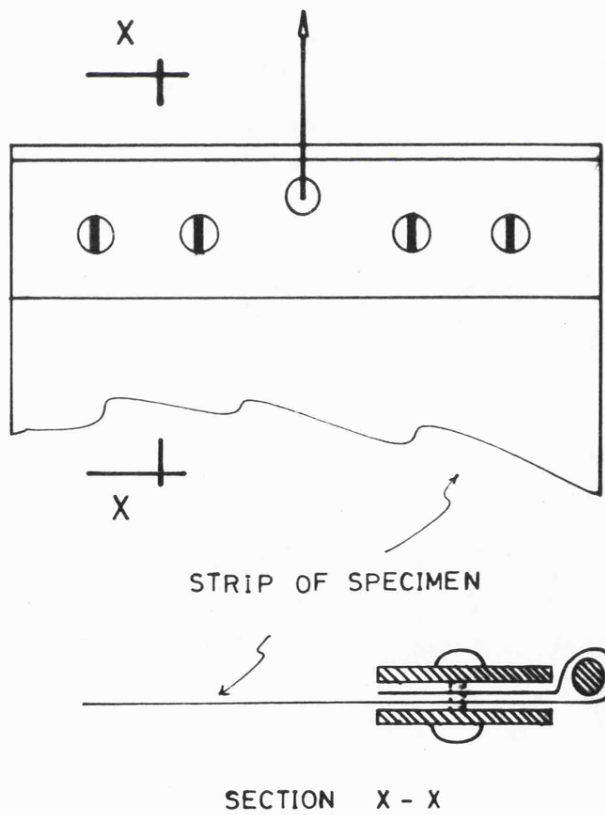
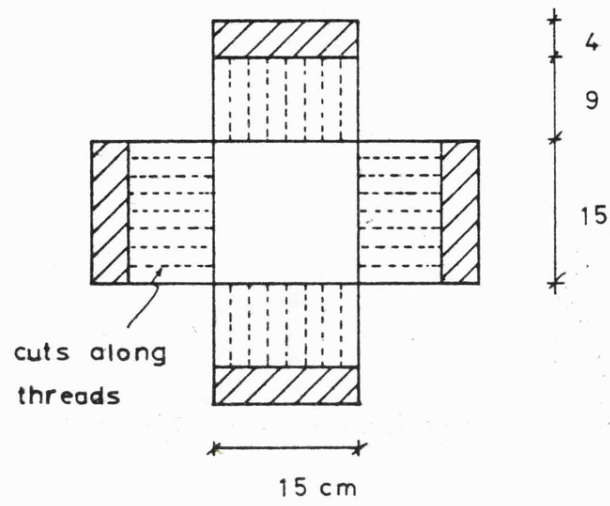
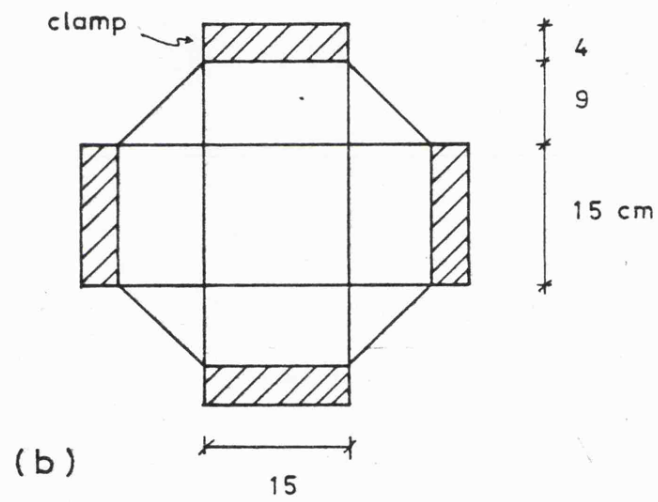


FIG (6·3)

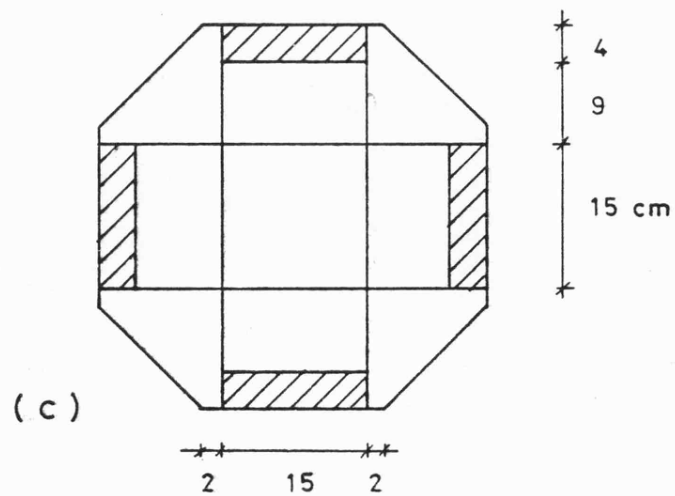
CLAMP ARRANGEMENT



(a)



(b)



(c)

FIG (6 · 4)

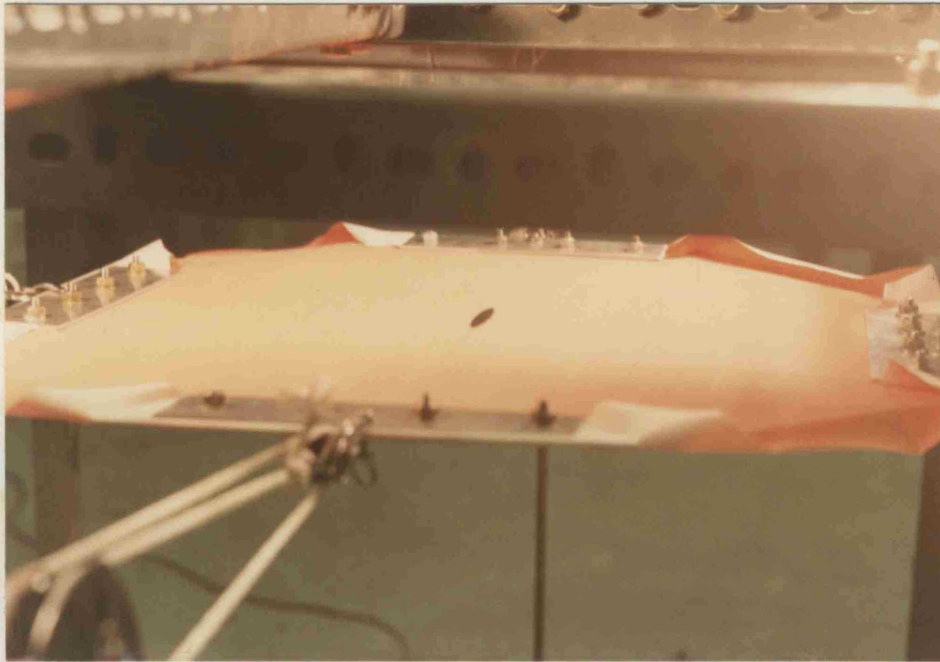


FIG (6.5)



FIG (6.6)



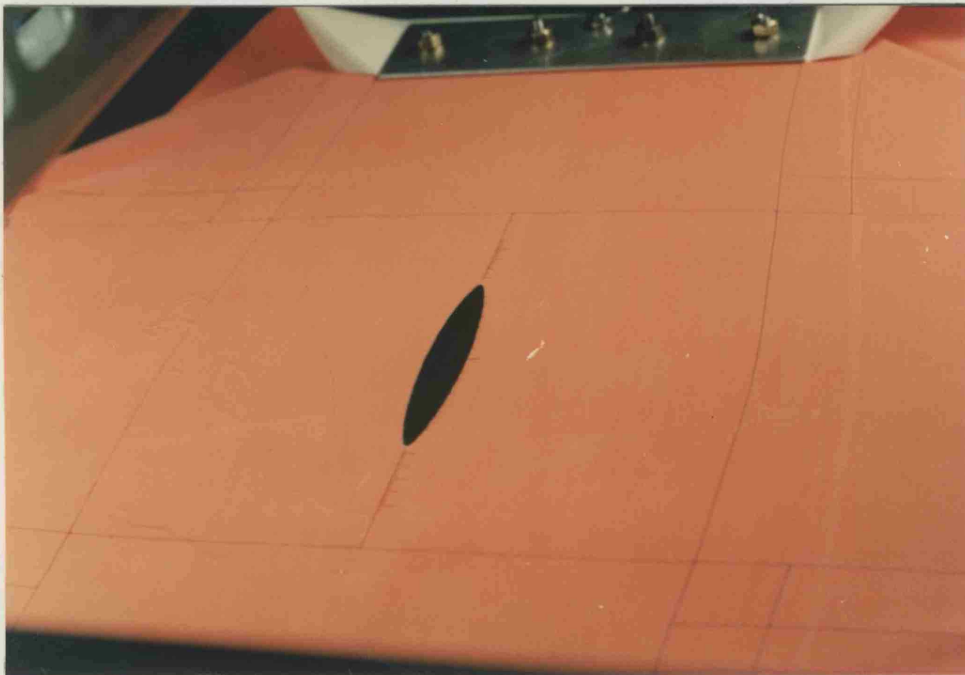


Fig (6.7) A test specimen with central slit subjected to a biaxial stress field

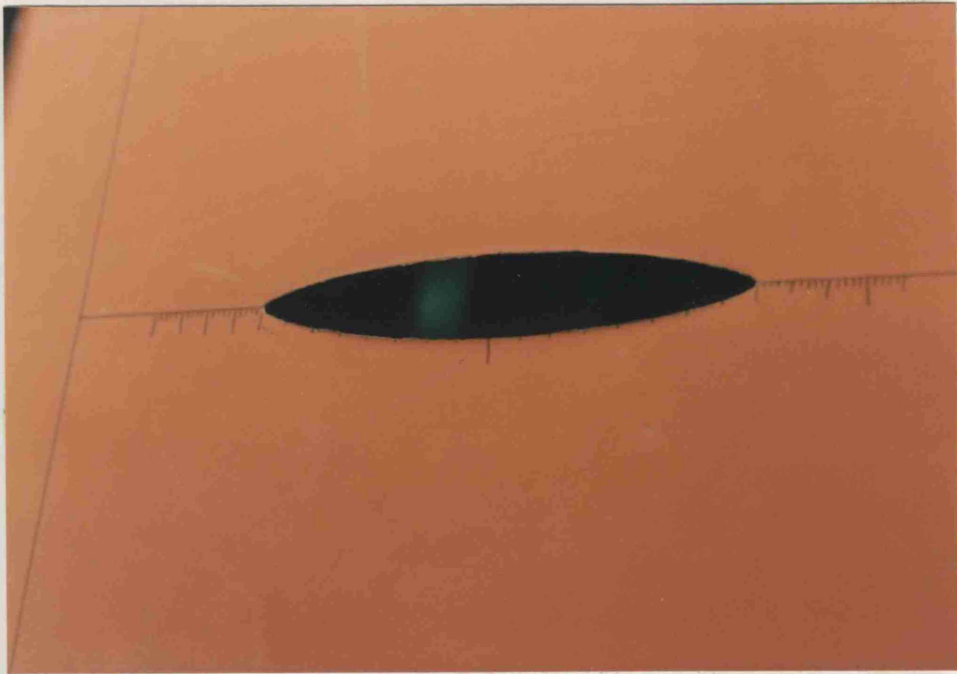


FIG (6.8)

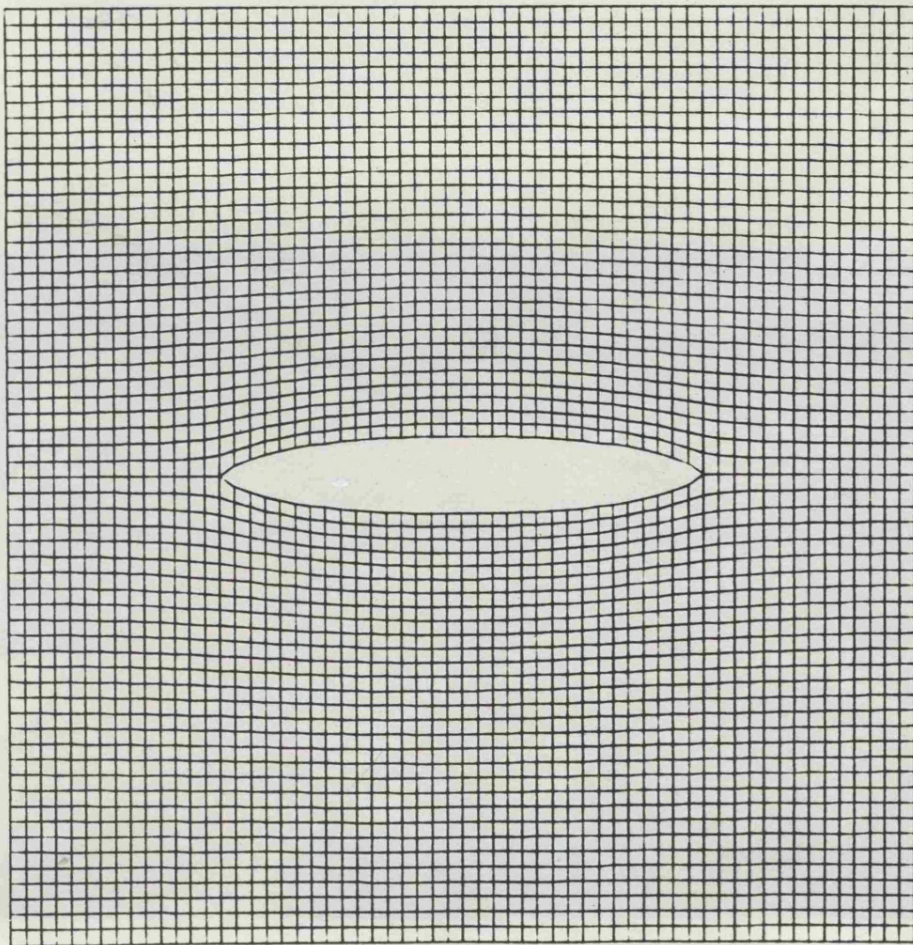


FIG (6.9)

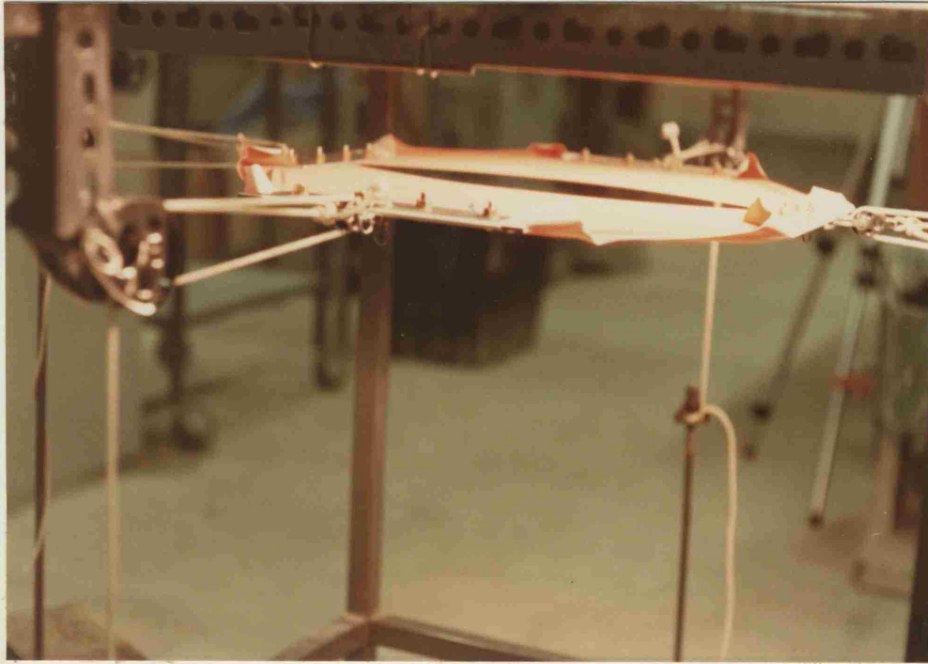


FIG (6.10)



FIG (6.11)

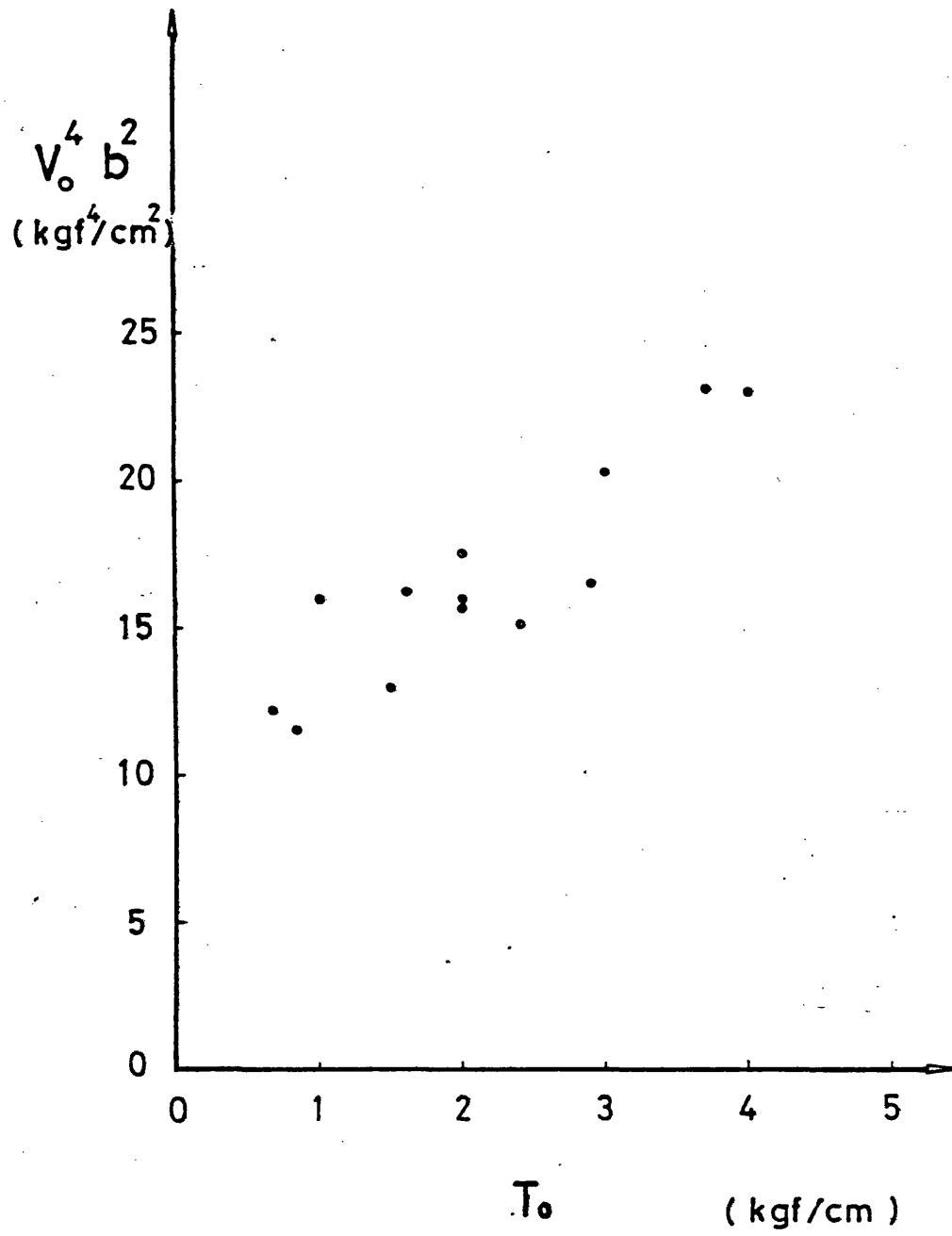


FIG ( 6·12 )



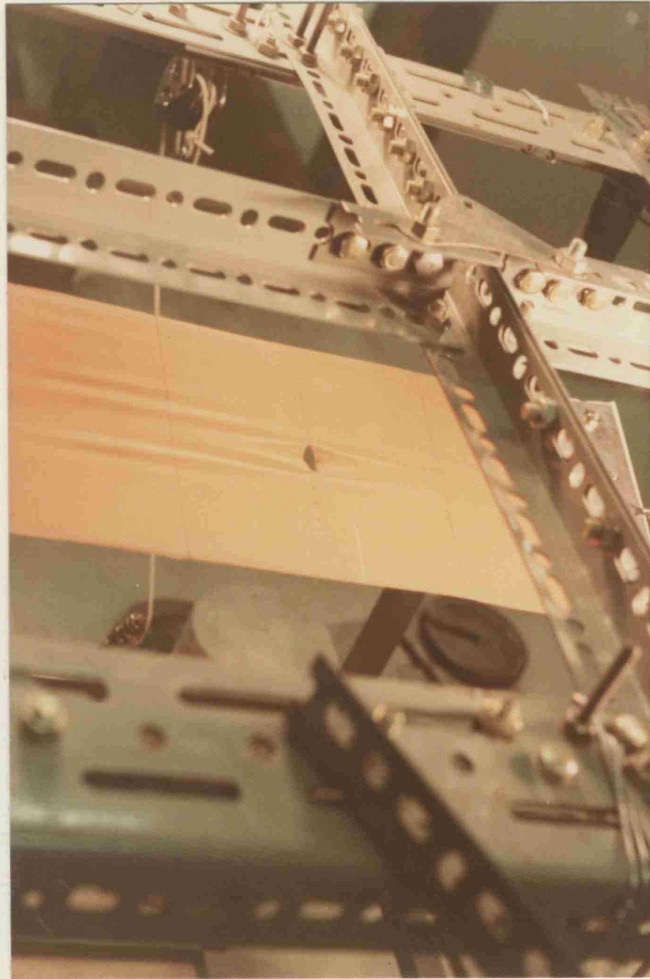


FIG (6.13)



FIG (6.14).

## CHAPTER 7

### CONCLUSIONS

## CHAPTER 7

### Conclusions

The experimental and analytical work conducted in this investigation confirms the validity and reliability of the theoretical expression proposed to predict the crack propagation behaviour of structural nets and fabrics. The study showed that the value of the fracture toughness depends only on the inherent material properties of the net, and is independent of all other external factors such as the net size, crack length or even the boundary tension.

The discrete analysis conducted offered a useful insight to the distribution of stresses in a fractured membrane subjected to tensile forces, specially for uncoated nets subjected to a uniaxial stress field, a case for which no mathematical treatment is available. and it showed that in a biaxial stress field, fixed grips loading, the relation between the critical boundary tension per cable and the crack tip stress is linear, i.e. that the concept of a stress concentration factor does exist, as in isotropic homogeneous materials.

Tests designed to simulate the boundary conditions adopted in deriving the proposed expressions can be used to determine the fracture toughness for light nets such as woven fabrics, especially since they behave roughly in an elastic manner (9), (14), (15), (28). Alternatively to avoid biaxial testing which is more difficult and expensive, the proposed relation between the biaxial and uniaxial strength can be used to evaluate the biaxial strength from a uniaxial test results.

The only remaining problem is in calculating accurately some material constants such as the value of the shear modulus of the coated fabric. However the present work does propose a test in an attempt to overcome this problem, and also Minami (9) conducted a study on the representation of material constants using a finite element method, and suggested a value for the ratio between the shear modulus and the modulus of elasticity, which can be used until better methods to evaluate such constants are devised.

The investigation drew the attention to the importance of joint slippage, especially in cable networks, and its effect on the redistribution of stresses. Further research in this topic is required to improve the methods of clamp design, which would eventually lead to a more efficient and safer structure.

Finally, the excellent correlation between the proposed expression and the different theoretical and experimental work previously published which apparently seemed to be contradictory established the validity and the reliability of the proposed solution.



## References

- (1) Griffith, A.A., "The phenomena of Rupture and flow in solids",  
Phil. Trans. Roy. Soc (London), Vol 221, Oct 21, 1920  
pp 163 - 198.
- (2) Irwin, G.R., Kies, J.A., "Fracturing and fracture dynamics"  
Weld.J.Res. suppl. 1952 17,95 S.
- (3) Orowan, E., "Energy criteria of fracture", Weld.J.Res. suppl.  
1955 20, 157 S.
- (4) Happold, E., Dickson, M.G.T., "Introductory paper: Review of  
the current state of the industry", Proceedings of the symposium  
on Air supported Structures: The state of the Art.  
The Institution of Structural Engineers, London, England, 1980,  
PP 5 - 22.
- (5) Happold, E., Cook, M., "A Review of Airhouses in Use", IABSE  
Colloquium in Inspection and Maintenance, Cambridge. July 1978.
- (6) Topping, A.D., "An introduction to Biaxial Stress Problems in  
fabric structures", Aerospace Engineering, Vol 20, No. 4, April 1961.  
pp 18-19, 53-58
- (7) Abbott, N.J., Skelton, J., "Crack propagation in woven fabrics"  
Journal of Coated fibrous materials, Vol 1, April 1972, pp 234-  
252.
- (8) Skelton, J., "Tearing behaviour of woven fabrics", Proceedings of  
the NATO advanced study institute on Mechanics of flexible fibre  
assemblies, Kilini, Greece, August 1979.
- (9) Minami, H., "Strength of coated fabrics with cracks", Journal  
of coated fabrics, Vol 7, No. 4, April 1978, pp 269 - 292.

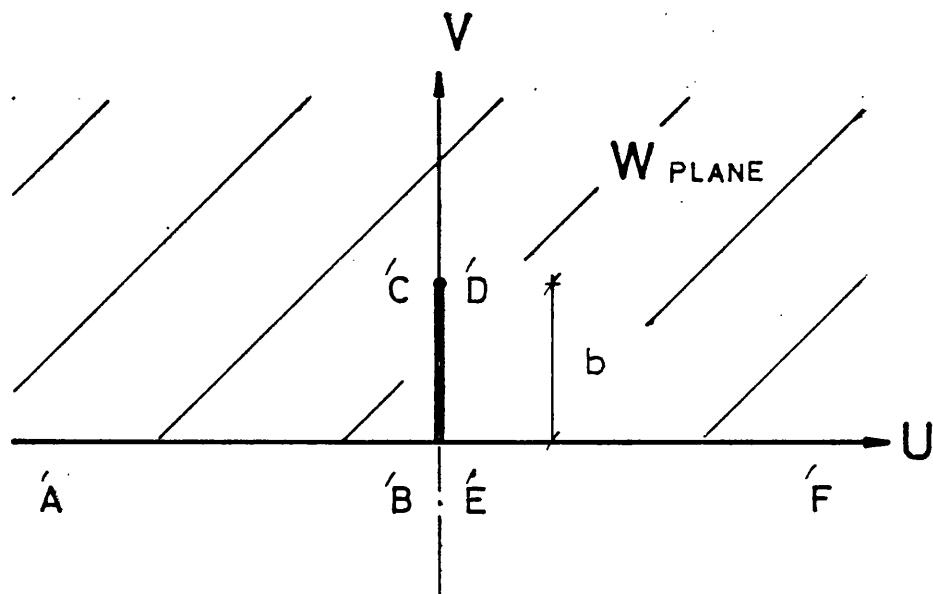
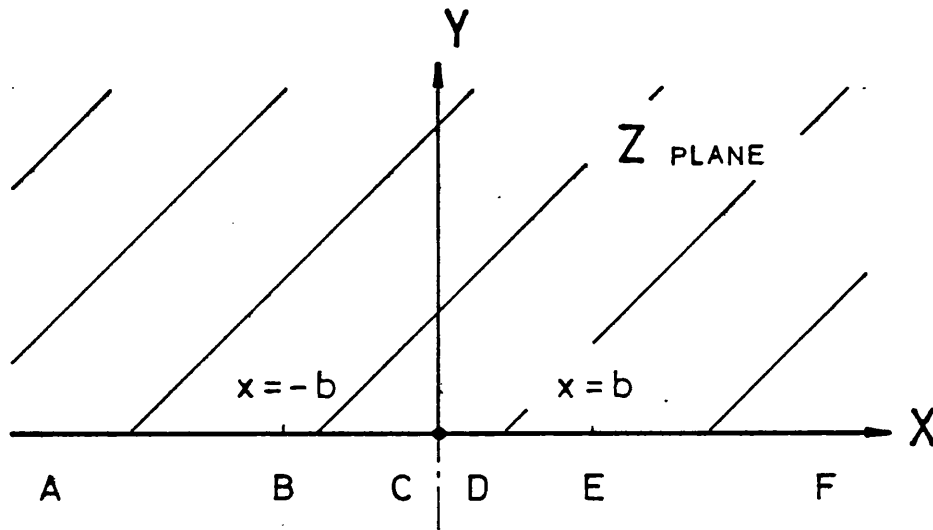
- (10) Hedgepeth, J.M., "Stress concentrations in filamentary structures", Technical Note D - 882, NASA, Washington, May 1961.
- (11) Anderson, S.L., et al, "Textiles and their testing" his majesty's stationery office, selected government Research reports, Vol 4, pp 1-4, 1949.
- (12) Topping, A.D., "The critical slit length of pressurized coated fabric cylinders", Journal of coated fabrics, Vol 3, Oct 1973, pp 96 - 110.
- (13) Deaton, J.W., Bursting strength of film and fabric plastic cylinders containing an axial slit; Transactions, 3rd Aerospace Expandable and Modular structures conference, May 1967, Miami Beach; AFAPL TR 68-17, pp 255 - 281.
- (14) KO., L, William, "Fracture behaviour of a Nonlinear woven fabric material", Journal of composite materials, Vol 9, Oct 1975, pp 361-369.
- (15) Racah E, "Crack propagation testing of coated fabrics used in surface stressed flexible structures", internal report, University of Bath, England July 1980.
- (16) "Air supported structures", draft for development 50:1976, British Standards Institution, London, England, 1976
- (17) Huisman, W.J.J., Bleker, B., "Composed skin design", IASS, International symposium on air-supported structures, Venice, Italy, June 1977.
- (18) Corten, H.T., "Fracture Mechanics of composites", Fracture-an advanced Treatise, Liebowitz, H., ed., Vol 7, academic press, New York, 1972, pp 675 - 769.
- (19) Morse, Philip. M and Feshbach, H., "Methods of theoretical physics" McGraw-Hill book company, Inc, May 1953.

- (20) Inglis, C.E., (1913) "Stresses in a plate due to the presence of cracks and sharp corners," Trans. Inst. Naval Archit. 55, 219.
- (21) Lawn, B.R., Wilshaw, T.R., "Fracture of brittle solids", Cambridge University Press. 1975
- (22) Williams, D., Crack propagation in sheet metal material - some conclusions deduced from a combination of theory and experiment, c.p. No 467, A.R.C. Technical report. 1960.
- (23) R.B.Anderson and J.L. Sullivan., Fracture Mechanics of through-cracked pressure vessels, NASA TN D-3252, Feb.1966.
- (24) R.Thomson, C.Hsieh, and V.Rana, "Lattice Trapping of fracture cracks", Journal of Applied Physics, Vol 42, No.8, July 1971.
- (25) C.Hsieh, and R. Thomson, "Lattice theory of fracture and crack creep", Journal of Applied Physics, Vol 44, No.5, May 1973.
- (26) I.A. Gaafar., "The behaviour of net structures subjected to static loads",MSc thesis, University of Strathclyde, 1978.
- (27) Barnes, M.R., "Form-finding and analysis of tension space structures by dynamic relaxation", PhD thesis, The City University October 1977.
- (28) G.W.Zender and J.W.Deaton, "Strength of filamentary sheets with one or more fibers broken", NASA TN D- 1609, March 1963.
- (29) P. Krishna., "Cable suspended roofs", McGraw-Hill book company 1978.
- (30) Hans.W. Reinhardt, "On the Biaxial testing and strength of coated fabrics", Experimental mechanics, February 1976.
- (31) "Nets in nature and Technics" a publication of the institution for lightweight structures (IL), University of Stuttgart, 1972.

## APPENDIX (1)

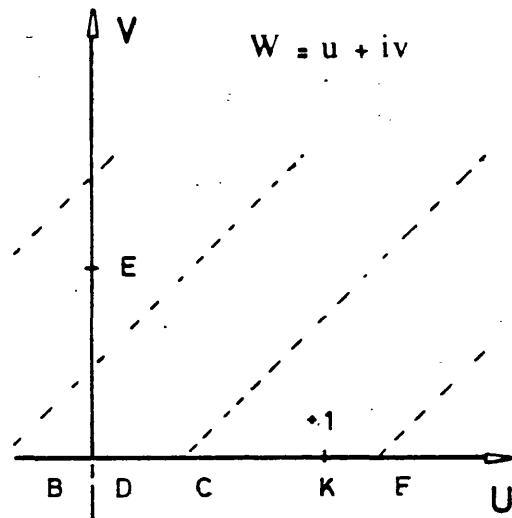
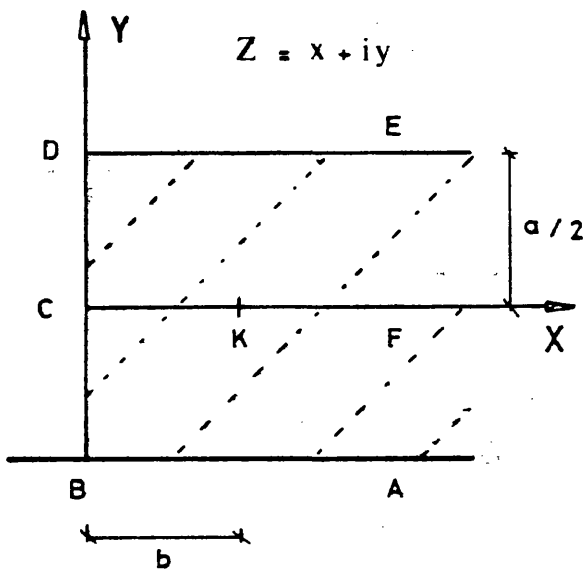
Appendix (1.1)

\* Infinite boundary case :

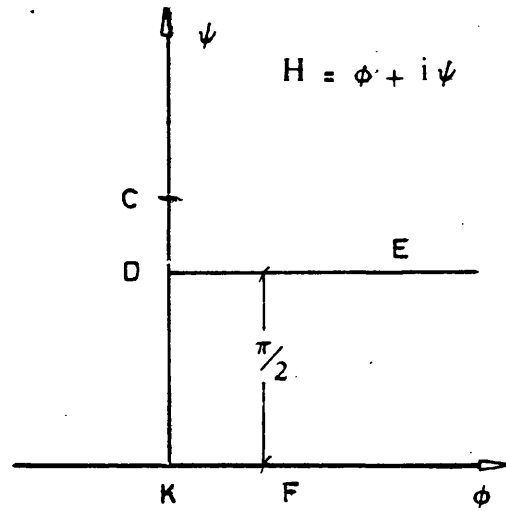
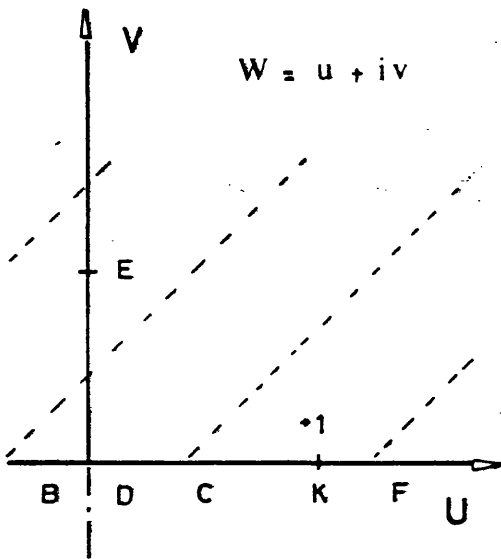


$$W = U + iV = \sqrt{Z^2 - b^2}$$

\* Fixed grips case :



$$W = \frac{\cosh\{\pi Z/a\}}{\cosh\{\pi b/a\}}$$



$$H = \cosh^{-1}(w)$$

$$\therefore H = \phi + i\psi = \cosh^{-1} \left\{ \frac{\cosh\{\pi Z/a\}}{\cosh\{\pi b/a\}} \right\}$$

APPENDIX (1.2)\*FIXED GRIPS LOADING CASE

$$\text{Area of the crack} = 4 \int_0^b \phi \cdot dx$$

$$= 4 \int_0^b \frac{Ta}{\pi} \cos^{-1} \left[ \frac{\cosh \left( \frac{\pi x}{ac} \right)}{\cosh \left( \frac{\pi b}{ac} \right)} \right] dx$$

This integration cannot be evaluated, but since

$$\frac{\partial W_r}{\partial b} = - V_o Ta \cdot \tanh \left( \frac{\pi b}{ac} \right)$$

and integrating with respect to b

$$\begin{aligned} \therefore W_r &= - V_o Ta \int \tanh \left( \frac{\pi b}{ac} \right) db \\ &= - V_o Ta \left[ \frac{ac}{\pi} \cdot \ln \cosh \left( \frac{\pi b}{ac} \right) \right] \\ &= - V_o T a^2 \frac{c}{\pi} \cdot \ln \cosh \left( \frac{\pi b}{ac} \right) \end{aligned}$$

$$\begin{aligned} \therefore \text{Area of the crack} &= \frac{W_r}{-\frac{1}{2} V_o} \\ &= 2 T \frac{a^2}{\pi} c \cdot \ln \cosh \left( \frac{\pi b}{ac} \right) \end{aligned}$$

Appendix (1.3)Fixed grips case: evaluating the strain energy released  $W_r$ :

$$\frac{\partial}{\partial b} [W_r] = - \frac{T_o^2}{AE} \cdot a \cdot \tanh \left\{ \frac{\pi b}{a \sqrt{T}} \right\}$$

$$W_r = \int - \frac{T_o^2}{AE} \cdot a \cdot \tanh \left\{ \frac{\pi b}{a \sqrt{T}} \right\} \cdot db$$

$$= - \frac{T_o^2}{AE} \cdot a \int \tanh \left\{ \frac{\pi b}{a \sqrt{T}} \right\} \cdot db$$

$$= - \frac{T_o^2}{AE} \cdot a \left\{ \frac{a \sqrt{T}}{\pi} \cdot \ln \cosh \left\{ \frac{\pi b}{a \sqrt{T}} \right\} \right\}$$

$$\therefore W_r = - \frac{a^2 T_o^2 (T)^{\frac{1}{2}}}{\pi AE} \cdot \ln \cosh \left\{ \frac{\pi b}{a \sqrt{T}} \right\}$$



## APPENDIX (2)

Discrete analysis program

```

integer dfile,rfile,c,h,l
dimension cor(500,4),ncon(500,2),difx(500),dify(500),difz(500),
&alen(500),ext(500),ae(500),p(500,3),tx(500),ty(500),ten(500),
&tenx(500),teny(500),u(500),v(500),uu(30),vv(30),
&r(30),q(500),ol(500)
write(6,5)
5 format(" number of data file")
read(5,10)dfile
write(6,15)
15 format(" number of results file")
read(5,10)rfile
10 format(i2)
read(dfile,20)n,ns,nv,nu
20 format(v)
write(rfile,25)n,ns,nv,nu
25 format(i3,1x,i3,1x,i3,1x,i3)
do 40 i=1,ns
40 read(dfile,45)(ncon(i,j),j=1,2)
45 format(v)
do 50 i=1,ns
50 write(rfile,55)(ncon(i,j),j=1,2)
55 format(i3,1x,i3)
do 60 i=1,n
60 read(dfile,65)(cor(i,j),j=1,4)
65 format(v)
do 66 i=1,ns
66 read(dfile,65)ol(i)
do 70 i=1,nu
70 read(dfile,65)(p(i,j),j=1,3)
do 76 i=1,ns
difx(i)=cor(ncon(i,2),2)-cor(ncon(i,1),2)
dify(i)=cor(ncon(i,2),3)-cor(ncon(i,1),3)
difz(i)=cor(ncon(i,2),4)-cor(ncon(i,1),4)
76 continue
write(6,77)
77 format(" number of cycles")
read(5,20)ncycles
do 80 i=1,nu
u(i)=0.0
v(i)=0.0
80 continue
h=1
l=1
c=1
530 continue
550 do 900 ij=1,nu
if(l.eq.1)go to 600
cor(ij,2)=cor(ij,2)-u(ij)
u(ij)=0.0
600 ii=1
700 continue
cor(ij,2)=cor(ij,2)+u(ij)

```

```

do 755 i=1,ns
if(ncon(i,1).eq.ij)go to 740
if(ncon(i,2).eq.ij)go to 740
go to 755
740 continue
difx(i)=cor(ncon(i,2),2)-cor(ncon(i,1),2)
alen(i)=sqrt(difx(i)**2+dify(i)**2+difz(i)**2)
ext(i)=alen(i)-ol(i)
if(ext(i).gt.0.0)go to 752
ten(i)=0.0
go to 754
752 ae(i)=7.0
753 ten(i)=ae(i)*ext(i)/ol(i)
754 tenx(i)=ten(i)*difx(i)/alen(i)
755 continue
do 760 j=1,n
760 tx(j)=0.0
do 770 i=1,ns
if(ncon(i,1).eq.ij)go to 765
if(ncon(i,2).eq.ij)go to 765
go to 770
765 continue
tx(ncon(i,1))=tx(ncon(i,1))-tenx(i)
tx(ncon(i,2))=tx(ncon(i,2))+tenx(i)
770 continue
r(ii)=tx(ij)-p(ij,1)
if(abs(r(ii)).lt.0.01)go to 897
ii=ii+1
if(ii.gt.2)go to 795
if(r(ii-1))785,897,790
785 uu(ii)=9.0
go to 895
790 uu(ii)=-9.0
go to 895
795 if(ii.gt.3)go to 800
uu(ii)=uu(ii-1)/2.0
go to 895
800 if(ii.eq.4)go to 828
if(ii.eq.5)go to 827
if(ii.eq.6)go to 826
if(ii.eq.7)go to 825
if(ii.eq.8)go to 822
if(ii.eq.9)go to 821
if(ii.eq.10)go to 820
if(ii.eq.11)go to 819
if(ii.eq.12)go to 818
if(ii.eq.13)go to 817
if(ii.gt.13)go to 816
805 uuu=r(ii-1)/r(ii-2)
if(uuu)810,810,811
810 uu(ii)=(uu(ii-1)+uu(ii-2))/2.0
go to 895

```

```

811 uu(ii)=(uu(ii-1)+uu(ii-3))/2.0
go to 895
816 if(r(ii-1).lt.0.0.and.r(ii-2).lt.0.0.and.r(ii-3).lt.0.0.and
&r(ii-4).lt.0.0.and.r(ii-5).lt.0.0.and.r(ii-6).lt.0.0.and.r(ii-7).
&lt.0.0.and.r(ii-8).lt.0.0.and.r(ii-9).lt.0.0.and.r(ii-10).lt.
&0.0.and.r(ii-11).lt.0.0.and.r(ii-12).lt.0.0.and.r(ii-13).lt.0.0)go to 888
if(r(ii-1).gt.0.0.and.r(ii-2).gt.0.0.and.r(ii-3).gt.0.0.and.r(ii-4).
&gt.0.0.and.r(ii-5).gt.0.0.and.r(ii-6).gt.0.0.and.r(ii-7).gt.0.0.and.
&r(ii-8).gt.0.0.and.r(ii-9).gt.0.0.and.r(ii-10).gt.0.0.and.r(ii-11).
&gt.0.0.and.r(ii-12).gt.0.0.and.r(ii-13).gt.0.0)go to 888
817 if(r(ii-1).lt.0.0.and.r(ii-2).lt.0.0.and.r(ii-3).lt.0.0.and.
&r(ii-4).lt.0.0.and.r(ii-5).lt.0.0.and.r(ii-6).lt.0.0.and.r(ii-7).
&lt.0.0.and.r(ii-8).lt.0.0.and.r(ii-9).lt.0.0.and.r(ii-10).lt.0.0.and.r(
&ii-11).lt.0.0.and.r(ii-12).lt.0.0)go to 887
if(r(ii-1).gt.0.0.and.r(ii-2).gt.0.0.and.r(ii-3).gt.0.0.and.r(ii-4).
&gt.0.0.and.r(ii-5).gt.0.0.and.r(ii-6).gt.0.0.and.r(ii-7).gt.0.0.and.
&r(ii-8).gt.0.0.and.r(ii-9).gt.0.0.and.r(ii-10).gt.0.0.and.r(ii-11).
&gt.0.0.and.r(ii-12).gt.0.0)go to 887
818 if(r(ii-1).lt.0.0.and.r(ii-2).lt.0.0.and.r(ii-3).lt.0.0.and.
&r(ii-4).lt.0.0.and.r(ii-5).lt.0.0.and.r(ii-6).lt.0.0.and.r(ii-7).lt.0.0.
&and.r(ii-8).lt.0.0.and.r(ii-9).lt.0.0.and.r(ii-10).lt.0.0.and.r(ii-11)
&lt.0.0)go to 886
if(r(ii-1).gt.0.0.and.r(ii-2).gt.0.0.and.r(ii-3).gt.0.0.and.r(ii-4).
&gt.0.0.and.r(ii-5).gt.0.0.and.r(ii-6).gt.0.0.and.r(ii-7).gt.0.0.and.r(ii-8).
&gt.0.0.and.r(ii-9).gt.0.0.and.r(ii-10).gt.0.0.and.r(ii-11).gt.0.0)go to 886
819 if(r(ii-1).lt.0.0.and.r(ii-2).lt.0.0.and.r(ii-3).lt.0.0.
&and.r(ii-4).lt.0.0.and.r(ii-5).lt.0.0.and.r(ii-6).lt.0.0.and.
&r(ii-7).lt.0.0.and.r(ii-8).lt.0.0.and.r(ii-9).lt.0.0.and.
&r(ii-10).lt.0.0)go to 885
if(r(ii-1).gt.0.0.and.r(ii-2).gt.0.0.and.r(ii-3).gt.0.0.and.
&r(ii-4).gt.0.0.and.r(ii-5).gt.0.0.and.r(ii-6).gt.0.0.and.
&r(ii-7).gt.0.0.and.r(ii-8).gt.0.0.and.r(ii-9).gt.0.0.and.
&r(ii-10).gt.0.0)go to 885
820 if(r(ii-1).lt.0.0.and.r(ii-2).lt.0.0.and.r(ii-3).lt.0.0.and.
&r(ii-4).lt.0.0.and.r(ii-5).lt.0.0.and.r(ii-6).lt.0.0.and.r(ii-7).
&lt.0.0.and.r(ii-8).lt.0.0.and.r(ii-9).lt.0.0)go to 884
if(r(ii-1).gt.0.0.and.r(ii-2).gt.0.0.and.r(ii-3).gt.0.0.and.
&r(ii-4).gt.0.0.and.r(ii-5).gt.0.0.and.r(ii-6).gt.0.0.and.r(ii-7).
&gt.0.0.and.r(ii-8).gt.0.0.and.r(ii-9).gt.0.0)go to 884
821 if(r(ii-1).lt.0.0.and.r(ii-2).lt.0.0.and.r(ii-3).lt.0.0.and.
&r(ii-4).lt.0.0.and.r(ii-5).lt.0.0.and.r(ii-6).lt.0.0.and.r(ii-7).
&lt.0.0.and.r(ii-8).lt.0.0)go to 883
if(r(ii-1).gt.0.0.and.r(ii-2).gt.0.0.and.r(ii-3).gt.0.0.and.
&r(ii-4).gt.0.0.and.r(ii-5).gt.0.0.and.r(ii-6).gt.0.0.and.r(ii-7).
&gt.0.0.and.r(ii-8).gt.0.0)go to 883
822 if(r(ii-1).lt.0.0.and.r(ii-2).lt.0.0.and.r(ii-3).lt.0.0.and.
&r(ii-4).lt.0.0.and.r(ii-5).lt.0.0.and.r(ii-6).lt.0.0.and.r(ii-7).
&lt.0.0)go to 882
if(r(ii-1).gt.0.0.and.r(ii-2).gt.0.0.and.r(ii-3).gt.0.0.and.r(ii-4).
&gt.0.0.and.r(ii-5).gt.0.0.and.r(ii-6).gt.0.0.and.r(ii-7).
&gt.0.0)go to 882
825 if(r(ii-1).lt.0.0.and.r(ii-2).lt.0.0.and.r(ii-3).lt.0.0.and.

```

```

&r(ii-4).lt.0.0.and.r(ii-5).lt.0.0.and.r(ii-6).lt.0.0)go to 881
if(r(ii-1).gt.0.0.and.r(ii-2).gt.0.0.and.r(ii-3).gt.0.0.and.
&r(ii-4).gt.0.0.and.r(ii-5).gt.0.0.and.r(ii-6).gt.0.0)go to 881
826 if(r(ii-1).lt.0.0.and.r(ii-2).lt.0.0.and.r(ii-3).lt.0.0.and.
&r(ii-4).lt.0.0.and.r(ii-5).lt.0.0)go to 880
if(r(ii-1).gt.0.0.and.r(ii-2).gt.0.0.and.r(ii-3).gt.0.0.and.
&r(ii-4).gt.0.0.and.r(ii-5).gt.0.0)go to 880
827 if(r(ii-1).lt.0.0.and.r(ii-2).lt.0.0.and.r(ii-3).lt.0.0.and.
&r(ii-4).lt.0.0)go to 870
if(r(ii-1).gt.0.0.and.r(ii-2).gt.0.0.and.r(ii-3).gt.0.0.and.
&r(ii-4).gt.0.0)go to 870
828 if(r(ii-1).lt.0.0.and.r(ii-2).lt.0.0.and.r(ii-3).lt.0.0)go to 850
if(r(ii-1).gt.0.0.and.r(ii-2).gt.0.0.and.r(ii-3).gt.0.0)go to 850
go to 805
850 uu(ii)=(uu(ii-1)+uu(ii-4))/2.0
go to 895
870 uu(ii)=(uu(ii-1)+uu(ii-5))/2.0
go to 895
880 uu(ii)=(uu(ii-1)+uu(ii-6))/2.0
go to 895
881 uu(ii)=(uu(ii-1)+uu(ii-7))/2.0
go to 895
882 uu(ii)=(uu(ii-1)+uu(ii-8))/2.0
go to 895
883 uu(ii)=(uu(ii-1)+uu(ii-9))/2.0
go to 895
884 uu(ii)=(uu(ii-1)+uu(ii-10))/2.0
go to 895
885 uu(ii)=(uu(ii-1)+uu(ii-11))/2.0
go to 895
886 uu(ii)=(uu(ii-1)+uu(ii-12))/2.0
go to 895
887 uu(ii)=(uu(ii-1)+uu(ii-13))/2.0
go to 895
888 uu(ii)=(uu(ii-1)+uu(ii-14))/2.0
895 u(ij)=uu(ii)-uu(ii-1)
go to 700
897 u(ij)=uu(ii)
900 continue
if(l.eq.1)go to 950
n=1
do 940 i=1,nu
if(abs(u(i)-q(i)).lt.0.1)go to 940
n=n+1
940 continue
if(n.eq.1)go to 970
950 do 960 ij=1,nu
q(ij)=u(ij)
960 continue
l=l+1
go to 550
970 continue

```

```

990 do 1200 ij=1,nv
if(c.eq.1)go to 995
cor(ij,3)=cor(ij,3)-v(ij)
v(ij)=0.0
995 ii=1
1000 continue
cor(ij,3)=cor(ij,3)+v(ij)
do 1065 i=1,ns
if(ncon(i,1).eq.ij)go to 1040
if(ncon(i,2).eq.ij)go to 1040
go to 1065
1040 continue
dify(i)=cor(ncon(i,2),3)-cor(ncon(i,1),3)
alen(i)=sqrt(difx(i)**2+dify(i)**2+difz(i)**2)
ext(i)=alen(i)-ol(i)
if(ext(i).gt.0.0)go to 1062
ten(i)=0.0
go to 1064
1062 ae(i)=7.0
1063 ten(i)=ae(i)*ext(i)/ol(i)
1064 teny(i)=ten(i)*dify(i)/alen(i)
1065 continue
do 1070 j=1,n
1070 ty(j)=0.0
do 1075 i=1,ns
if(ncon(i,1).eq.ij)go to 1073
if(ncon(i,2).eq.ij)go to 1073
go to 1075
1073 continue
ty(ncon(i,1))=ty(ncon(i,1))-teny(i)
ty(ncon(i,2))=ty(ncon(i,2))+teny(i)
1075 continue
r(ii)=ty(ij)-p(ij,2)
if(abs(r(ii)).lt.0.01)go to 1197
ii=ii+1
if(ii.gt.2)go to 1095
if(r(ii-1))1085,1197,1090
1085 vv(ii)=9.0
go to 1195
1090 vv(ii)=-9.0
go to 1195
1095 if(ii.gt.3)go to 1100
vv(ii)=vv(ii-1)/2.0
go to 1195
1100 if(ii.eq.4)go to 1128
if(ii.eq.5)go to 1127
if(ii.eq.6)go to 1126
if(ii.eq.7)go to 1125
if(ii.eq.8)go to 1124
if(ii.eq.9)go to 1123
if(ii.eq.10)go to 1122
if(ii.eq.11)go to 1121

```

```

if(ii.eq.12)go to 1120
if(ii.eq.13)go to 1119
if(ii.gt.13)go to 1118
1105 vvv=r(ii-1)/r(ii-2)
if(vvv)1110,1110,1111
1110 vv(ii)=(vv(ii-1)+vv(ii-2))/2.0
go to 1195
1111 vv(ii)=(vv(ii-1)+vv(ii-3))/2.0
go to 1195
1118 if(r(ii-1).lt.0.0.and.r(ii-2).lt.0.0.and.r(ii-3).lt.0.0.and.r(ii-4).
&lt.0.0.and.r(ii-5).lt.0.0.and.r(ii-6).lt.0.0.and.r(ii-7).lt.0.0.and.
&r(ii-8).lt.0.0.and.r(ii-9).lt.0.0.and.r(ii-10).lt.0.0.and.r(ii-11).
&lt.0.0.and.r(ii-12).lt.0.0.and.r(ii-13).lt.0.0)go to 1188
if(r(ii-1).gt.0.0.and.r(ii-2).gt.0.0.and.r(ii-3).gt.0.0.and.r(ii-4).
&gt.0.0.and.r(ii-5).gt.0.0.and.r(ii-6).gt.0.0.and.r(ii-7).gt.0.0.and.
&r(ii-8).gt.0.0.and.r(ii-9).gt.0.0.and.r(ii-10).gt.0.0.and.r(ii-11).gt.
&0.0.and.r(ii-12).gt.0.0.and.r(ii-13).gt.0.0)go to 1188
1119 if(r(ii-1).lt.0.0.and.r(ii-2).lt.0.0.and.r(ii-3).lt.0.0.and.r(ii-4).lt.
&0.0.and.r(ii-5).lt.0.0.and.r(ii-6).lt.0.0.and.r(ii-7).lt.0.0.and.r(ii-8).
&lt.0.0.and.r(ii-9).lt.0.0.and.r(ii-10).lt.0.0.and.r(ii-11).lt.0.0.and.
&r(ii-12).lt.0.0)go to 1187
if(r(ii-1).gt.0.0.and.r(ii-2).gt.0.0.and.r(ii-3).gt.0.0.and.r(ii-4).gt.
&0.0.and.r(ii-5).gt.0.0.and.r(ii-6).gt.0.0.and.r(ii-7).gt.0.0.and.r(ii-8).
&gt.0.0.and.r(ii-9).gt.0.0.and.r(ii-10).gt.0.0.and.r(ii-11).gt.0.0.and.
&r(ii-12).gt.0.0)go to 1187
1120 if(r(ii-1).lt.0.0.and.r(ii-2).lt.0.0.and.r(ii-3).lt.0.0.and.r(ii-4).lt.
&0.0.and.r(ii-5).lt.0.0.and.r(ii-6).lt.0.0.and.r(ii-7).lt.0.0.and.r(ii-8).lt.
&0.0.and.r(ii-9).lt.0.0.and.r(ii-10).lt.0.0.and.r(ii-11).lt.0.0)go to 1186
if(r(ii-1).gt.0.0.and.r(ii-2).gt.0.0.and.r(ii-3).gt.0.0.and.r(ii-4).
&gt.0.0.and.r(ii-5).gt.0.0.and.r(ii-6).gt.0.0.and.r(ii-7).gt.0.0.and.
&r(ii-8).gt.0.0.and.r(ii-9).gt.0.0.and.r(ii-10).gt.0.0.and.r(ii-11).gt.
&0.0)go to 1186
1121 if(r(ii-1).lt.0.0.and.r(ii-2).lt.0.0.and.r(ii-3).lt.0.0.and.
&r(ii-4).lt.0.0.and.r(ii-5).lt.0.0.and.r(ii-6).lt.0.0.and.r(ii-7).
&lt.0.0.and.r(ii-8).lt.0.0.and.r(ii-9).lt.0.0.and.r(ii-10).lt.0.0)
&go to 1185
if(r(ii-1).gt.0.0.and.r(ii-2).gt.0.0.and.r(ii-3).gt.0.0.and.
&r(ii-4).gt.0.0.and.r(ii-5).gt.0.0.and.r(ii-6).gt.0.0.and.r(ii-7).
&gt.0.0.and.r(ii-8).gt.0.0.and.r(ii-9).gt.0.0.and.r(ii-10).gt.
&0.0)go to 1185
1122 if(r(ii-1).lt.0.0.and.r(ii-2).lt.0.0.and.r(ii-3).lt.0.0.and.
&r(ii-4).lt.0.0.and.r(ii-5).lt.0.0.and.r(ii-6).lt.0.0.and.r(ii-7).
&lt.0.0.and.r(ii-8).lt.0.0.and.r(ii-9).lt.0.0)go to 1184
if(r(ii-1).gt.0.0.and.r(ii-2).gt.0.0.and.r(ii-3).gt.0.0.and.
&r(ii-4).gt.0.0.and.r(ii-5).gt.0.0.and.r(ii-6).gt.0.0.and.r(ii-7).
&gt.0.0.and.r(ii-8).gt.0.0.and.r(ii-9).gt.0.0)go to 1184
1123 if(r(ii-1).lt.0.0.and.r(ii-2).lt.0.0.and.r(ii-3).lt.0.0.and.
&r(ii-4).lt.0.0.and.r(ii-5).lt.0.0.and.r(ii-6).lt.0.0.and.r(ii-7).
&lt.0.0.and.r(ii-8).lt.0.0)go to 1183
if(r(ii-1).gt.0.0.and.r(ii-2).gt.0.0.and.r(ii-3).gt.0.0.and.
&r(ii-4).gt.0.0.and.r(ii-5).gt.0.0.and.r(ii-6).gt.0.0.and.r(ii-7).
&gt.0.0.and.r(ii-8).gt.0.0)go to 1183

```

```

1124 if(r(ii-1).lt.0.0.and.r(ii-2).lt.0.0.and.r(ii-3).lt.0.0.and.
&r(ii-4).lt.0.0.and.r(ii-5).lt.0.0.and.r(ii-6).lt.0.0.and.r(ii-7).
&lt.0.0)go to 1182
if(r(ii-1).gt.0.0.and.r(ii-2).gt.0.0.and.r(ii-3).gt.0.0.and.r(ii-4).
&gt.0.0.and.r(ii-5).gt.0.0.and.r(ii-6).gt.0.0.and.r(ii-7).gt.0.0)go to 1182
1125 if(r(ii-1).lt.0.0.and.r(ii-2).lt.0.0.and.r(ii-3).lt.0.0.and.
&r(ii-4).lt.0.0.and.r(ii-5).lt.0.0.and.r(ii-6).lt.0.0)go to 1181
if(r(ii-1).gt.0.0.and.r(ii-2).gt.0.0.and.r(ii-3).gt.0.0.and.r(ii-4).
&gt.0.0.and.r(ii-5).gt.0.0.and.r(ii-6).gt.0.0)go to 1181
1126 if(r(ii-1).lt.0.0.and.r(ii-2).lt.0.0.and.r(ii-3).lt.0.0.and.
&r(ii-4).lt.0.0.and.r(ii-5).lt.0.0)go to 1180
if(r(ii-1).gt.0.0.and.r(ii-2).gt.0.0.and.r(ii-3).gt.0.0.and.
&r(ii-4).gt.0.0.and.r(ii-5).gt.0.0)go to 1180
1127 if(r(ii-1).lt.0.0.and.r(ii-2).lt.0.0.and.r(ii-3).lt.0.0.and.
&r(ii-4).lt.0.0)go to 1170
if(r(ii-1).gt.0.0.and.r(ii-2).gt.0.0.and.r(ii-3).gt.0.0.and.
&r(ii-4).gt.0.0)go to 1170
1128 if(r(ii-1).lt.0.0.and.r(ii-2).lt.0.0.and.r(ii-3).lt.0.0)go to 1150
if(r(ii-1).gt.0.0.and.r(ii-2).gt.0.0.and.r(ii-3).gt.0.0)go to 1150
go to 1105
1150 vv(ii)=(vv(ii-1)+vv(ii-4))/2.0
go to 1195
1170 vv(ii)=(vv(ii-1)+vv(ii-5))/2.0
go to 1195
1180 vv(ii)=(vv(ii-1)+vv(ii-6))/2.0
go to 1195
1181 vv(ii)=(vv(ii-1)+vv(ii-7))/2.0
go to 1195
1182 vv(ii)=(vv(ii-1)+vv(ii-8))/2.0
go to 1195
1183 vv(ii)=(vv(ii-1)+vv(ii-9))/2.0
go to 1195
1184 vv(ii)=(vv(ii-1)+vv(ii-10))/2.0
go to 1195
1185 vv(ii)=(vv(ii-1)+vv(ii-11))/2.0
go to 1195
1186 vv(ii)=(vv(ii-1)+vv(ii-12))/2.0
go to 1195
1187 vv(ii)=(vv(ii-1)+vv(ii-13))/2.0
go to 1195
1188 vv(ii)=(vv(ii-1)+vv(ii-14))/2.0
1195 v(ij)=vv(ii)-vv(ii-1)
go to 1000
1197 v(ij)=vv(ii)
1200 continue
if(c.eq.1)go to 1250
n=1
do 1240 i=1,nv
if(abs(v(i)-q(i)).lt.0.1)go to 1240
n=n+1
1240 continue
if(n.eq.1)go to 1500

```



```
1250 do 1300 ij=1,nv
    q(ij)=v(ij)
1300 continue
    c=c+1

go to 990
1500 continue
if(h.eq.ncycles)go to 1700
    h=h+1
go to 950
1700 continue
do 1750 i=1,n
1750 write(rfile,1800)(cor(i,j),j=1,4)
1800 format(f5.1,1x,f9.4,1x,f9.4,1x,f9.4)
do 1840 i=1,ns
1840 write(rfile,2000)ol(i)
do 1900 i=1,nu
1900 write(rfile,2000)(p(i,j),j=1,3)
2000 format(f9.4,1x,f9.4,1x,f9.4)
do 2010 i=1,ns
2010 write(rfile,2020)i,ten(i)
2020 format("ten(",i3,")=",f9.4)
    close(5)
    close(6)
stop
end
```

## APPENDIX ( 3 )

Joint slippage program.

```

integer dfile,d2file,rfile
dimension cor(500,4),ncon(500,2),difx(500),dify(500),
&alen(500),ext(500),ae(500),ten(500),r(30),ol(500),jsl(600,2),
&s(500),dift(30),ss(90)
write(6,5)
5 format(" number of data files")
read(5,10)dfile,d2file
write(6,15)
15 format(" number of results file")
read(5,10)rfile
10 format(v)
read(dfile,10)n,ns
do 40 i=1,ns
40 read(dfile,45)(ncon(i,j),j=1,2)
45 format(v)
55 format(i3,1x,i3)
do 60 i=1,n
60 read(dfile,45)(cor(i,j),j=1,4)
do 66 i=1,ns
66 read(dfile,45)ol(i)
read(d2file,45)n1,n1,n2,n3
do 67 i=1,n1
67 read(d2file,45)(jsl(i,j),j=1,2)
do 90 i=n3,ns
cor(ncon(i,1),3)=-cor(ncon(i,2),3)
ol(i)=ol(i)*2.0
90 continue
1700 continue
do 1750 i=1,n
1750 write(rfile,1800)(cor(i,j),j=1,4)
1800 format(f5.1,1x,f9.4,1x,f9.4,1x,f9.4)
do 1840 i=1,ns
1840 write(rfile,1845)ol(i)
1845 format(f9.4)
do 1850 i=1,n1
1850 write(rfile,55)(jsl(i,j),j=1,2)
do 2050 i=1,n1
s(i)=0.0
2050 continue
do 2075 i=1,ns
difx(i)=cor(ncon(i,2),2)-cor(ncon(i,1),2)
dify(i)=cor(ncon(i,2),3)-cor(ncon(i,1),3)
alen(i)=sqrt(difx(i)**2+dify(i)**2)
2075 continue
2086 do 2500 ij=1,n1
s(ij)=0.0
2088 ii=1
2090 continue
ol(jsl(ij,1))=ol(jsl(ij,1))+s(ij)
ol(jsl(ij,2))=ol(jsl(ij,2))-s(ij)
ext(jsl(ij,1))=alen(jsl(ij,1))-ol(jsl(ij,1))
ext(jsl(ij,2))=alen(jsl(ij,2))-ol(jsl(ij,2))

```

```

if(ext(jsl(ij,1)).gt.0.0)go to 2095
ten(jsl(ij,1))=0.0
go to 2100
2095 ae(jsl(ij,1))=7.0
ten(jsl(ij,1))=ae(jsl(ij,1))*ext(jsl(ij,1))/ol(jsl(ij,1))
2100 if(ext(jsl(ij,2)).gt.0.0)go to 2200
ten(jsl(ij,2))=0.0
go to 2290
2200 ae(jsl(ij,2))=7.0
ten(jsl(ij,2))=ae(jsl(ij,2))*ext(jsl(ij,2))/ol(jsl(ij,2))
2290 dift(ii)=ten(jsl(ij,1))-ten(jsl(ij,2))
if(dift(ii))2300,2420,2295
2295 r(ii)=dift(ii)-0.7037
go to 2301
2300 r(ii)=dift(ii)+0.7037
2301 if(ii.gt.1)go to 2302
if(abs(dift(ii)).lt.0.7037)go to 2420
2302 if(abs(r(ii)).lt.0.001)go to 2420
ii=ii+1
if(ii.gt.2)go to 2305
if(r(ii-1))2304,2420,2303
2303 ss(ii)=0.2
go to 2400
2304 ss(ii)=-0.2
go to 2400
2305 if(ii.gt.3)go to 2306
ss(ii)=ss(ii-1)/2.0
go to 2400
2306 if(ii.eq.4)go to 2340
if(ii.eq.5)go to 2335
if(ii.eq.6)go to 2330
if(ii.eq.7)go to 2325
if(ii.eq.8)go to 2324
if(ii.eq.9)go to 2323
if(ii.eq.10)go to 2322
if(ii.eq.11)go to 2321
if(ii.eq.12)go to 2320
if(ii.eq.13)go to 2319
if(ii.gt.13)go to 2318
2308 sss=r(ii-1)/r(ii-2)
if(sss)2310,2310,2311
2310 ss(ii)=(ss(ii-1)+ss(ii-2))/2.0
go to 2400
2311 ss(ii)=(ss(ii-1)+ss(ii-3))/2.0
go to 2400
2318 if(r(ii-1).lt.0.0.and.r(ii-2).lt.0.0.and.r(ii-3).lt.0.0.
&and.r(ii-4).lt.0.0.and.r(ii-5).lt.0.0.and.r(ii-6).lt.0.0.and.
&r(ii-7).lt.0.0.and.r(ii-8).lt.0.0.and.r(ii-9).lt.0.0.and.r(ii-10).
&lt.0.0.and.r(ii-11).lt.0.0.and.r(ii-12).lt.0.0.and.r(ii-13).
&lt.0.0)go to 2397
if(r(ii-1).gt.0.0.and.r(ii-2).gt.0.0.and.r(ii-3).gt.0.0.
&and.r(ii-4).gt.0.0.and.r(ii-5).gt.0.0.and.r(ii-6).gt.0.0.

```

```

&and.r(ii-7).gt.0.0.and.r(ii-8).gt.0.0.and.r(ii-9).gt.0.0.and.
&r(ii-10).gt.0.0.and.r(ii-11).gt.0.0.and.r(ii-12).gt.0.0.
&and.r(ii-13).gt.0.0)go to 2397
2319 if(r(ii-1).lt.0.0.and.r(ii-2).lt.0.0.and.r(ii-3).lt.0.0.
&and.r(ii-4).lt.0.0.and.r(ii-5).lt.0.0.and.r(ii-6).lt.0.0.and.
&r(ii-7).lt.0.0.and.r(ii-8).lt.0.0.and.r(ii-9).lt.0.0.and.
&r(ii-10).lt.0.0.and.r(ii-11).lt.0.0.and.r(ii-12).lt.0.0)go to 2396
if(r(ii-1).gt.0.0.and.r(ii-2).gt.0.0.and.r(ii-3).gt.0.0.and.
&r(ii-4).gt.0.0.and.r(ii-5).gt.0.0.and.r(ii-6).gt.0.0.and.r(ii-7).
&gt.0.0.and.r(ii-8).gt.0.0.and.r(ii-9).gt.0.0.and.r(ii-10).gt.
&0.0.and.r(ii-11).gt.0.0.and.r(ii-12).gt.0.0)go to 2396
2320 if(r(ii-1).lt.0.0.and.r(ii-2).lt.0.0.and.r(ii-3).lt.0.0.
&and.r(ii-4).lt.0.0.and.r(ii-5).lt.0.0.and.r(ii-6).lt.0.0.and.
&r(ii-7).lt.0.0.and.r(ii-8).lt.0.0.and.r(ii-9).lt.0.0.and.
&r(ii-10).lt.0.0.and.r(ii-11).lt.0.0)go to 2395
if(r(ii-1).gt.0.0.and.r(ii-2).gt.0.0.and.r(ii-3).gt.0.0.and.
&r(ii-4).gt.0.0.and.r(ii-5).gt.0.0.and.r(ii-6).gt.0.0.and.
&r(ii-7).gt.0.0.and.r(ii-8).gt.0.0.and.r(ii-9).gt.0.0.and.
&r(ii-10).gt.0.0.and.r(ii-11).gt.0.0)go to 2395
2321 if(r(ii-1).lt.0.0.and.r(ii-2).lt.0.0.and.r(ii-3).
&lt.0.0.and.r(ii-4).lt.0.0.and.r(ii-5).lt.0.0.and.r(ii-6).lt.0.0.
&and.r(ii-7).lt.0.0.and.r(ii-8).lt.0.0.and.r(ii-9).lt.0.0.
&and.r(ii-10).lt.0.0)go to 2394
if(r(ii-1).gt.0.0.and.r(ii-2).gt.0.0.and.r(ii-3).gt.0.0.
&and.r(ii-4).gt.0.0.and.r(ii-5).gt.0.0.and.r(ii-6).gt.0.0.
&and.r(ii-7).gt.0.0.and.r(ii-8).gt.0.0.and.r(ii-9).gt.0.0.
&and.r(ii-10).gt.0.0)go to 2394
2322 if(r(ii-1).lt.0.0.and.r(ii-2).lt.0.0.and.r(ii-3).lt.0.0.
&and.r(ii-4).lt.0.0.and.r(ii-5).lt.0.0.and.r(ii-6).lt.0.0.
&and.r(ii-7).lt.0.0.and.r(ii-8).lt.0.0.and.r(ii-9).lt.0.0)go to 2393
if(r(ii-1).gt.0.0.and.r(ii-2).gt.0.0.and.r(ii-3).gt.0.0.and.
&r(ii-4).gt.0.0.and.r(ii-5).gt.0.0.and.r(ii-6).gt.0.0.
&and.r(ii-7).gt.0.0.and.r(ii-8).gt.0.0.and.r(ii-9).gt.0.0)go to 2393
2323 if(r(ii-1).lt.0.0.and.r(ii-2).lt.0.0.and.r(ii-3).lt.0.0.
&and.r(ii-4).lt.0.0.and.r(ii-5).lt.0.0.and.r(ii-6).lt.0.0.
&and.r(ii-7).lt.0.0.and.r(ii-8).lt.0.0)go to 2392
if(r(ii-1).gt.0.0.and.r(ii-2).gt.0.0.and.r(ii-3).gt.0.0.and.
&r(ii-4).gt.0.0.and.r(ii-5).gt.0.0.and.r(ii-6).gt.0.0.
&and.r(ii-7).gt.0.0.and.r(ii-8).gt.0.0)go to 2392
2324 if(r(ii-1).lt.0.0.and.r(ii-2).lt.0.0.and.r(ii-3).lt.0.0.and.
&r(ii-4).lt.0.0.and.r(ii-5).lt.0.0.and.r(ii-6).lt.0.0.
&and.r(ii-7).lt.0.0)go to 2391
if(r(ii-1).gt.0.0.and.r(ii-2).gt.0.0.and.r(ii-3).gt.0.0.and.
&r(ii-4).gt.0.0.and.r(ii-5).gt.0.0.and.r(ii-6).gt.0.0.
&and.r(ii-7).gt.0.0)go to 2391
2325 if(r(ii-1).lt.0.0.and.r(ii-2).lt.0.0.and.r(ii-3).lt.0.0.and.
&r(ii-4).lt.0.0.and.r(ii-5).lt.0.0.and.r(ii-6).lt.0.0)go to 2390
if(r(ii-1).gt.0.0.and.r(ii-2).gt.0.0.and.r(ii-3).gt.0.0.and.
&r(ii-4).gt.0.0.and.r(ii-5).gt.0.0.and.r(ii-6).gt.0.0)go to 2390
2330 if(r(ii-1).lt.0.0.and.r(ii-2).lt.0.0.and.r(ii-3).lt.0.0.
&and.r(ii-4).lt.0.0.and.r(ii-5).lt.0.0)go to 2380
if(r(ii-1).gt.0.0.and.r(ii-2).gt.0.0.and.r(ii-3).gt.0.0.and.

```

```

&r(ii-4).gt.0.0.and.r(ii-5).gt.0.0)go to 2380
2335 if(r(ii-1).lt.0.0.and.r(ii-2).lt.0.0.and.r(ii-3).lt.0.0.
&and.r(ii-4).lt.0.0)go to 2370
if(r(ii-1).gt.0.0.and.r(ii-2).gt.0.0.and.r(ii-3).gt.0.0.
&and.r(ii-4).gt.0.0)go to 2370
2340 if(r(ii-1).lt.0.0.and.r(ii-2).lt.0.0.and.r(ii-3).lt.0.0)go to 2350
if(r(ii-1).gt.0.0.and.r(ii-2).gt.0.0.and.r(ii-3).gt.0.0)go to 2350
go to 2308
2350 ss(ii)=(ss(ii-1)+ss(ii-4))/2.0
go to 2400
2370 ss(ii)=(ss(ii-1)+ss(ii-5))/2.0
go to 2400
2380 ss(ii)=(ss(ii-1)+ss(ii-6))/2.0
go to 2400
2390 ss(ii)=(ss(ii-1)+ss(ii-7))/2.0
go to 2400
2391 ss(ii)=(ss(ii-1)+ss(ii-8))/2.0
go to 2400
2392 ss(ii)=(ss(ii-1)+ss(ii-9))/2.0
go to 2400
2393 ss(ii)=(ss(ii-1)+ss(ii-10))/2.0
go to 2400
2394 ss(ii)=(ss(ii-1)+ss(ii-11))/2.0
go to 2400
2395 ss(ii)=(ss(ii-1)+ss(ii-12))/2.0
go to 2400
2396 ss(ii)=(ss(ii-1)+ss(ii-13))/2.0
go to 2400
2397 ss(ii)=(ss(ii-1)+ss(ii-14))/2.0
2400 s(ij)=ss(ii)-ss(ii-1)
2410 go to 2090
2420 s(ij)=ss(ii)
ol(jsl(ij,1))=ol(jsl(ij,1))-s(ij)
ol(jsl(ij,2))=ol(jsl(ij,2))+s(ij)
2500 continue
write(rfile,2510)
2510 format(" situation of joints",/)
do 2520 ij=1,nl
2520 write(rfile,2522)ij,s(ij)
2522 format(1x,"s(",i3,")=",f9.4)
3000 continue
close(5)
close(6)
stop
end

```